Gabriel Santos da Silva

Using Diversity Combining Techniques and Extended Spreading Factors to Improve Performance and Reduce OFDM Receiver Complexity in IEEE 802.15.4g

Uso de Técnicas de Combinação de Diversidade e Fatores de Espalhamento Estendidos para Melhorar a Performance e Reduzir a complexidade do Receptor OFDM em IEEE 802.15.4.g

Campinas

2018

Gabriel Santos da Silva

Using Diversity Combining Techniques and Extended Spreading Factors to Improve Performance and Reduce OFDM Receiver Complexity in IEEE 802.15.4g

Uso de Técnicas de Combinação de Diversidade e Fatores de Espalhamento Estendidos para Melhorar a Performance e Reduzir a complexidade do Receptor OFDM em IEEE 802.15.4.g

Dissertação apresentada à Faculdade de Engenharia Elétrica e de Computação da Universidade Estadual de Campinas como parte dos requisitos exigidos para a obtenção do título de Mestre em Engenharia Elétrica, na Área de Telecomunicações e Telemática.

Dissertation presented to the Faculty of Electrical Engineering and Computing of the University of Campinas in partial fulfillment of the requirements for the degree of Master in Electrical Engineering, in the area of Telecommunications and Telematics

Orientador: Prof. Dr. Renato da Rocha Lopes

Co-orientador Prof. Dr. Eduardo Rodrigues de Lima

Este exemplar corresponde à versão final da tese defendida pelo aluno Gabriel Santos da Silva, e orientada pelo Prof. Dr. Renato da Rocha Lopes

Campinas

2018

Ficha catalográfica
Universidade Estadual de Campinas
Biblioteca da Área de Engenharia e Arquitetura
Rose Meire da Silva - CRB 8/5974

Informações para Biblioteca Digital

Título em outro idioma: Uso de técnicas de combinação de diversidade e fatores de espalhamento estendidos para melhorar a performance e reduzir a complexidade do receptor OFDM em IEEE 802.15.4g
Palavras-chave em inglês:
Protocols for Wireless Application (Computer Network Protocol)
Wireless communication system
Orthogonal frequency division multiplexing
Área de concentração: Telecomunicações e Telemática
Titulação: Mestre em Engenharia Elétrica
Banca examinadora:
Renado da Rocha Lopes
Gustavo Fraidenraich
Cláudio Ferreira Dias
Data de defesa: 09-08-2018
Programa de Pós-Graduação: Engenharia Elétrica

COMISSÃO JULGADORA - DISSERTAÇÃO DE MESTRADO

Candidato: Gabriel Santos da Silva   **RA:** 149985

Data da Defesa: 09 de Agosto de 2018

Título da Tese: "Using Diversity Combining Techniques and Extended Spreading Factors to Improve the Performance and Reduce OFDM Receiver Complexity in IEEE 802.15.4g"

Título da Tese em outro idioma: "Uso de Técnicas de Combinação de Diversidade e Fatores de Espalhamento Estendidos para Melhorar a Performance e Reduzir a Complexidade do Receptor OFDM em IEEE 802.15.4g"

Prof. Dr Renato da Rocha Lopes (Presidente, FEEC/UNICAMP)
Prof. Dr. Cláudio Ferreira Dias (Consultoria)
Prof. Dr. Gustavo Fraidenraich (FEEC/UNICAMP)

A ata de defesa, com as respectivas assinaturas dos membros da Comissão Julgadora, encontra-se no processo de vida acadêmica do aluno.

Dedico este trabalho a todos que me ajudaram a torná-lo possível.

Agradecimentos

Primeiramente agradeço ao Prof. Dr. Renato Lopes, por ter me aceito como seu aluno de mestrado, e pela orientação dedicada a mim ao longo do trabalho; e ao Dr. Eduardo Rodrigues de Lima, por ter me dado a oportunidade de fazer parte do seu time no Instituto de Pesquisas Eldorado, pelo conhecimento repassado a mim nas áreas de processamento digital de sinais e sistemas de comunicação, e pela confiança depositada em meu trabalho em todo estes anos. Ambos foram essenciais para a conclusão deste trabalho.

Quero estender meu agradecimento também a todos os meus colegas de trabalho do Instituto de Pesquisas Eldorado que me ajudaram em muitos momentos, compartilhando seu tempo, paciência e conhecimento. Em espcial cito Augusto F. R. Queiroz e Cesar G. Chaves que me auxiliaram em vários pontos durante a elaboração do trabalho e de artigos referentes ao mesmo. Agradeço à UNICAMP/FFEC, seus professores e demais funcionários; e ao Instituto de Pesquisas Eldorado por permitir que parte do meu trabalho dedicado a ele desse origem à minha tese de mestrado.

Agradeço imensamente à minha família, meus pais Gilson Bento da Silva e Valéria de Fátima Santos Silva, por todo o apoio que me deram até hoje. Sem o amor de vocês teria sido impossível superar esse desafio. Por último, agradeço a todas as pessoas que de alguma forma contribuíram com este trabalho. Em especial cito Átila de M. T. Moretto, pelo companheirismo nesses tantos anos, José Arnaldo B. Filho, por me incentivar sempre, e Júnior Marques, pelo grande carinho compartilhado nessa última etapa do trabalho.

"Roads you have never ridden to places you have never seen and people you have never met. Days end. A different sunset, a different resting point, a different perspective. A little less road waits for you tomorrow. A little more road lies behind you. Choose your road. Ride it well."

(Alastair Humphreys)

Abstract

IEEE 802.15.4g is an amendment of the IEEE 802.15.4 standard focused on Smart Utility Networks (SUN), and devoted to the communication requirements of Low Rate Wireless Personal Area Network (LR-WPAN). Nowadays, due to its characteristics, the amendment focuses on Smart Ubiquitous Network applications, such as Smart City and Internet of Things (IoT). One of the three Physical Layers (PHYs) defined in the standard is the Multi-Rate and Multi-Regional Orthogonal Frequency Division Multiplexing (MR-OFDM). In addition to other features, the MR-OFDM employs frequency spreading to reduce the Peak-to-Average Power Ratio (PAPR) of the OFDM symbol. Under some channel assumptions, this frequency spreading can also introduce frequency diversity to the PHY.

This work proposes a method to perform frequency despreading that exploits diversity in the IEEE 802.15.4g MR-OFDM PHY. The method follows two approaches: the use of diversity combining techniques and the proposal of new Modulation and Coding Scheme (MCS) configurations using extended spreading factors. In a channel with Rayleigh distribution and assuming uncorrelated subcarriers, the proposed method shows improvements up to 10.35 dB when compared to the MR-OFDM performing frequency despreading using original configurations. The method is valid even in the presence of channel estimation errors and large channel coherence bandwidths. The work is part of a larger project which aims at the implementation of an Integrated Circuit capable of handling the three PHYs defined in the IEEE802.15.4g, not only the MR-OFDM. Thus, the method must be fully compliant to the standard and focus on the MR-OFDM receiver implementation complexity.

Keywords: IEEE 802.15.4g; OFDM; Frequency Diversity; Diversity Combining Techniques; Spreading Factor.

Resumo

IEEE 802.15.4g é um adendo da norma IEEE 802.15.4 focada em *Smart Utility Network* (SUN), e dedicada a requisitos de comunicação no contexto de *Low Rate* (LR) *Wireless Personal Area Network* (WPAN). Hoje em dia, devido às suas características, o adendo foca em apliações de *Smart Ubiquitous Network*, como cidades inteligentes e Internet das Coisas (IoT). Uma das três Camadas Físicas (PHYs) definidas na norma é a *Multi-Rate and Multi-Regional Orthogonal Frequency Division Multiplexing* (MR-OFDM). Além de outras características, o MR-OFDM emprega o método *Frequency Spreading* (FS) para reduzir a *Peak-to-Average Power Ratio* (PAPR) do símbolo OFDM. Sob algumas premissas do canal, este trabalho mostra que o FS também pode introduzir diversidade em frequência à camada física.

Este trabalho propõe um método para reverter o espalhamento de frequência que explora diversidade em IEEE 802.15.4g MR-OFDM. O método segue duas abordagens: o uso de técnicas de combinação de diversidade e a proposta de novas configurações de *Modulation and Coding Scheme* (MCS) usando fatores de espalhamento estendidos. Em um canal com distribuição *Rayleigh* e assumindo subportadoras não correlacionadas, o método proposto mostra melhorias de até 10.35 dB quando comparado ao MR-OFDM, revertendo o espalhamento de frequência de forma direta, usando configurações originais. O método é válido mesmo na presença de erros na estimativa do canal e bandas de coerência largas. O trabalho faz parte de um projeto maior que visa a implementação de um circuito integrado capaz de suportar as três camadas físicas definias em IEEE 802.15.4g, não apenas o MR-OFDM. Devido a isso, o método deve ser totalmente compatível com a norma e focar na complexidade de implementação do receptor MR-OFDM.

Palavras-chaves: IEEE 802.15.4g; OFDM; Diversidade em Frequência; Técnicas de Combinação de Diversidade; Fator de Espalhamento.

List of Figures

List of Tables

Contents

1 Introduction

The performance of wireless communication systems depends on the communication reliability, which in turn depends on the strength of the transmitted signal. Usually, in multipath fading scenarios, the probability of occurrence of deep fades may be high, and the communication scheme will suffer from errors due to the signal degradation. Current and emerging wireless communication systems employ some form of diversity in order to mitigate the effect of multipath fading, enhancing transmission reliability (TSE; VISWANATH, 2005; SALEHI; PROAKIS, 2007). Diversity improves the system performance over fading channels, ensuring that the signal passes through multiple paths that fade independently. Therefore, the probability of occurrence of deep fades in all signal copies is low and at least one signal replica should have reasonable power at the receiver (TU; DUTKIEWICZ, 2009).

Diversity can be introduced in transmission or reception, and in three domains: time, space and frequency. In frequency, under some channel assumptions, diversity is exploited transmitting the signal over different carrier frequencies. This can be achieved, for instance, in Orthogonal Frequency Division Multiplexing (OFDM), a multi-carrier system, where the information symbols are transmitted over a set of non-interfering orthogonal subcarriers, which experience flat fading. Hence, a symbol can be transmitted over different subcarriers, and if these subcarriers are uncorrelated, which happens when they are separated in frequency by a distance larger than the channel coherence bandwidth, the system presents frequency diversity.

The IEEE802.15.4g is an amendment to the IEEE802.15.4 standard, which contains Physical Layer (PHY) specifications devoted to Smart Metering Utility Networks (SUN) applications on the context of Low-Rate Wireless Personal Area Network (LR-WPAN)(IEEE, 2012). The amendment defines several frequency bands, bandwidths and data rates, which are obtained through three PHYs, among them the Multi-Rate and Multi-Regional Orthogonal Frequency Division Multiplexing (MR-OFDM). This PHY employs, in addition to other techniques, frequency spreading. In this case, the modulated symbols are replicated on different carriers, and phase rotations are applied to the copied data tones. In contrast to frequency diversity, however, the goal here is to reduce the Peak-to-Average Power Ratio (PAPR) of the OFDM symbol.

The main contribution of this work is to exploit the diversity that may be introduced in the MR-OFDM PHY through the FS technique, even though the objective of the method according to the standard is to reduce the OFDM symbol PAPR. To that end a method to revert the frequency spreading is proposed in this work following two

approaches: employing diversity combining techniques, and proposing new MR-OFDM configurations employing extended spreading factors. The first approach uses Selection Combining (SC), Maximal Ratio Combining (MRC) and Selection Combining Maximal Ratio Combining (SMRC) as diversity combining techniques. Besides the SMRC, this work proposes another hybrid technique, the Selection Frequency Despreading (SFD), which is described in Chapter 3. The second approach employs different combinations of modulation and spreading factor not foreseen yet by the IEEE 802.15.4g standard but still compliant to the data rates defined in (IEEE, 2012). A new spreading factor, $8\times$, is proposed as well, providing more configuration possibilities.

To assess the impact of our proposal, the Bit Error Rate (BER) of the proposed method is obtained through simulations in an environment developed in Matlab. This work presents the simulation results, discussing the performances and comparing them with theoretical BER curves. Furthermore, hardware architectures are designed in VHDL based on the simulated models, integrated in a MR-OFDM transceiver in order to validate their functionality, and prototyped in FPGA. The FPGA prototyping corroborates the simulated performances; and provides synthesis results for hardware complexity analyses.

The remainder of this thesis is structured as follows. Chapter 2 contextualizes the work. It describes the theoretical basis for OFDM, as well as one of its main drawback, the PAPR, and wireless channel models. Moreover, it introduces the diversity concept, providing an overview of the most known diversity combining techniques. Finally, this chapter describes the IEEE 802.15.4g standard, focusing on the MR-OFDM PHY and the frequency spreading technique. Chapter 3 details the contribution of this work. It explains the proposed method along with BER improvement employing diversity combining techniques and extended spreading factors. Chapter 4 presents the simulation results for the frequency despreading proposed method, employing all the addressed diversity combining techniques and extended spreading factors. The results are obtained through a simulation environment implemented in Matlab, which is also detailed in this chapter. Chapter 5 corroborates the simulated results by discussing the MR-OFDM system prototyped in FPGA. Moreover, it presents the hardware architecture for all the possibilities of the proposed method, comparing their complexity. Finally, last chapter is about the conclusion and final considerations of this work.

2 Background

2.1 Orthogonal Frequency-Division Multiplexing (OFDM)

OFDM is a particular type of multi-carrier technique that has gained popularity in a number of applications, such as Wi-Fi (IEEE 802.11a/g/n), WiMAX, Digital Video/Audio Broadcasting (DVB-T/DAB), among others (MARCHETTI *et al.*, 2009). The basic idea of multi-carrier schemes is to divide a single data stream into different subcarriers. In the context of OFDM, these subcarriers are all arranged with a minimum frequency interval that does not harm the orthogonality between them. Hence, the available bandwidth can be used with high spectral efficiency.

As shown in (WEINSTEIN; EBERT, 1971), the modulation and demodulation in OFDM systems can be implemented as an N-point Inverse Discrete Fourier Transform (IDFT) and Discrete Fourier Transform (DFT), respectively. A modulated OFDM signal using the IDFT can be expressed as

$$x_n = \frac{1}{N} \sum_{k=0}^{N-1} X_k e^{j\frac{2\pi kn}{N}}. \tag{2.1}$$

The IDFT transforms the frequency-domain sequence $\{X_k, \ k = 1, ..., N\}$ into a time-domain sequence $\{x_n, \ n = 1, ..., N\}$. For the demodulation, using the DFT, the signal x_n is converted back from a time-domain sequence into a frequency-domain sequence by

$$X_k = \sum_{k=0}^{N-1} x_n e^{-j\frac{2\pi kn}{N}}. \tag{2.2}$$

As a multi-carrier technique, OFDM can surpass some limitations of single-carrier schemes on wireless channels. For instance, single-carrier systems reduce the transmitted symbol duration in order to achieve a high data rate. Thus, they suffer from a more severe Inter-Symbol Interference (ISI) due to the dispersive fading of wireless channels. On the other hand, OFDM employs the Cyclic Prefix (CP) to tackle ISI.

The CP is formed by a repetition of the last N_{cp} subcarriers usually appended at the beginning of the OFDM symbol (GOLDSMITH, 2005). In (IEEE, 2012), the CP adopts 1/4 of the number of subcarriers within an OFDM symbol. Even though it incurs in power, bandwidth and data rate penalties, under the condition that the CP length is at least equal to the channel length, the linear convolution of the transmitted signal with the discrete-time channel is converted into a circular convolution. As a result, the effects of the ISI are completely removed (BAHAI *et al.*, 2004), which is exemplified in Fig. 1. It depicts both cases, transmission with and without CP, highlighting the existence or absence of interference from the previous OFDM symbol.
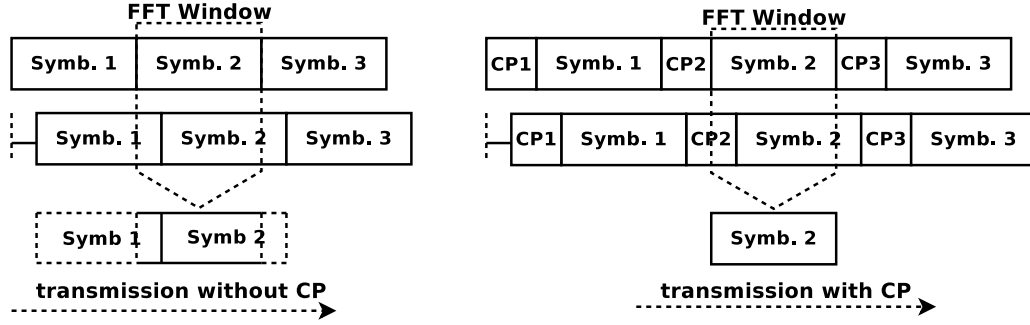
Figure 1 – OFDM Cyclic Prefix

Despite its advantages, OFDM has some disadvantages as well. One example is that with large number of subcarriers OFDM will usually have large Peak-to-Average Power Ratio (PAPR). It happens when the subcarriers within an OFDM symbol are added up coherently (MARCHETTI *et al.*, 2009). Due to multi-carrier modulation, some instantaneous output power might be higher than the system mean power, which requires power amplifiers that are linear over a large range of input amplitudes. These amplifiers are expensive and have low efficiency. Moreover, if the peak power is out of the linear power amplifier range, it might cause non-linear distortion to the system, resulting in severe performance degradation (SENGAR, 2012).

2.1.1   Wireless Channel Model for OFDM

To better understand an OFDM system advantages and disadvantages, it is important to understand the basic characteristics of wireless channels. The transmitted signal is affected by the channel as it goes through the path from the transmitter to the receiver, depending on the distance between the two antennas (path loss), the path taken by the signal (shadowing), and the environment - buildings and other objects - around the path (multipath fading) (JAIN, 2007).

These three phenomena are grouped into large-scale or small-scale propagation effects. Path loss and shadowing are referred as large-scale since they cause signal variations over large distances, while multipath fading is classified as small-scale attenuation since the variations caused by it occurs over very short distances (GOLDSMITH, 2005). Fig. 2 shows the effects of each one of the phenomena as the function of distance and received power over transmitted power. This work focuses only on the small-scale propagation effects.

The multipath fading is related to the signal reflections caused by the objects located around the path of the wireless signal. These reflection might reach the receiver with different amplitudes and phases, which may combine coherently or incoherently, thus increasing or decreasing the received power. If a single pulse is transmitted over a multipath channel there will be multiple copies at the receiver at different times, since
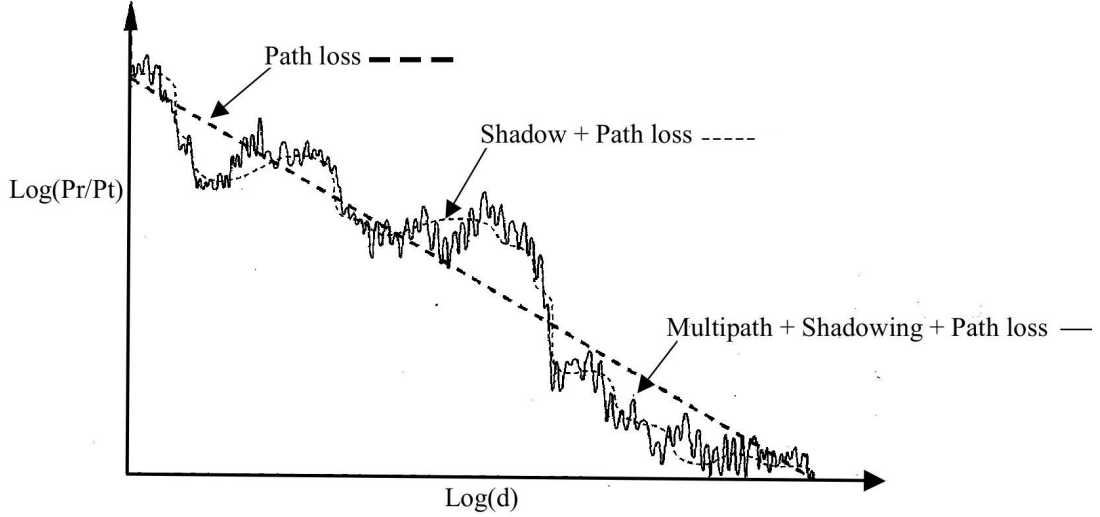
Figure 2 – Path loss, shadowing, and multipath Fading (GOLDSMITH, 2005)

different paths have different lengths. Thus, the channel impulse response described as a discrete number of impulses as follows

$$h(t, \tau) = \sum_{i=1}^{N} \alpha_i(t) e^{-j\theta_i(t)} \delta(\tau - \tau_i(t)), \tag{2.3}$$

where N stands for the number of the channel coefficients, and $\alpha_i(t)$, $\theta_i(t)$ and $\tau_i(t)$ stand for the amplitude, phase and delay spread of the ith multipath component, respectively.

Even though this is just one of several possible channel fading models, a multipath fading channel can be described as a Rayleigh fading if the multiple reflective paths are numerous and there is no dominant signal (e.g., direct line of sight signal) component (SKLAR, 1997). The contribution of each path in the multipath channel can be modeled as a circular symmetric complex random variable, and if the number of paths is large enough, the channel impulse response can reasonably be modeled as a zero-mean independent and identically distributed (iid) Gaussian random variable in the form $h_I + jh_Q$ (TSE; VISWANATH, 2005).

For a variance of σ^2 for both in-phase and quadrature components, the signal envelope, $|h| = \sqrt{h_I^2 + h_Q^2}$, is statistically described by the Rayleigh probability density function (PDF)

$$p_{|h|}(x) = \frac{x}{\sigma^2} e^{-\frac{x^2}{2\sigma^2}}, x \geq 0. \tag{2.4}$$

For $|h|^2$, the received signal power is exponentially distributed with mean $2\sigma^2$ as in

$$p_{|h|^2}(x) = \frac{1}{2\sigma^2} e^{-\frac{x}{2\sigma^2}}, x \geq 0. \tag{2.5}$$

Also, as h_I and h_Q are i.i.d., the phase θ is uniformly distributed and independent of $|h|$. So, h has a Rayleigh-distributed amplitude and uniform phase, and the two are mutually independent (GOLDSMITH, 2005).

Apart from the multi-path fading models, this fading can be separated into two types due to the time dispersive nature of the channel - flat and frequency selective fading (MITRA, 2009). These types of fading depend on the relation between signal and channel parameters - bandwidth, delay and symbol period -, characterizing the channel according to its coherence bandwidth (B_c) and time delay spread (σ_τ).

The B_c is the frequency bandwidth for which the channel characteristics remain similar, i.e., the channel is considered to pass all the frequency components with almost equal gain and linear phase. The B_c is inversely related to the channel time delay spread (σ_τ), which is the time interval between the arrival of the first received signal component and the last received signal component of the same transmitted single pulse. When the channel B_c is greater than the signal bandwidth (B_s), hence, σ_τ is smaller than the duration of the transmitted symbol (T_s), the channel is considered flat fading. On the other hand, for a frequency selective fading, $B_s > B_c$ and $T_s < \sigma_\tau$. Both cases, flat and frequency selective fading, are depicted in Fig. 3.
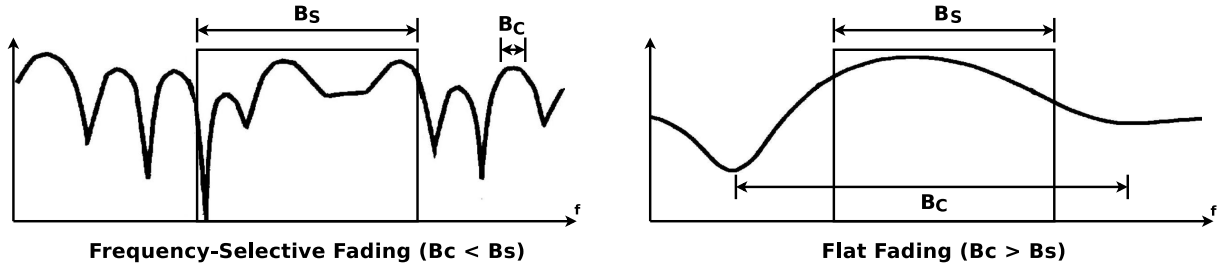
Figure 3 – Channel coherence bandwidth B_c and signal bandwidth B_s (SKLAR, 1997)

Assuming that a signal with a bandwidth, $B_s = 1/T_s$, is transmitted by an OFDM system with N_{sc} subcarriers, then the subcarrier spacing is given by $B_{sc} = B_s/N_{sc}$, and, consequently, the symbol period for each subcarrier is $T_{sc} = N_{sc}T_s$. Thus, N_{sc} can be chosen in a way that $B_{sc} < B_c$. Regardless of this relation between B_{sc} and B_c, if the channel presents frequency selective fading, some subcarriers can undergo these deep fades and the signal power of such subchannels could be strongly attenuated, decreasing their Signal-to-Noise Ratio (SNR).

Several methods have been proposed in order to compensate this effect, such as channel coding and diversity. The idea is normally to transmit redundant information on the symbols, such as replicas. As a result, a deep fade must affect both the symbol and the redundant information to be detrimental, which is less likely. This topic is more detailed in the following sections, focusing on diversity combining techniques.

2.1.2   Peak-to-Average Power Ratio (PAPR)

In OFDM systems the transmitted symbol is formed by the superposition of modulated symbols through the IDFT. For some of the symbol combinations, this combination

may produce signals with high envelope peaks in the constructive superposition case, or signals completely faded in the destructive case. This large dynamic range causes a significant variation in the instantaneous signal power (peak power) when compared to the average (mean) signal power (KOZHAKHMETOV, 2008). A measure of this variation is the peak to average power ratio (PAPR), which is defined as

$$PAPR[x_n] = \frac{max[|x_n|^2]}{E[|x_n|^2]}, \tag{2.6}$$

where $max[|x_n|^2]$ is the maximum instantaneous (peak) power, $E[|x_n|^2]$ is the average power and $E[.]$ denotes the expected value.

The PAPR analysis are based on a single modulation interval, i.e., an OFDM symbol, and since the CP is a repetition of the last N_{cp} samples of the OFDM symbol, it does not affect PAPR (LI; STUBER, 2006). The MR-OFDM symbol is formed by complex symbols modulated with conventional modulation schemes (PSK and QAM constellations) added together. Assuming that these modulations all have the same average power for all mappings, i.e., $E[|x_n|^2] = 1$ (IEEE, 2012; LI; STUBER, 2006), (2.6) is rewritten as

$$PAPR[x_n] = \frac{max[|\sum_{k=0}^{N-1} X_k e^{j\frac{2\pi kn}{N}}|^2]}{E[|\sum_{k=0}^{N-1} X_k e^{j\frac{2\pi kn}{N}}|^2]} \leq \frac{N^2 max[|X_k|]^2}{N} \leq N max[|X_k|]^2. \tag{2.7}$$

Based on (2.7), it is possible to conclude that the PAPR increases linearly with the number of subcarriers, N.

To compare the PAPR reduction obtained by different strategies, we normally use the Complementary Cumulative Distribution Function (CCDF) of the PAPR. It shows the probability that the OFDM signal with N subcarriers (or the probability of all subcarriers) will have PAPR at or above a certain level z. As defined in Section 2.1.1, due the central limit theorem, the envelope of the OFDM signal follows a Rayleigh distribution. So, for a system with N subcarriers, the variable $x_{max}^2 = max[|x_n|^2]$ is a random variable with Cumulative Distribution Function (CDF) equals to $F_{x_{max}^2}(z) = (1 - e^{-z/N})^N$. The CCDF can be obtained through this CDF as

$$\text{Prob}(PAPR > z) = \text{Prob}(x_{max}^2 > zN) = 1 - F_{x_{max}^2}(zN) = 1 - (1 - e^{-z})^N. \tag{2.8}$$

Large PAPR requires that system devices, such as power amplifier, Analog to Digital Converter (ADC) and Digital to Analog Converter (DAC), must have large linear dynamic ranges (SENGAR, 2012). Power amplifiers are linear only over a finite range of input amplitudes. Thus, in order to prevent saturation and clipping of the OFDM signal peaks, the amplifiers must sacrifice their power efficiency, which causes high power consumption. (LI; STUBER, 2006). Otherwise, if the peaks exceed the linear range of the amplifier, they go into saturation, resulting in Inter Carrier Interference (ICI) due to loss of orthogonality and other problems caused by the device nonlinearity. Furthermore,

the PAPR may affect the quantization resolution of DAC and ADC. High peaks consume a lot of this resolution, degrading the SNR of the system through the increase of the quantification noise (MOLISCH, 2012).

Several methods have been proposed to mitigate the high peaks in the OFDM signal, enabling the use of OFDM in wireless networks despite their large PAPR. The approaches for these methods are: the proposal of new amplifiers concepts for increasing the transmitter power efficiency even with large PAPR (DINIS *et al.*, 1996), the optimization of existing amplifiers (JONG *et al.*, 1999), and the reduction of the transmitted signals PAPR. The last approach comprises clipping and filtering, constrained coding, and selective mapping (KOZHAKHMETOV, 2008).

The technique employed by the MR-OFDM frequency spreading for PAPR reduction is similar to the Selective Mapping (SM) and Partial Transmit Sequence (PTS). In all the mentioned techniques - frequency spreading, SM and PTS - the symbols within an OFDM symbol suffer different phase rotations following different sequences. In SM and frequency spreading the symbol weighting is performed in frequency domain, and in PTS, on the other hand, the weighting is performed in time domain (VARAHRAM; ALI, 2011; MISHRA, 2012). The MR-OFDM frequency spreading is more detailed in following sections.

2.2 Diversity Combining

Current and emerging wireless communications systems employ some form of diversity in order to mitigate the effect of multipath fading and/or shadowing from buildings and objects, enhancing transmission reliability (SALEHI; PROAKIS, 2007). Diversity basic concept is transmitting and/or receiving a signal redundantly over independent fading channels in such a way that multiple independent and uncorrelated or slightly correlated versions of this signal are obtained at the receiver. The probability of occurrence of deep fades in all signal copies is low, and at least one signal replica should have reasonable power at the receiver (TU; DUTKIEWICZ, 2009). Then, these multiple replicas are combined in a way that the fading of the resultant signal is reduced, increasing the overall SNR.

Diversity can be introduced in transmission or reception, and in three domains: time, frequency and space. In time diversity, the symbols are transmitted in different time slots, being separated by the channel coherence time. Frequency diversity is achieved by transmitting the same signal at different carrier frequencies (multi-carrier systems), where the carriers are separated by the coherence bandwidth of the channel. Finally, space diversity employs multiple receive antennas. Regardless of the manner, the redundant signals are separated - time slots, carrier frequencies, or antennas, it is performed in such

a way that the fading amplitudes corresponding to each signal replica are approximately independent (GOLDSMITH, 2005).

Usually in literature systems are described employing spatial diversity. With antenna array, the independent fading paths are realized without an increase of additional system resources such as transmit signal power or bandwidth. However, this method is not suitable for portable devices due to the space requirements and hardware complexity (DIETZE, 2001). So, depending on the domain where the diversity is introduced, different trade-off analysis among performance, power consumption, bandwidth efficiency, and implementation complexity have to be performed.

2.2.1 Diversity Combining Techniques

Each independent and uncorrelated replica of the signal is referred to as a diversity branch. The diversity branches can be combined in several ways which vary in complexity and overall performance (GOLDSMITH, 2005). The different types of combining employed on the replicas are known as diversity combining techniques. The diversity combining techniques can be grouped according to their operation principles: combination by selection, combination by addition and hybrid methods. In combination by selection, only the diversity branch considered as the most suitable branch is selected based on some criterion. In combination by addition, the diversity branches are weighted and linearly combined. Finally, in hybrid methods, a specific number of diversity branches are selected based on some criterion and combined according to a conventional diversity combining technique (POLYDOROU, 2004).

In this document, the diversity combining model assumes that the fading follows the Rayleigh distribution, as expressed in (2.4), and is independent to the other branch. In its turn, the noise for each diversity branch is described as a Gaussian distribution

$$p(n) = \frac{1}{\sigma\sqrt{2\pi}} e^{-\frac{(n-\mu)^2}{2\sigma^2}}, \tag{2.9}$$

where mean $\mu = 0$ and variance $\sigma^2 = N_0/2$ (MITIĆ *et al.*, 2015). Finally, as detailed in Section 2.1.1, the received signal power is exponentially distributed, thus, the instantaneous value of the SNR per bit in each diversity branch, γ_m, is expressed as a function of energy per bit E_b and spectral density of noise power N_0 as

$$p(\gamma_m) = \frac{1}{E_b/N_0} e^{-\frac{\gamma}{E_b/N_0}}. \tag{2.10}$$

Unlike the techniques that employ combination by selection, combining techniques can be linear and their outputs can be obtained as a function of a weighted sum of the signals from the independent fading paths, where different paths can be multiplied by different weights. At the combiner output, the resultant signal has a SNR represented by

γ_Σ, with a distribution that depends on the number of diversity paths, fading distribution on each path and diversity combining technique applied to the system (GOLDSMITH, 2005). Several figures of merit are used to accurately analyze the performance of diversity receiver in fading, in this work the BER is adopted as figure of merit. The system BER can be calculated by

$$BER = P_e = \int_0^\infty P_b(\gamma) p_{\gamma_\Sigma}(\gamma) \, \mathrm{d}\gamma, \tag{2.11}$$

where $p_{\gamma_\Sigma}(\gamma)$ is the PDF of the combined SNR for a determined diversity combining technique and $P_b(\gamma)$ is the probability of bit error for a determined modulation and fading distribution. In the following sections, it is assumed BPSK modulation, so, $P_b(\gamma)$ is

$$P_b(\gamma) = \frac{1}{2}\mathrm{erfc}\left(\sqrt{\gamma}\right). \tag{2.12}$$

This work focuses on the Selection Combining, Maximal Ratio Combining, and Selection Maximal Ratio Combining techniques, which encompass the theoretical worst and best performance cases in diversity techniques. Another technique usually described in this context is the Equal Gain Combining (STÜBER, 2000), but it is not portrayed in this document.

2.2.1.1 Selection Combining (SC)

Selection Combining (SC) is considered the simplest diversity combining technique and the one with the worst performance. SC general form is based on monitoring all the diversity branches and selecting the one with the highest SNR (MITIĆ *et al.*, 2015), as shown in Fig. 4. The main disadvantage of SC is that the signals must be monitored at a faster rate than the occurrence of fading (CHANDRASEKARAN, 2005). Measuring SNR in a short time is difficult, in fact, the adopted selection criterion in practice is the highest signal level, i.e., $S + N$.
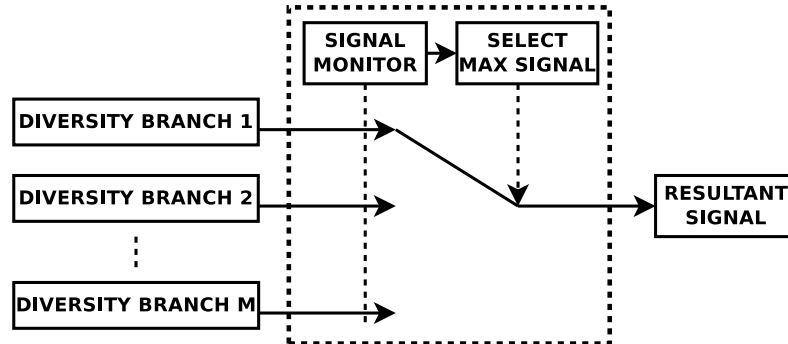
Figure 4 – Selection Combining

Instead of a combining method, SC can be considered as a selection procedure. The output from the combiner applying selection combining scheme provides a SNR equals to $\gamma_\Sigma = max\{\gamma_1, ..., \gamma_M\}$, where M stands for the maximum number of available diversity

branches. In this method, since only one diversity branch is used, there is no need to sum the branches in a co-phased way.

A closed-form expression for the BER using SC is calculated using the PDF of γ_Σ and the bit error probability, P_b, as in (2.11). This PDF is expressed as

$$p_{\gamma_\Sigma}(\gamma) = \frac{M}{E_b/N_0} e^{-\frac{\gamma}{E_b/N_0}} (1 - e^{-\frac{\gamma}{E_b/N_0}})^{M-1}. \tag{2.13}$$

Assuming that $E_b/N_0 = \gamma$, for a Rayleigh fading distribution and BPSK modulation, the BER is calculated integrating the conditional error rate over γ (GOLDSMITH, 2005) as

$$P_e = \int_0^\infty \frac{1}{2}\text{erfc}(\sqrt{\gamma}) \frac{M}{E_b/N_0} e^{-\frac{\gamma}{E_b/N_0}} (1 - e^{-\frac{\gamma}{E_b/N_0}})^{M-1} \, d\gamma =$$

$$= \frac{1}{2} \sum_{m=0}^{M} (-1)^m \binom{M}{m} \left(1 + \frac{m}{E_b/N_0}\right)^{-1/2}. \tag{2.14}$$

For other fading distributions and modulations, P_e is evaluated numerically or by approximation. Fig. 5 depicts the SC performance according to BER, for different number of diversity branches, M.
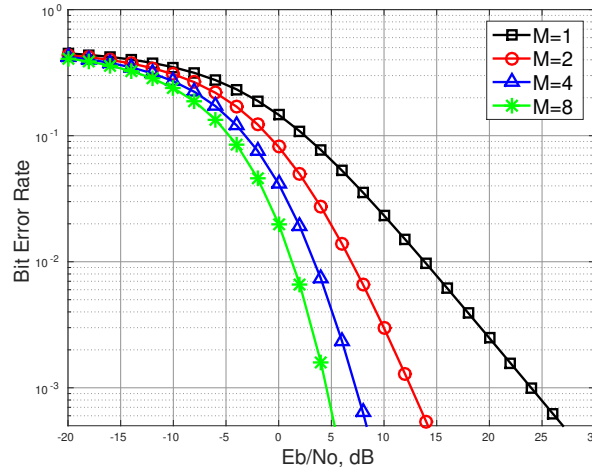
Figure 5 – BER for SC with BPSK modulation in Rayleigh channel

2.2.1.2 Maximal Ratio Combining (MRC)

Maximal Ratio Combining (MRC) is the optimal technique of signal linear combination, providing the theoretical maximum gain that can be obtained with the use of diversity (YACOUB, 2001). On the other hand, it is considered as the most complex diversity combining technique. Unlike the techniques based on combination by selection where the output of the combiner equals the signal on one of the branches, in MRC the signals from the diversity branches are weighted and then combined in a co-phased way (MITIĆ *et al.*, 2015). It is depicted in Fig. 6.

To optimize the MRC resultant signal, the weights are chosen in a way that the branches considered stronger are further amplified, while the ones considered weaker are
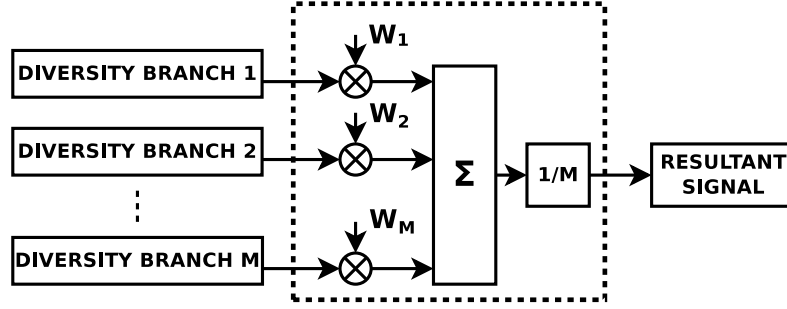
Figure 6 – Maximal Ratio Combining

attenuated. By Cauchy-Schwarz inequality (LEE, 1982), the SNR at the MRC combiner output achieves its maximum when the weights are proportional to the branches channel frequency response. Assuming the total noise power equals N_0 and $W_{k,m} = 1/H_{k,m}$, it can be seen that the combined SNR is

$$\gamma_\Sigma = \sum_{m=1}^{M} \frac{|H_{k,m}W_{k,m}|^2 E_b}{N_0} = \sum_{m=1}^{M} \frac{|H_{k,m}H_{k,m}^*|^2 E_b}{|H_{k,m}H_{k,m}^*|N_0} = \sum_{m=1}^{M} \frac{|H_{k,m}|^2 E_b}{N_0} = \sum_{m=1}^{M} \gamma_m. \quad (2.15)$$

Thus, γ_Σ is the sum of the SNR on each branch, increasing linearly with the number of diversity branches M (GOLDSMITH, 2005).

The PDF of γ_Σ is obtained through the manipulation of chi-square random variables. Since $|H_{k,m}|$ represents the independent fading with Rayleigh distribution on each branch, then $|H_{k,m}|^2$ is a chi-square random variable with two degrees of freedom. As γ_Σ is a sum of M of these variables, its PDF is a chi-square random variable with $2M$ degrees of freedom (GOLDSMITH, 2005). The closed equation for γ_Σ PDF is

$$p_{\gamma_\Sigma}(\gamma) = \frac{\gamma^{M-1}e^{-\frac{\gamma}{Eb/N_0}}}{Eb/N_0(M-1)!}, \ \gamma \geq 0. \quad (2.16)$$

From (**??**), the system error rate can be calculated using the bit error probability assuming BPSK modulation and Rayleigh fading distribution, and integrating the conditional error rate over γ (SIMON; ALOUINI, 2005). It leads to

$$P_e = \int_0^\infty \frac{1}{2}|erfc(\sqrt{\gamma})\frac{\gamma^{M-1}e^{-\frac{\gamma}{E_b/N_0}}}{E_b/N_0(M-1)!} \ \mathrm{d}\gamma =$$
$$= \left(\frac{1-\mu}{2}\right)^M \frac{1}{(M-1)!} \sum_{m=0}^{M-1} \frac{(M-1+m)!}{m!}\left(\frac{1+\mu}{2}\right)^m, \quad (2.17)$$

where

$$\mu = \sqrt{\frac{E_b/N_0}{1+E_b/N_0}}. \quad (2.18)$$

Fig. 7 depicts the BER performance of the MRC technique according to the number of diversity branches.
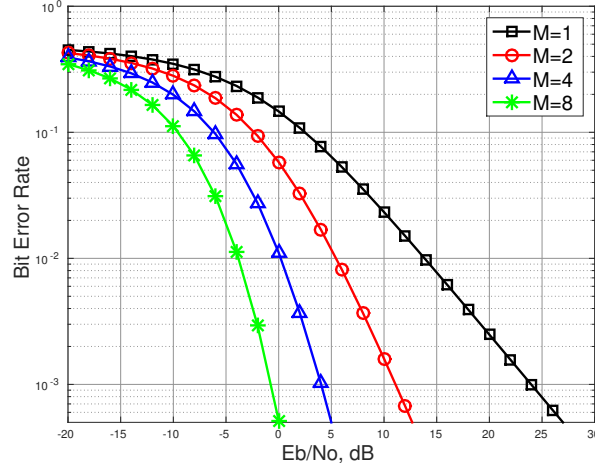
Figure 7 – BER for MRC with BPSK modulation in Rayliegh channel

2.2.1.3 Selection Maximal Ratio Combining (SMRC)

MRC provides the best performance with the highest complexity since it depends on the knowledge of channel (fade amplitude and phase) on each diversity branch. SC, on the other hand, provides the worst performance with the least complexity since it selects only one branch (SIMON; ALOUINI, 2005). The performance gap between these two methods motivates studies of the Selection Maximal Ratio Combining (SMRC) hybrid diversity technique that provides an intermediate performance with an intermediate complexity.

The SMRC selects, out of M total branches, the L strongest signals according to the SC criterion; then they are weighted optimally, co-phased and summed, according to the MRC. The SMRC is depicted in Fig. 8. For the SMRC to be worthwhile, the complexity reduction obtained weighting and combining L branches instead of M branches must makes up for the performance loss.
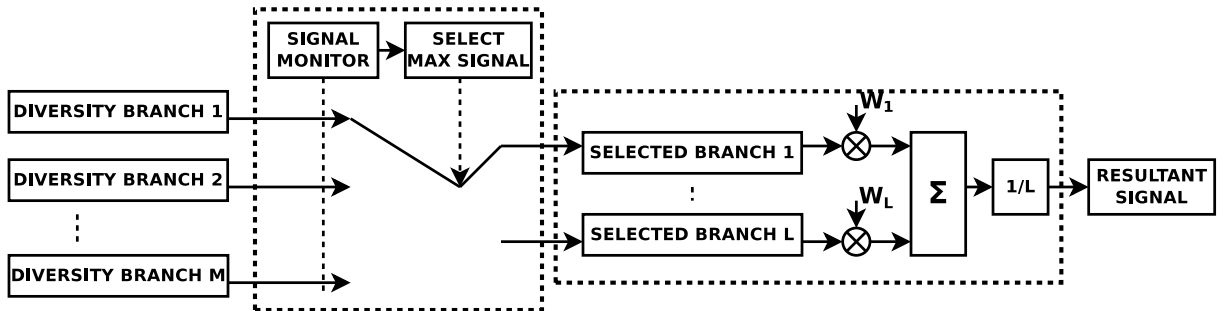
Figure 8 – Selection Maximal Ratio Combining

For the SMRC, the available expressions of the figures of merit only exist for particular solutions in which a very limited number of branches and fading environment are tackled. The system performance is evaluated by the average probability of error and to calculate it, the PDF of γ_Σ is necessary. At the SMRC-combiner output, it can be

calculated differentiating the CDF of γ_Σ with respect to γ (SIMON; ALOUINI, 2005). The methods yields to

$$p_{\gamma_\Sigma}(\gamma) = \binom{M}{L}\left[\frac{\gamma^{L-1}e^{-\frac{\gamma}{E_b/N_0}}}{(E_b/N_0)^L(L-1)!} + \frac{1}{E_b/N_0}\sum_{m=1}^{M-L}(-1)^{L+m-1}\binom{M-L}{m}\left(\frac{L}{m}\right)^{L-1}\right.$$
$$\left. e^{-\frac{\gamma}{E_b/N_0}}\left(e^{-\frac{m\gamma}{LE_b/N_0}} - \sum_{l=0}^{L-2}\frac{1}{m!}\left(\frac{-m\gamma}{LE_b/N_0}\right)^l\right)\right]. \quad (2.19)$$

As expected, the PDF at the SMRC-combiner output can be reduced to the well-known PDF of the SNR at the MRC-combiner output when $L = M$, and to the SNR at the SC-combiner output when $L = 1$. Both PDFs are the upper-bound and lower-bound of the SNR respectively.

Based on (2.11), (2.12) and (2.19), for BPSK modulation with Rayleigh fading channel, a closed-form for the total BER of the system employing SMRC is presented as

$$P_e = \binom{M}{L}\sum_{m=0}^{M-L}\frac{(-1)^m\binom{M-L}{m}}{1+m/L}I_{L-1}\left(\frac{\pi}{2}; E_b/N_0, \frac{E_b/N_0}{1+m/L}\right), \quad (2.20)$$

where $I_n(\theta; c1, c2)$ is an integral defined as a closed form in (SIMON; ALOUINI, 2005). Also, in (ENG *et al.*, 1996), the same numerical results for $L = 2$ and $L = 3$ are provided.

2.3   IEEE 802.15.g Standard

The IEEE 802.15.4g is an amendment of the IEEE 802.15.4 standard approved by the IEEE on March 2012, focusing on Smart Utility Network (SUN) applications in the context of Low-Rate Wireless Personal Area Network (LR-WPAN). The IEEE 802.15.4 is defined by the IEEE 802 standard committee and its IEEE 802.15 working group, as pictured in Fig. 9. IEEE 802 is in charge of standardization on technical specification for Local Area Networks (LAN), Metropolitan Area Networks (MAN), and Personal Area Networks (PAN); while 802.15 is responsible for Wireless PAN (WPAN) technical standards (KATO, 2015).
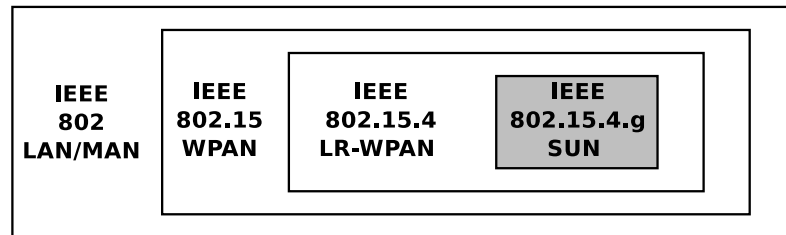
Figure 9 – IEEE 802.15.4g in the context of IEEE standards

SUN is an advanced wireless communication network that allows interoperability among smart grid devices such as smart meters. It enables multiple applications to operate

over shared network resources, providing control and monitoring of utilities systems as gas metering, automated demand, and distribution, etc.

Frequently, SUNs are required to cover geographically widespread areas containing a large number of stationary endpoints with minimal infrastructure. Hence, SUN devices are designed to operate in very large-scale, low-power wireless applications and often require the use of the maximum power available under applicable regulations, in order to provide long-range, point-to-point connections (IEEE, 2012).

Nowadays, the global demand for an advanced, intelligent, and cost-effective utility management system is a top priority, mobilizing efforts from industry, academia and regulators. In 2011, at the time that the IEEE 802.15.4g standard was being developed, the Wireless Smart Utility Network (Wi-SUN) Alliance was established as a global organization focused on IEEE802.15.4/4g standardization work. Due to the characteristics of IEEE802.15.4g, the Wi-SUN Alliance is still active, seeking to establish and promote technology standards in order to encourage new Smart Ubiquitous Network applications, such as Smart City and Internet of Things (IoT) markets. The main activities of the Wi-SUN alliance are

- plan technical standards that coordinate various wireless systems and standardize power levels, data rates, modulations, and frequency bands, among other parameters;

- establish and manage the certification process based on the same technical standards;

- plan and hold interoperability testing events;

- run promotion activities.

To date, Wi-SUN Alliance members include many global and national organizations from Australia, Brazil, Canada, Europe, India, Japan, Korea, and the United States (WI-SUN, 2017).

The aim of the IEEE 802.15.4g is to offer a standard that describes a PHY and Medium Access Layer (MAC) in order to embrace global and regional specifications. The amendment defines several frequency bands, bandwidths and data rates. The frequency band ranges from 169 MHz to 1 GHz, also allowing for operation at 2.4 GHz for unlicensed usage, while the bandwidth ranges from tens of kHz to several MHz, supporting data rates from few kbps to 1 Mbps (IEEE, 2012).

As SUN communication range, robustness, and coexistence characteristics have not been met by other existing IEEE 802.15 standards, three PHYs are proposed to encompass these different frequencies and channels in different regions. The PHYs are Multi-Rate

and Multi-Regional Frequency Shift Keying (MR-FSK), Multi-Rate and Multi-Regional Offset Quadrature Phase-Shift Keying (MR-O-QPSK), and MR-OFDM. A SUN device is an entity containing an implementation of the medium access control (MAC) sublayer specified in (IEEE, 2012) and the MR-FSK PHY. Optionally, it can contain the MR-OFDM or the MR-O-QPSK PHY.

The MR-FSK PHY achieves good transmit power efficiency with low implementation complexity due to the constant envelope of the transmit signal; however, this PHY is weak against interference due to its low bandwidth efficiency. It supports various frequency bands in various regions, including the U.S., China, Japan, and Korea. The MR-O-QPSK PHY shares common characteristics with the O-QPSK PHY defined by the IEEE 802.15.4 standard. Its performance can be improved in the presence of multipath fading using coding; besides, it also supports spread spectrum techniques. Finally, the MR-OFDM provides higher data rates at higher spectral efficiency, as well as reliable data communication, even in a poor wireless environment with multipath fading and shadowing. On the other hand, it has a more complex structure, which results in a more costly implementation (IEEE, 2012). This work provides performance improvements for a receiver based on the MR-OFDM PHY, focusing on the standard compliance and the PHY hardware complexity.

2.3.1 MR-OFDM Physical Layer

As the name suggests, the MR-OFDM PHY is based on OFDM, widely used in modern digital communication systems, such as Wi-fi (IEEE 802.11 a/g/n) and WiMAX. It defines four operation modes, each characterized by the number of subcarriers within an OFDM symbol (from 128 tones for option 1 down to 16 tones for option 4). From the 14 frequency bands covered in (IEEE, 2012), the MR-OFDM PHY is adopted in 470 MHz, 780 MHz, 863 MHz, 902 MHz, 917 MHz, 920 MHz, 950 MHz, and 2450 MHz. However, not all of these frequency bands support all operation modes.

The main parameters for the MR-OFDM PHY operation modes are summarized in Table 1. As defined in (IEEE, 2012), the subcarrier spacing is constant and equal to $10416,66\overline{6}$ Hz, which, multiplied by the number of active tones plus the DC tone, results in the PHY nominal bandwidth (from 1.094 MHz down to 156 kHz). The sampling rate corresponds to a base symbol duration of 96 μs and to the respective number of subcarriers, ranging from $1.333\overline{3}$ MSamples/s down to $0.166\overline{6}$ MSamples/s.

The PHY supports data rates ranging from 50 kb/s to 800 kb/s depending on the adopted modulation scheme (BPSK, QPSK and 16-QAM), code-rate (1/2 and 3/4) and spreading factor (no frequency spreading, 2× and 4×). The combination of these parameters is defined as Modulation and Coding Scheme (MCS) and all the possible MCS configurations are shown in Table 2.

Table 1 – OFDM parameters of the MR-OFDM mode

Parameters	Option 1	Option 2	Option 3	Option 4
Nominal Bandwidth (KHz)	1094	552	281	156
Channel spacing (KHz)	1200	800	400	200
Tone Spacing (KHz)	10.416$\overline{6}$	10.416$\overline{6}$	10.416$\overline{6}$	10.416$\overline{6}$
FFT Size	128	64	32	16
Active Tones	104	52	26	14
Pilot/Data/DC Tones	8/96/1	4/48/1	2/24/1	2/12/1
Symbol Duration (μs)	120	120	120	120
Base Symbol Duration (μs)	96	96	96	96
CP Duration (μs)	24	24	24	24
Sampling Rate (MSamples/s)	1.333$\overline{3}$	0.666$\overline{6}$	0.333$\overline{3}$	0.166$\overline{6}$

Table 2 – MR-OFDM data-rate for each Modulation and Coding Scheme (MCS)

Config.	Modulation	Code Rate	Spread Factor	Data Rate (kb/s)			
				Option 1	Option 2	Option 3	Option 4
MCS0	BPSK	1/2	4×	100	50	-	-
MCS1	BPSK	1/2	2×	200	100	50	-
MCS2	QPSK	1/2	2×	400	200	100	50
MCS3	QPSK	1/2	–	800	400	200	100
MCS4	QPSK	3/4	–	-	600	300	150
MCS5	16-QAM	1/2	–	-	800	400	200
MCS6	16-QAM	3/4	–	-	-	600	300

The MCS adopted in transmission is communicated to the receiver through the Rate field of the PHY Header (PHR), which composes the MR-OFDM PHY Protocol Data Unit (PPDU). This PPDU is formatted as illustrated in Fig. 10, being composed of Synchronization Header (SHR), PHR, Packet Service Data Unit (PSDU), Tail and Pad. The SHR, composed by the Short Training Field (STF) and the Long Training Field (LTF), is used in the receiver for frame synchronization, phase and frequency correction, and frequency channel estimation. The PHR, besides the MCS, carries other frame configurations, which turn this field detection into a crucial step in the reception. The PSDU is the PHY payload, i.e. the data to be transmitted along with other tones. Together with the TAIL and PAD fields, it composes the Data Field of the PPDU (ALVES *et al.*, 2016).

Operating with the MR-OFDM parameters and data rates established therein the standard (IEEE, 2012), the reference modulator depicted in Fig. 11 builds the PPDU, encoding the data received from the MAC layer. The following section will detail the
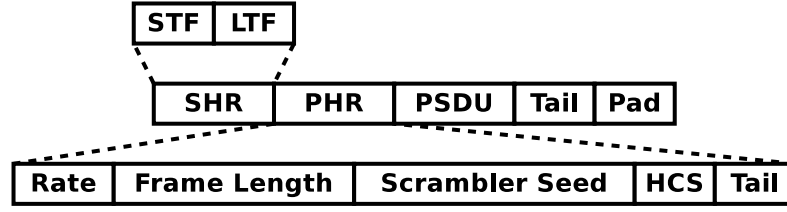
Figure 10 – Format of the MR-OFDM PPDU

highlighted block, Frequency Spreading. The functionality of the other blocks presented in this diagram is not relevant in the scope of this work.
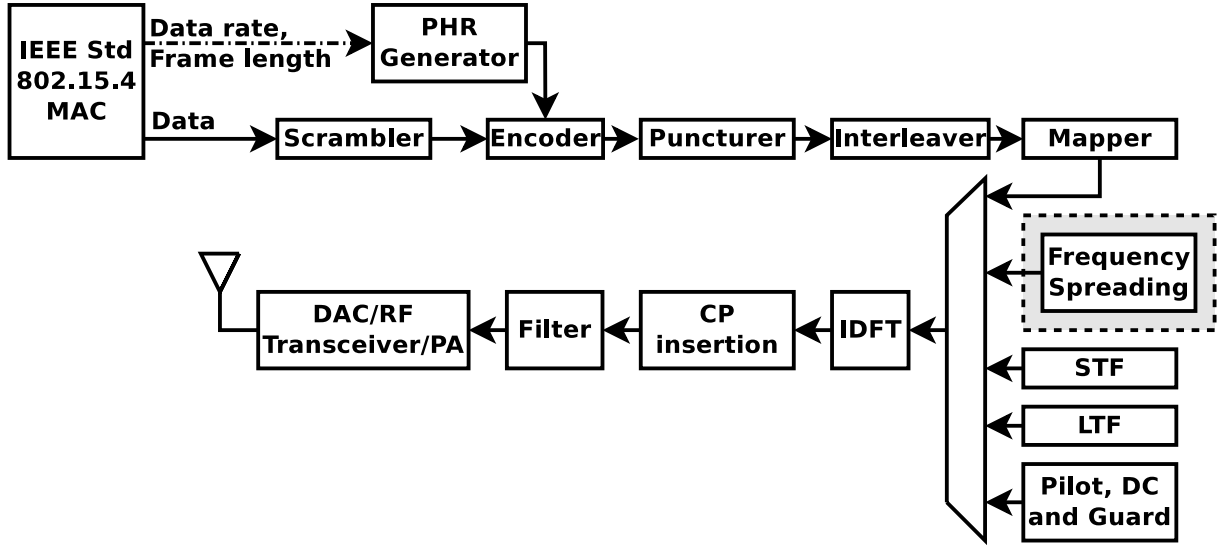
Figure 11 – Reference modulator diagram for MR-OFDM

2.3.1.1 MR-OFDM Frequency Spreading

The MR-OFDM frequency spreading is a method of replicating PSK symbols on different subcarriers. It replicates only PSK symbols because it is employed by the MCS 0, 1 and 2, configurations that do not employ the 16-QAM modulation (Table 2). The standard describes the method according to the number of supported repetitions: 2×, 4× or no repetition.

For all the option cases, the available bandwidth is divided into N_d+1 tones, where N_d stands for the number of data tones in an OFDM symbol. These tones are separated by the subcarrier spacing, B_{sc}. Index 0 corresponds to the central tone, being referred as the DC tone, and it is omitted since it does not carry any information (IEEE, 2012). The remaining N_d tones containing the actual and replicated data are indexed from $-N_d/2$ to -1 and 1 to $N_d/2$, as depicted in Fig. 12.

In this particular use of frequency spreading, phase rotations are applied to each repetition of the data to reduce the PAPR of the OFDM symbol (IEEE, 2012). Depending on the repetition subset and the subcarrier position in the subset, the technique applies a

No Spreading

Original Data	

-Nd/2   -1   1   Nd/2

Frequency Spreading by 2X

Repetition 1	**Original Data**

-Nd/2   -1   1   Nd/2

Frequency Spreading by 4X

Repetition 1	**Repetition 2**	**Original Data**	**Repetition 3**

-Nd/2   -Nd/4+1   -Nd/4   -1   1   Nd/4   Nd/4+1   Nd/2
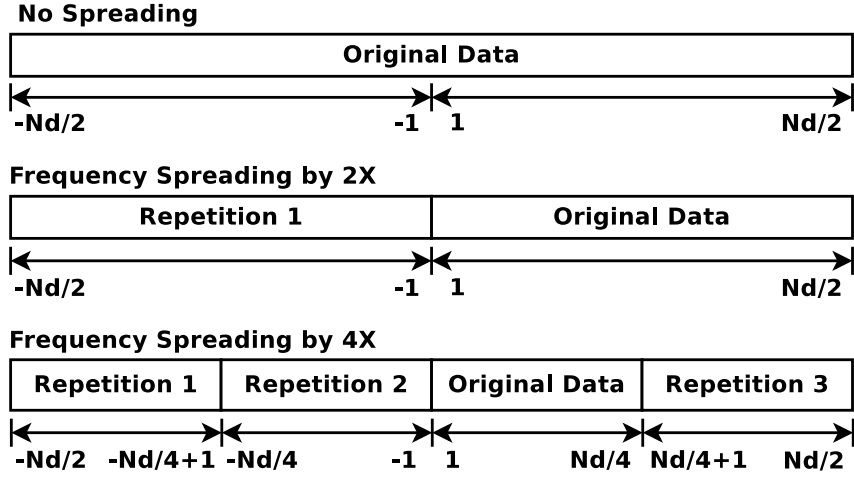
Figure 12 – MR-OFDM Frequency Spreading structure

specific phase rotation belonging to the set $(\pm 1, \pm j)$. These rotations can be represented by $e^{\frac{j2\pi C_{k,m}}{4}}$, where k stands for the subcarrier index and m for the repetition subset index.

For the spreading factor 2x, the original symbols are placed into positive frequencies numbered from 1 to $N_d/2$, and the replicas are placed into negative frequencies from $-N_d/2$ to -1. The rotated replicas are given by

$$D_{(k-\frac{N_d}{2}-1)} = D_k e^{\frac{j2\pi(2k-1)}{4}}, \text{ for } k = 1, ..., N_d/2. \quad (2.21)$$

Adopting the spreading factor 4x, the original symbols are placed into the lower half of the positive frequencies (from 1 to $N_d/4$), while the replicas are placed into the negative frequencies (from $-N_d/2$ to -1) and the upper half of the positive frequencies (from $N_d/4 + 1$ to $N_d/2$). The replicas are given by

$$D_{(k+\frac{N_d}{4})} = D_k e^{\frac{j2\pi(k-1)}{4}},$$
$$D_{(k-\frac{N_d}{2}-1)} = D_k e^{\frac{j2\pi(2k-1)}{4}},$$
$$D_{(k-\frac{N_d}{4}-1)} = D_k e^{\frac{j2\pi(3k-1)}{4}}, \text{ for } k = 1, ..., N_d/4. \quad (2.22)$$

Finally, the MR-OFDM also offers the no spreading option, where the original data are placed into all data carrying tones, as shown in the top for of Fig. 12. For this case, no phase rotation is applied to the original data. Consequently, there is no PAPR reduction. The spreaded data are defined as data tones, and, along with the other tones - DC, pilot and null, constitute an OFDM symbol, X_k, for $k = 1, ..., FFT_{size}$.

Under some channel assumptions, such as frequency selective fading and channel coherence bandwidth, the MR-OFDM frequency spreading introduces frequency diversity to the system. This work proposes a method to revert the spreading applied in the transmission exploiting the mentioned diversity. It is described in the following chapter.

3 Proposed Method for MR-OFDM Frequency Despreading

This work is part of a project that aims at the implementation of an Integrated Circuit (IC) capable of handling the 3 PHYs defined in the IEEE802.15.4g standard. However its main focus is the BER improvement of the MR-OFDM receiver through the reversal of the frequency spreading that is applied in the MR-OFDM transmitter. Fig. 13 shows the block diagram of the MR-OFDM Receiver implemented based on the reference modulator depicted in Fig. 11 and the estimation of channel frequency response. The highlighted block is the one responsible for the frequency despreading and will be detailed in the following section. The functionality of the other blocks presented in the diagram is not in the scope of this work.
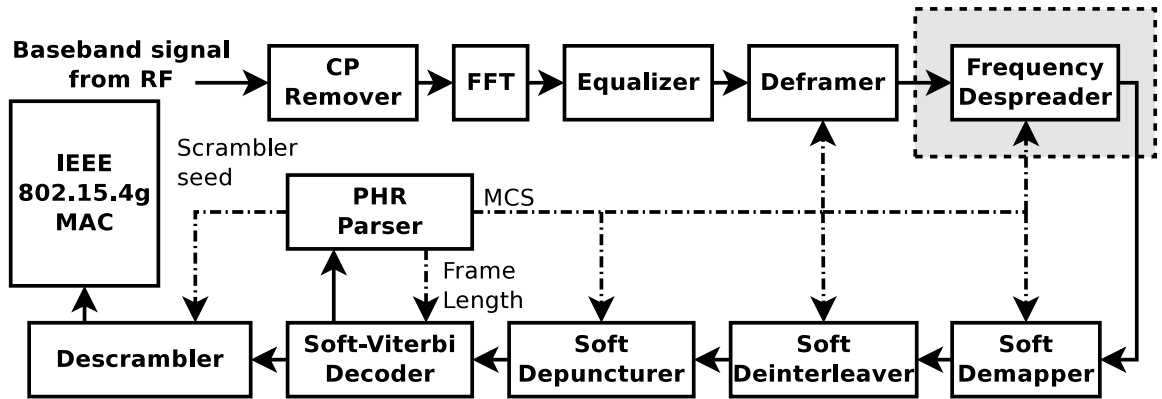
Figure 13 – Diagram for MR-OFDM receiver

As already mentioned in Section 2.1, the subcarriers of the OFDM system may face deep fades due to frequency selectivity. One such scenario is depicted in Fig. 14. In this case, a deep fade occurs at the center of the signal band, decreasing the signal power and, consequently, decreasing the SNR for the subcarriers that occupy the center of the band. Channel coding and diversity are powerful techniques to combat small-scale fading.
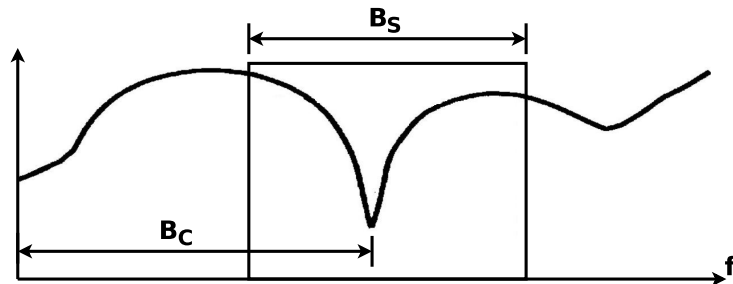
Figure 14 – Null at signal band center ($B_c > B_s$) (SKLAR, 1997)

In the context of frequency spreading, it is assumed that the difference in frequency between a subcarrier transmitting an original modulated symbol and a subcarrier transmitting this symbol replica is larger than the channel coherence bandwidth, B_c. Hence, these two replicas go through uncorrelated paths, so that the spreading technique provides frequency diversity to the system. In MR-OFDM each group of replicas is a diversity branch. Assuming that the OFDM symbol is transmitted along with a Cyclic Prefix larger enough to eliminate Inter-Symbol Interference (ISI), the received signal for the mth branch can be described as

$$R_{k,m} = |H_{k,m}|e^{j\theta_{k,m}}X_k + N_{k,m}. \tag{3.1}$$

X_k represents the transmitted symbol, while $|H_{k,m}|$, θ_k and $N_{k,m}$ are the random channel amplitude, channel phase and the Additive White Gaussian Noise (AWGN) for a specific position k in the same branch (MITIĆ *et al.*, 2015), respectively.

To improve IEEE802.15.4g MR-OFDM performance, a frequency despreading method that exploits this diversity is proposed based on two approaches: diversity combining techniques used in addition to the frequency despreading; and new MCS configurations employing extended spreading factors. In the following section, a straightforward frequency despreading is described. Both approaches are detailed further in this chapter.

3.1 MR-OFDM Frequency Despreding (FD)

In the MR-OFDM receiver, an incoming OFDM symbol, r_n, is first stripped of the CP, and then converted to the frequency domain through the FFT as in (2.2), resulting in R_k symbols, for $k = 1, ..., N$. As per the standard, these symbols are separated into DC, pilot, null and data tones. As described in Section 2.3.1.1, frequency spreading is applied only to data tones, thus, frequency despreading must be performed only on the N_d data tones as well. They are grouped according to the number of repetitions adopted in the MR-OFDM transmitter: no frequency spreading, frequency spreading by $2\times$ and $4\times$.

In Fig. 15, regardless of the number of repetition adopted previously, it is possible to see that all subcarriers related to the same transmitted symbol, for example symbol A, are placed in the same position within the repetition groups. Furthermore, in different data subsets, the subcarriers related to the same transmitted symbol are represented in different ways. For example, the symbol A is also represented as A', A'' and A''', referring to the phase rotation applied on each subcarrier in the transmission.

These rotations are not related to channel phase compensation, but to transmitted signal PAPR reduction, and must be reverted when the subcarriers are grouped. Thus, the symbols are rotated by the negated form of the phases in the transmitter, referred as $e^{\frac{-j2\pi C_{k,m}}{4}}$, where k stands for the data tone index and m for the repetition group index.
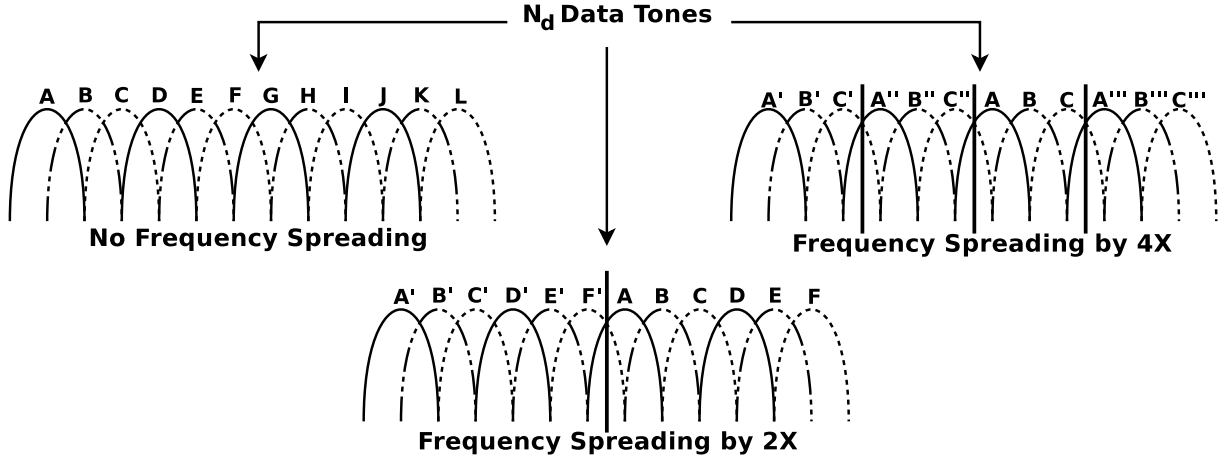
Figure 15 – Data tones grouping

For the case where the Transmitter employed frequency spreading by $2\times$, the derotated symbols are given by

$$R_{k,1} = R_{(k-\frac{N_d}{2}-1)} e^{\frac{-j2\pi(2k-1)}{4}},$$
$$R_{k,2} = R_k, \text{ for } k = 1, ..., N_d/2, \tag{3.2}$$

while, for the case where the frequency spreading by $4\times$ is employed, they are given by

$$R_{k,1} = R_{(k-\frac{N_d}{2}-1)} e^{\frac{-j2\pi(2k-1)}{4}},$$
$$R_{k,2} = R_{(k-\frac{N_d}{4}-1)} e^{\frac{-j2\pi(3k-1)}{4}},$$
$$R_{k,3} = R_k,$$
$$R_{k,4} = R_{(k+\frac{N_d}{4})} e^{\frac{-j2\pi(k-1)}{4}}, \text{ for } k = 1, ..., N_d/4. \tag{3.3}$$

Finally, all subcarriers related to a specific position k in the data subsets are accumulated and averaged, resulting in an estimation of the transmitted symbol.

The whole process is called Frequency Despreading (FD) and reverts the frequency spreading in a straightforward manner, not fully exploiting the frequency diversity provided by the MR-OFDM system. In order to mitigate channel effects, prior to FD, the incoming OFDM symbol must be equalized using the Channel State Information (CSI), $\hat{H}_k$, expressed as $\hat{X}_k = \frac{R_k}{\hat{H}_k}$, for $k = 1, ..., N_d$. FD is depicted in Fig. 16, and its resultant signal is expressed by

$$Y_k = \frac{1}{M} \sum_{m=1}^{M} \hat{X}_{k,m}, \text{ for } k = 1, ..., N_d/M. \tag{3.4}$$

3.2 Diversity Combining Techniques applied to MR-OFDM

In order to improve the performance obtained with FD the diversity combining techniques described in Section 2.2.1 - SC, MRC and SMRC - are applied to the MR-OFDM
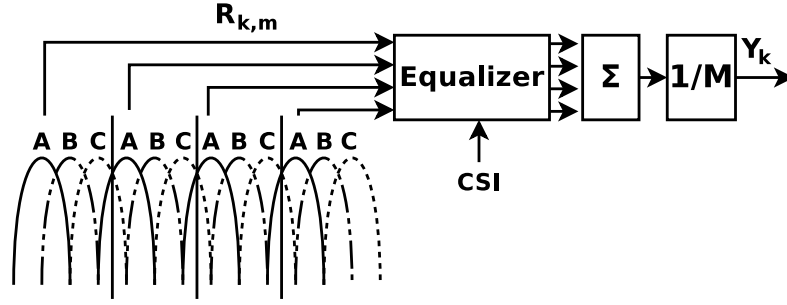
Figure 16 – Subcarriers combining after PAPR phase derotation for FD by $4\times$

receiver. The uncorrelated groups of subcarriers can go through a selection procedure and/or being weighted and combined, instead of just being accumulated and averaged, as it is done in FD. The following sections describe the mentioned techniques in the MR-OFDM context and proposes a hybrid technique between SD and FD, which will be referred to as Selection Frequency Despreading (SFD).

3.2.1 SC applied to MR-OFDM

In the MR-OFDM the subcarrier repetition groups after frequency spreading are considered diversity branches. Thus, the SC performs the selection on the M subcarriers related to the same position k in their respective data tones subset. These subcarriers have undergone PAPR phase rotation according to (3.2) or (3.3). The selection criterion is based on the subcarrier with the most suitable CSI.

As in Section 3.1, SC is performed on equalized symbols in order to mitigate channel effects. SC resultant signal is calculated by

$$Y_k = \hat{X}_{k,max} = \frac{R_{k,max}}{\hat{H}_{k,max}}, \tag{3.5}$$

where $\hat{X}_{k,max}$ is the equalized and derotated symbol related to the strongest channel, given by $|H_{k,max}| = \max\{|H_{k,1}|, \ldots, |H_{k,M}|\}$. Fig. 17 depicts the SC selecting the most suitable equalized subcarrier.
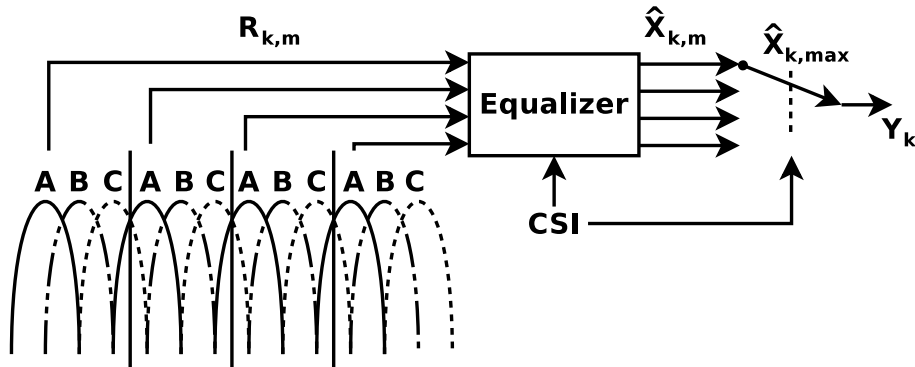
Figure 17 – SC applied to subcarriers after PAPR phase derotation

The SC can use a more complex selection procedure, selecting not only the subcarrier with the most suitable channel gain, but the L most suitable subcarriers. Still in the MR-OFDM context, the same combination adopted in the FD can be applied to the selected branches for each data tone. This technique, a hybrid between SD and FD, will be referred to as Selection Frequency Despreding (SFD). The basic concept of using selection and combining procedures is to exploit appropriately the amount of diversity offered by the channel since the SC usually uses only one diversity path (SIMON; ALOUINI, 2005). The SFD combiner output can be rewritten as

$$Y_k = \frac{1}{L} \sum_{l=1}^{L} \hat{X}_{k,l}, \text{ for } l = 1, ..., L < M, \tag{3.6}$$

where $\hat{X}_{k,l}$ are the L equalized and derotated symbols with highest channel gains. The subcarrier selection and combining are shown in Fig. 18.

If $L = 1$ the SFD reduces to the SC, on the other hand, if $L = M$ the hybrid technique is equivalent to FD. Finally, if $1 < L < M$, the SFD is expected to provide a performance gain when compared to SC and FD, since it is less sensitive to the combining loss of the branches with lowest SNR (ENG *et al.*, 1996). For this method to be worthwhile when compared to FD, the gain obtained in combining L branches instead of M branches must be higher than the additional complexity due to the selection process.
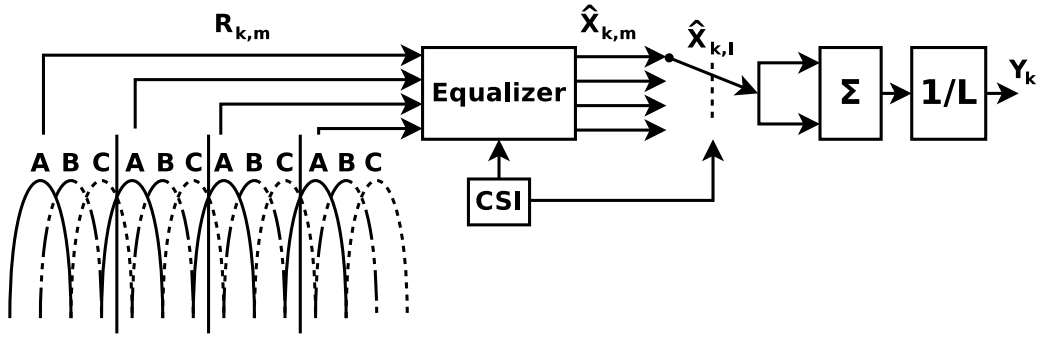
Figure 18 – SFD applied to subcarriers after PAPR phase derotation

3.2.2   MRC applied to MR-OFDM

Applied to MR-OFDM, MRC is performed in two steps. Incoming symbols are grouped and undergo the PAPR phase rotation described in Section 3.1. Then, MRC is performed on $R_{k,m}$, i.e., the subcarriers are weighted and then summed in a coherent fashion. It is described in Fig. 19.

Employing the estimated channel gain as optimal weights on each subcarrier, the

MRC combined output is expressed as

$$Y_k = \sum_{m=1}^{M} W_{k,m} R_{k,m} = \frac{\sum\limits_{m=1}^{M} R_{k,m} \hat{H}_{k,m}^*}{\sum\limits_{m=1}^{M} \left| \hat{H}_{k,m} \right|^2}, \text{ for } m = 1, ..., M. \quad (3.7)$$

where $\hat{H}$ is the estimated channel response, $\hat{H}_{k,m}^*$ is the conjugate of the estimated channel response and $\left| \hat{H}_{k,m} \right|^2$ is the channel power for each subcarrier. This process is performed on received symbols instead of equalized ones as it provides signal equalization within combining process. In practical systems, the MRC performance might be severely affected by possible estimation errors in channel estimation methods.
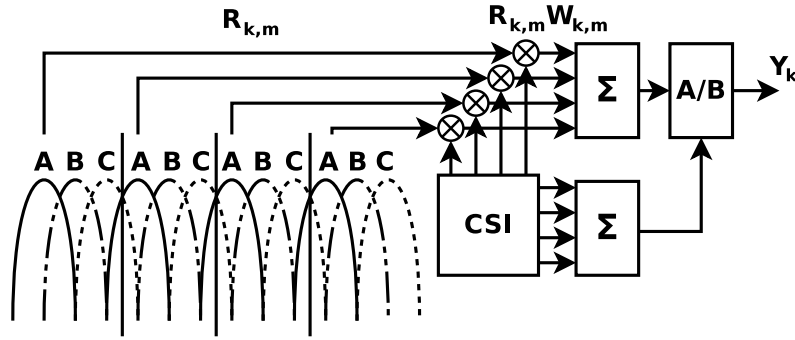
Figure 19 – MRC applied to subcarriers after PAPR phase derotation

Based on Fig. 19, the MRC does not stand out as the most complex diversity combining technique when compared to SC and SFD. All these mentioned schemes need CSI. SC and SFD use it as selection criterion and for incoming signal equalization, while MRC uses it for diversity branches weighting. A deeper analysis of the method complexity is provided in future chapters.

3.2.3 Selection Maximal Ratio Combining (SMRC)

As a hybrid of MRC and SC, besides the steps performed by MRC, SMRC performs another step related to subcarrier selection. Thus, in the first step, incoming symbols are grouped and undergo PAPR phase rotation, providing $R_{k,m}$ symbols. The second step performs selection, monitoring all the M subcarriers for each position k and selecting the L subcarriers with highest $\left| \hat{H}_l \right|^2$, where $L < M$. Finally, in the third step, the selected symbols are combined using MRC. Fig. 20 shows all these steps.

As in MRC, the optimal weight applied on each subcarrier is the estimated channel gain. SMRC resultant signal can be expressed as

$$Y_k = \frac{\sum\limits_{l=1}^{L} R_{k,l} \hat{H}_{k,l}^*}{\sum\limits_{l=1}^{L} \left| \hat{H}_{k,l} \right|^2}, \text{ for } l = 1, ..., L < M, \quad (3.8)$$

where $\hat{H}_{k,l}^*$ is the conjugate of the estimated channel response and $\left|\hat{H}_{k,l}\right|^2$ is the channel power for the lth selected subcarrier. Also as in MRC, this operation is performed on received symbols instead on the equalized subcarriers as it provides signal equalization within the combining process.

If $L = 1$, only the strongest signal is chosen, thus, (3.8) reduces to (3.5), i.e., the SMRC is equivalent to SC. If $L = M$, all the diversity branches are chosen, thus, (3.8) reduces to (3.7), i.e., SMRC is equivalent to MRC. For the SMRC to be advantageous, the complexity reduction obtained weighting and combining L branches instead of M branches must makes up for the performance loss and the complexity of the selection step.
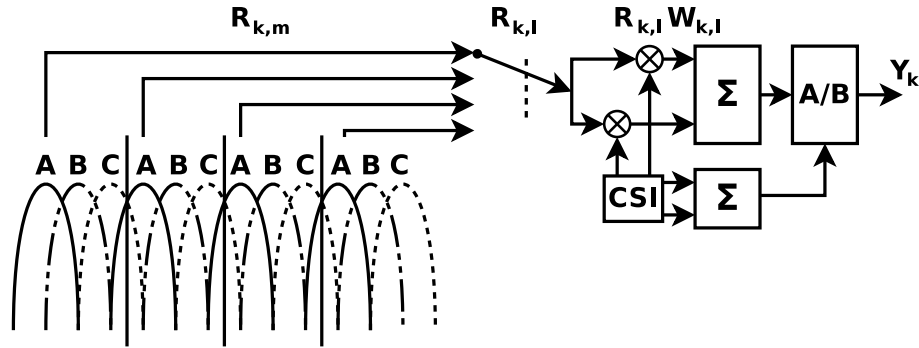
Figure 20 – SMRC applied to subcarriers after PAPR phase derotation

3.3 Extended Spreading Factor applied to MR-OFDM

The basic concept of employing extended spreading factor is that increasing the spreading factor, the frequency despreading method is able to provide a higher PAPR reduction and diversity gain to the system. However, increasing the number of repetition groups due to the spreading factor, the distance in frequency among the subcarriers that transmit the same symbol, $\Delta f_{B_{sc}}$, decreases. And, as already mentioned, $\Delta f_{B_{sc}}$ must be larger than the channel coherence bandwidth, B_c, for the frequency spreading to provide frequency diversity. So, this limits the number of diversity branches in a given bandwidth, thus limiting how much the spreading factors can be extended in MR-OFDM.

As already described in Section 2.3.1, the signal bandwidth in OFDM, B_s, can be expressed as the subcarrier spacing multiplied the number of active tones plus the DC tone. Thus, the signal bandwidth varies according to the option parameter listed in Table 1. Fig. 21, depicts the relation among B_s, B_{sc}, and $\Delta f_{B_{sc}}$. Furthermore, a rule of thumb for a channel to have frequency-selective fading is $B_s \geq 10B_c$ (FELICIE, 2012). Assuming the MR-OFDM operation mode as option 1, the channel B_c is limited as

$$10B_c \leq B_s =$$
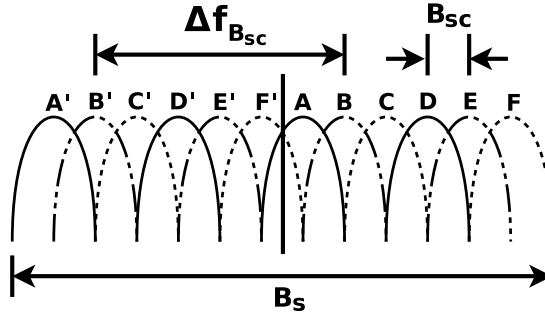
Figure 21 – Difference in frequency among subcarriers that transmit the same symbol

$$10B_c \leq (Active\ Tones + 1)B_{sc} =$$
$$10B_c \leq (104 + 1)B_{sc} =$$
$$B_c \leq 10B_{sc}. \tag{3.9}$$

Besides B_s, $\Delta f_{B_{sc}}$ is also expressed in terms of subcarrier spacing. This distance in frequency is obtained through the subcarrier spacing multiplied by the number of data tones and divided by the spreading factor. Once more assuming option 1, the maximum spreading factor is limited as

$$\Delta f_{B_{sc}} > B_c =$$
$$\Delta f_{B_{sc}} > 10B_{sc} =$$
$$\frac{Data\ Tones\ .\ B_{sc}}{Spreading\ Factor} > 10B_{sc} =$$
$$\frac{96B_{sc}}{Spreading\ Factor} > 10B_{sc} =$$
$$Spreading\ Factor \leq 9. \tag{3.10}$$

Even though the MR-OFDM supports spreading factors extended until $9\times$, to be compliant to (IEEE, 2012), the adopted maximum spreading factor is $8\times$. This choice takes into consideration the data rates summarized in Table 2. The data rate can be calculated through MCS configurations as

$$Data\ Rate_{(kb/s)} = (\frac{Data\ Tones\ .\ Bits\ per\ Symbol\ .\ Code\ Rate}{Spreading\ Factor\ .\ Symbol\ Duration_{(\mu s)}}). \tag{3.11}$$

The standard comprises Data Tones equals to 96, 48, 24 or 12 subcarriers; Bits per Symbol equals 1 for BPSK, 2 for QPSK and 4 for $16-$QAM modulation; and Code Rates equals $1/2$ and $3/4$. Independently of configuration, the Symbol Duration is constant and equals to 120 μs. Based on (3.11), to maintain the system data rate when using an extended spreading factor, the MR-OFDM must adopt a modulation with a higher number of bits per symbol. It results in a MCS configuration not foreseen by the standard. To better comprehend these new MCS configurations, the work adopts the notation $MCS_{(X,Y)}$, where X and Y stand for the selected modulation and spreading factor, respectively.

The proposed method focuses on employing extended spreading factors to $\text{MCS}_{(BPSK,4\times)}$, $\text{MCS}_{(BPSK,2\times)}$ and $\text{MCS}_{(QPSK,2\times)}$, which are the original MCS configurations with frequency spreading. Thus, initially, we propose $\text{MCS}_{(QPSK,4\times)}$ instead of $\text{MCS}_{(BPSK,2\times)}$. $\text{MCS}_{(QPSK,4\times)}$ does not present any extra implementation complexity to the system, and any drawback performance due to modulation since BPSK and QPSK present the same BER.

Another proposed configuration is $\text{MCS}_{(16-QAM,4\times)}$ instead of $\text{MCS}_{(QPSK,2\times)}$. Even though, originally, the 16-QAM is not used with frequency spreading, this modulation is part of the standard (IEEE, 2012) and does not add extra implementation complexity to the system. For $MCS_{(16-QAM,4\times)}$ to be worthwhile, the PAPR reduction and diversity gain have to compensate for the performance loss that the QAM modulation has compared to the PSK ones. The MCS proposals considering an extended spreading factor of $4\times$ are summarized in Table 3.

Table 3 – MCS Proposals for MR-OFDM adopting $4\times$

	Data Rate (Kbps)	Original Configuration	Proposed Configuration
MCS 1	200	BPSK, $2\times$	QPSK, $4\times$
MCS 2	400	QPSK, $2\times$	16-QAM, $4\times$

3.3.1   Frequency Spreading by $8\times$

Based on the maximum spreading factor established in the previous section and on the data rate compliance, the MCS proposals can also adopt the spreading factor of $8\times$ for an OFDM symbol composed by 128 subcarriers. Thus, the work proposes $\text{MCS}_{(QPSK,8\times)}$ instead of $\text{MCS}_{(BPSK,4\times)}$, and $\text{MCS}_{(16-QAM,8\times)}$ instead of $\text{MCS}_{(BPSK,2\times)}$. For $\text{MCS}_{(QPSK,8\times)}$ to be worthwhile, the PAPR reduction and diversity gain have to compensate the costs of the frequency spreading by $8\times$ implementation; and for the $\text{MCS}_{(16-QAM,8\times)}$, besides the implementation cost, it has to compensate the difference in performance between the modulations as well.

Additionally to the mentioned proposals, there is the possibility for the system to employ the frequency spreading by $8\times$ combined with a modulation that performs 5 bits to symbol mapping, such as the 32-QAM. Although this modulation transmits more bits per symbol, it tends to be even more susceptible to noise and interference than the 16-QAM (PURKAYASTHA; SARMA, 2015). Furthermore, the implementation of 32-QAM modulator and demodulator would increase the system complexity, which is the opposite of this work purpose. Thus, the use of this modulation is not part of this work. The MCS proposals considering an extended spreading factor of $8\times$ are summarized in Table 4.

Table 4 – MCS Proposals for MR-OFDM adopting 8×

	Data Rate (Kbps)	Original Configuration	Proposed Configuration
MCS 0	100	BPSK, 4×	QPSK, 8×
MCS 1	200	BPSK, 2×	16-QAM, 8×

Besides the diversity combining techniques, the spreading factor of 8× is the only functionality proposed in this method that adds extra implementation complexity to the transceiver. To reduce its implementation complexity, the phase rotations and their sequences of the frequency spreading by 8× must be as simple as possible, and at least provide the same PAPR reduction obtained with the other spreading factors. Thus, for the sake of simplicity, the proposed phases and sequences follow the patterns presented in the frequency spreading by 2× and 4×, instead of being optimized, as in similar techniques as Selective Mapping (SM) and Partial Transmit Sequence (PTS) (VARAHRAM; ALI, 2011; MISHRA, 2012).

As defined in Section 2.3.1.1, for frequency spreading by 2×, the copied symbols in the group defined as repetition 1 are multiplied by phase factors in the set $(0, \pm j)$. For frequency spreading by 4×, once again the repetition 1 group is multiplied by phase factors in the set $(0, \pm j)$, while for the other groups the phase factors belong to the set $(\pm 1, \pm j)$.

All the phase factors and sequences for the 4× case are depicted in Fig. 22. It is possible to notice that, the phase factor sets that are exclusive to this case present a smaller angle difference among the phase rotations, $\Delta\theta$, when compared to the repetition 1 set. For the repetition 1 set this difference is $\pi/2$. For the other sets, $\Delta\theta$ is $\pi/4$. Moreover, even though for repetition groups 2 and 3 the phase factors are the same, the direction of the phase sequence changes. For repetition 2 the sequence is $(\pi, \pi/2, 0, 3\pi/2)$, i.e., the sequence rotates to the right, and for repetition 3 is $(0, \pi/2, \pi, 3\pi/2)$, i.e, the sequence rotates to the left.
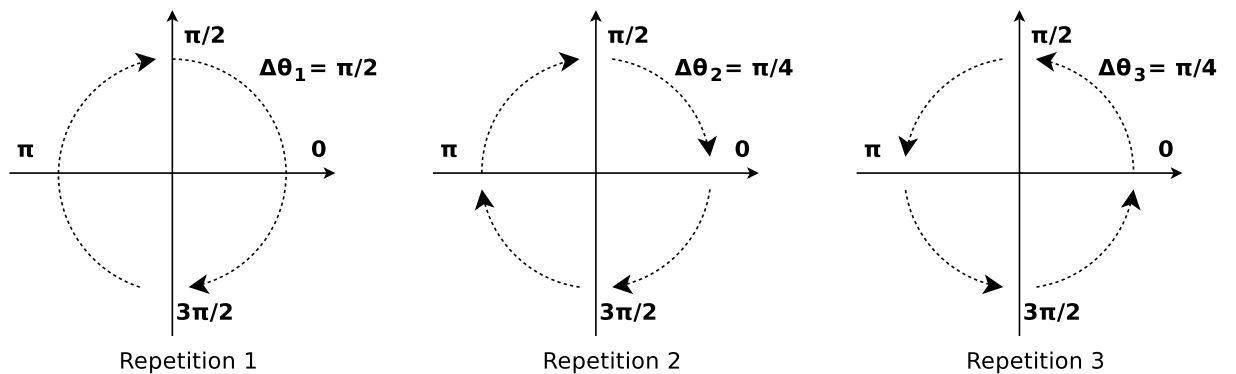
Figure 22 – Phase rotations for Frequency Spreading by 4×

Referring to the repetition groups position, it is possible to notice another pattern, as depicted in Fig. 23. In both cases, spreading factors $2\times$ and $4\times$, the lower data group of the positive data tones does not suffer phase rotation, and the lower group of the negative data tones maintains the set $(\pi/2, 3\pi/2)$. The repetition groups provided only by frequency spreading by $4\times$ are placed closer to $N_d/2$ and -1 indexes.
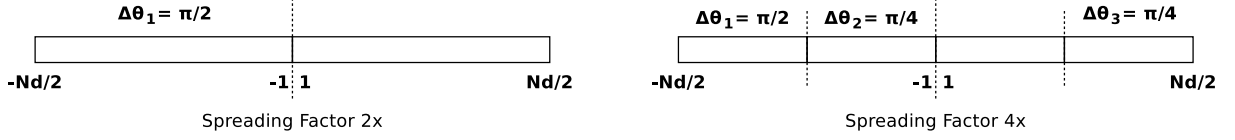
Figure 23 – Data subset positions

For spreading factor of $8\times$, taking into consideration the described patterns, the new phase factor sets use $\Delta\theta = \pi/8$ and $\pi/16$. Also, as the angle difference decreases, the repetition groups that employ them are placed closer to $N_d/2$ and -1 indexes. Finally, the phase sequences used in the repetition groups placed in the negative indexes rotate to the right, while the ones used in the groups placed in the positive indexes rotate to the left.

The resultant data tones for frequency spreading by $8\times$ are calculated by

$$
\begin{aligned}
R_{k,1} &= R_{(k-\frac{N_d}{2}-1)}e^{\frac{j2\pi(2k-1)}{4}}, & R_{k,5} &= R_k, \\
R_{k,2} &= R_{(k-\frac{3N_d}{8}-1)}e^{\frac{j2\pi(3k-1)}{4}}, & R_{k,6} &= R_{(k+\frac{N_d}{8})}e^{\frac{j2\pi(k-1)}{4}}, \\
R_{k,3} &= R_{(k-\frac{N_d}{4}-1)}e^{\frac{j\pi(k+4)}{4}}, & R_{k,7} &= R_{(k+\frac{N_d}{4})}e^{\frac{j\pi(7k+2)}{4}}, \\
R_{k,4} &= R_{(k-\frac{N_d}{8}-1)}e^{\frac{j\pi(16k+6)}{8}}, & R_{k,8} &= R_{(k+\frac{3N_d}{8})}e^{\frac{j\pi(k+13)}{8}}, \text{ for } k = 1, ..., N_d/8.
\end{aligned}
$$

(3.12)

The next chapters present simulation and synthesis results in order to verify the spreading factor $8\times$ viability based on the in the MR-OFDM PAPR reduction.

4 Simulation Results

The frequency despreading method proposed in this work is based on the use of diversity combining techniques and extended spreading factors. In order to maintain the data rates established in the standard (IEEE, 2012), new MCS configurations are proposed as well. Hence, besides employing extended spreading factors, these proposed MCS configurations also employ modulation with more bits per symbol. To assess the impact of our proposal, the Bit Error Rate (BER), Complementary Cumulative Distribution Function (CCDF) and implementation complexity of each diversity combining technique and proposed MCS were evaluated.

This chapter presents extensive simulations performed in an environment modeled using MATLAB, providing both BER and CCDF. The implementation complexity is addressed in the following chapter. The system BER verifies the performance improvement obtained with the frequency despreading method. The CCDF, in turn, is the probability of a random variable to be above a particular level. Thus, it is a way to evaluate the PAPR reduction provided by the use of extended spreading factor.

4.1 Simulation Environment

The simulation environment depicted in Fig. 24 was implemented in MATLAB in order to verify the frequency despreading method and its possibilities for diversity combining technique and MCS configurations. Compared to the MR-OFDM Transmitter and Receiver presented in Fig. 11 and Fig. 13, respectively, the environment is a simplified version of the MR-OFDM PHY, discarding the blocks that are not in the scope of this work.
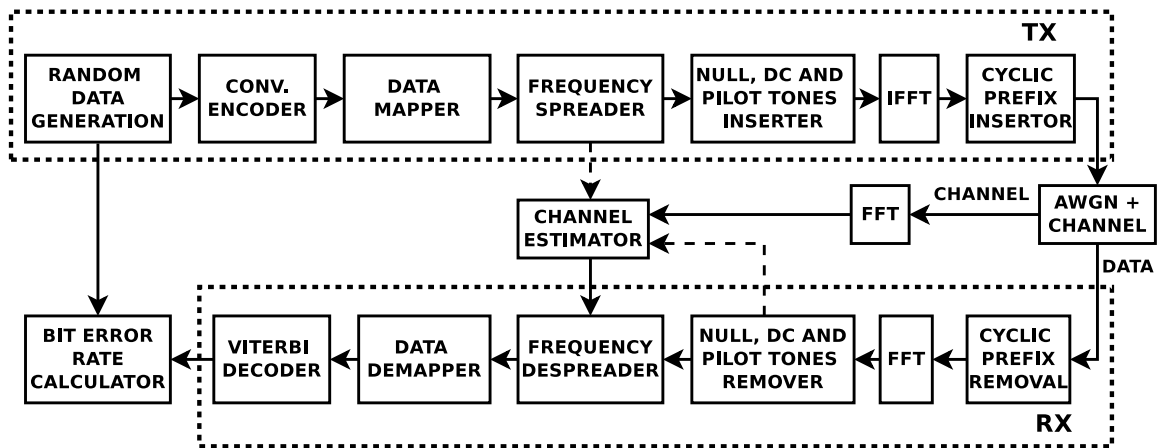
Figure 24 – MATLAB simulation environment

Initially, bits are generated randomly and encoded according to the adopted configurations (IEEE, 2012). The bits are mapped to symbols (in-phase (I) and quadrature (Q) components), using BPSK, QPSK or 16-QAM modulation; and the resultant symbols may be replicated on different tones according to the spreading factor $2\times$, $4\times$ and $8\times$. These replicas undergo through phase rotations to reduce the PAPR of the OFDM transmitted signal. Other tones (DC, null and pilot tones) are added to them, forming an OFDM symbol, which is converted from the frequency to the time domain using IFFT. To complete the transmitter waveform, the CP is appended to the symbol in order to avoid the ISI caused by the multipath channel properties (MOLISCH, 2012).

In the simulations, the communication channel is modeled according to the Rayleigh multipath channel model in (TSE; VISWANATH, 2005) as an n-tap channel, with real and imaginary parts of each tap being independent Gaussian random variables, and by inserting Additive Gaussian White Noise (AWGN) to the signal. At first, it is assumed frequency-selective fading with a coherence bandwidth that provides frequency diversity to the system for the spreading factors $2\times$, $4\times$ and $8\times$. Moreover, the simulations assume perfect CSI at the receiver, perfect synchronization, and no carrier frequency offset.

At the receiver, the CP is removed from each OFDM symbol, and then they are converted back to the frequency domain using FFT. In this domain, DC, null and pilot tones are removed from the incoming symbols, leaving only data tones. At this point of the data flow, depending on the diversity combining technique adopted by the frequency despreading method, data tones should be equalized. As part of frequency despreading, the data tones undergo different phase rotations to revert the rotations applied in the transmission to reduce PAPR. Then, the rotated symbols are grouped as depicted in Fig. 15. To conclude the despreading, the groups are combined or selected according to the chosen diversity combining technique. After despreading, symbols are demapped into bits. Subsequently, if they were previously encoded, the bits are decoded by the Viterbi hard decoder, providing the final bits. In possession of the bit sequence prior to the transmission and the equivalent sequence after the reception, it is possible to asses the performance of the system. The BER is obtained comparing both sequences and counting the number of differences between them.

Due to the number of data tones in Options 2, 3 and 4 and the limitation demonstrated in (3.10), Option 1 is the only operation mode that supports all the spreading factors, including the $8\times$. Thus, for simulation purposes, symbols are generated using only Option 1, and MCS 0, 1 and 2. The initial simulations consider perfect CSI knowledge, and, assuming no carrier frequency error nor synchronization error, the SHR field is not necessary, and, therefore, not generated. Also, in the simulation, the modules responsible for the receiver are assumed to have previous knowledge of the adopted configuration in the transmission, which eliminates the necessity of generating a PHR. Therefore, only the

PSDU field is randomly generated and processed by the simulation environment. Finally, the PSDU size is not necessarily compliant with the IEEE 802.15.4g standard, generating a sufficient number of bits to estimate the BER.

Further simulations are performed assuming scenarios that vary the channel coherence bandwidths and estimate the channel frequency response. The purpose is to verify the robustness of the frequency despreading method under the effects of channel estimation in low SNR and subcarrier correlation. In the simulations performed assuming perfect knowledge of the CSI, the channel frequency response of the modeled channel is employed directly in the equalization of the received signal, and in the diversity combining techniques as weighting factor and selection criterion. In order to analyze the effects of possible estimation errors, the modeled channel is applied in the transmitted OFDM symbols and estimated using pilot tones and pilot OFDM symbols. The channel estimates are then applied in the transmitted signal.

In order to simulate a scenario with controlled variation of the channel coherence bandwidth, B_C, the channel time delay spread, σ_τ, must vary accordingly, which can be obtained changing the number of taps used to model the channel. Assuming that the channel is no longer than the CP length to guarantee a circular convolution with the transmitted signal, the number of taps can assume values in the range of 2 to 32 for Option 1. It is worth mention that, for the simulations where the effects of the correlation among the subcarrier repetition groups are not analyzed, it is assumed a 10-tap channel.

4.2   Performance Results

Simulations results and analysis for the proposed frequency despreading method are presented in this section as a function of E_b/N_0. In particular, we compare the systems in terms of E_b/N_0, including comparisons to theoretical BER curves for BPSK, QPSK and 16-QAM modulations, and with MRC and SC diversity combining techniques. The results focus on the diversity gain obtained by the system when using a diversity combining technique with FD, the diversity gain provided by hybrid techniques according to the numbers of selected subcarriers, the improvement of these diversity gains according to the spreading factors, and the performance gains obtained with the MCS proposals.

4.2.1   Diversity Combining Technique Performances

The gains obtained by the conventional diversity combining techniques when compared to the FD are analyzed through BER curves for FD, SC and MRC, as shown in Fig. 25. The simulations in this figure adopt frequency spreading of 2×, BPSK modulation, and both, convolutional coding with code rate 1/2 and no coding. Even though the MR-OFDM always employs convolutional coding, the simulations assuming uncoded

system are performed to compare the results with the theoretical BER curves presented in literature, depicted in Fig. 5 and Fig. 7.

(a) Coded system

(b) Uncoded system
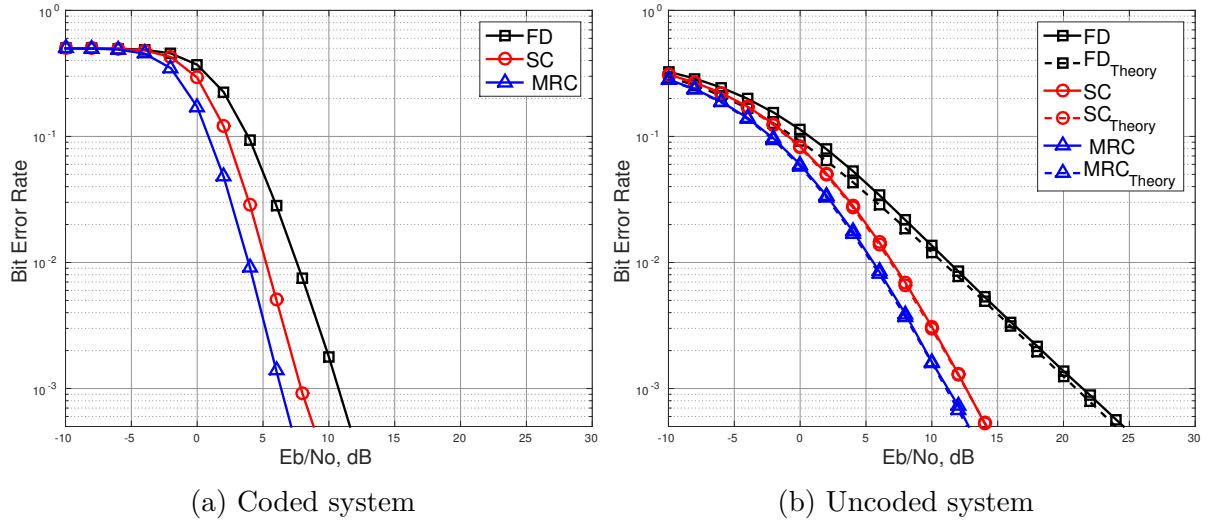
Figure 25 – Diversity combining technique performances for BPSK 2×

It is verified that, as detailed in Section 2.2.1, for the coded and uncoded cases the MRC presents the best performance, followed by SC and FD. To reach a BER of 10^{-3}, the FD needs 10.75 dB, the SC needs 7.84 dB, and the MRC needs 6.39 dB. Furthermore, the curves for the uncoded system are close to the theoretical ones. For other simulated modulations - QPSK and 16-QAM - and spreading factors - 4× and 8×, the behavior is the same, i.e., MRC with the best performance, SC with the intermediate and FD with the worst. The performance of FD, SC and MRC at E_b/N_0 (dB) for a BER of 10^{-3} assuming other spreading factors and modulations are summarized in Table 5.

Table 5 – Conventional combining techniques performance at E_b/N_0 (dB) for a BER of 10^{-3}

Modulation	Diversity Combining Techniques	Spreading Factors			
		1×	2×	4×	8×
BPSK	FD	14.01	10.75	7.72	4.71
	SC	14.04	7.84	4.05	1.90
	MRC	14.01	6.39	1.02	-3.05
QPSK	FD	16.25	12.90	9.31	5.94
	SC	16.30	8.77	4.75	2.52
	MRC	16.30	7.33	1.58	-2.64
16-QAM	FD	21.10	17.32	13.64	9.98
	SC	21.10	13.09	8.37	5.69
	MRC	21.10	11.62	5.11	0.68

Based on the results presented in Table 5, it is also possible to assess the performance improvement provided by the increment of the spreading factor for the FD, SC and

MRC techniques. Simulations assuming BPSK modulation and convolutional coding with code rate 1/2 are depicted in Fig. 26. To reach a BER of 10^{-3}, the FD needs 14.01 dB for the case without frequency spreading, 10.75 dB for frequency spreading by 2×, 7.72 dB for frequency spreading by 4×, and 4.71 dB for frequency spreading by 8×. Referring the spreading factor as M, when compared to the case without frequency spreading, the FD presents gains around $10\log_{10}(M)$ dB. Thus, there is a quasi-constant marginal return as M increases. It is verified by the difference in dB between the performances of two spreading factors, which is defined as $\Delta_{(M,N)}$. For the FD, $\Delta_{(8\times,4\times)} \approx \Delta_{(4\times,2\times)} \approx \Delta_{(2\times,1\times)} \approx 3$ dB.

Besides the FD case, Fig. 26 depicts BER curves for MRC and SC as well. It is possible to see that the performance improvements obtained by the increment of spreading factor are higher for both techniques, MRC and SC, when compared to FD. To reach a BER of 10^{-3}, the SC needs 7.84 dB for frequency spreading by 2×, 4.05 dB for frequency spreading by 4× and 1.90 dB for frequency spreading by 8×. The MRC, in turn, needs, for the same cases, 6.39 dB, 1.02 dB and -3.05 dB, respectively. Furthermore, for SC and MRC, instead of quasi-constant marginal return, there is a diminishing marginal return as M increases, i.e., $\Delta_{(8\times,4\times)} < \Delta_{(4\times,2\times)} < \Delta_{(2\times,1\times)}$.

In (TSE; VISWANATH, 2005), it is shown that, for MRC, the SNR of the resultant signal at the combiner output, γ_Σ, can be split into a product of two terms:

$$\sum_{m=1}^{M} \frac{|H_{k,m}|^2 E_b}{N_0} = \left(M\frac{E_b}{N_0}\right).\left(\frac{1}{M}\sum_{m=1}^{M}|H_{k,m}|^2\right). \tag{4.1}$$

For the first term, the improvement in the received SNR comes from increasing the total received energy from a single bit. The effective total received power of the signal increases linearly with M, so that using $M = 2^k$ yields a $3k$ dB gain. The second term is related to diversity gain. If the channel gains are fully correlated across all subcarriers related to the same position k, then there is no diversity gain no matter the number of paths. For the case where $H_{k,m}$ are independent there is diversity gain, but there is also a diminishing marginal return as M increases. Due to the law of large numbers the second term converges to 1 with increasing M, providing only a gain related to the first term. Hence, Fig. 26 suggests that FD provides, as gain, only the first term of (4.1), while MRC and SC also include a share of the second term due to the diversity gain.

Besides the conventional diversity combining techniques - SC and MRC, this work presents simulation results for the hybrid techniques - SFD and SMRC - as well. The performance of SFD and SMRC at E_b/N_0 (dB) for a BER of 10^{-3} assuming the spreading factors 4× and 8×, and all the possible modulations are summarized in Table 6. These performances depend directly on the number of selected subcarriers. So, for a better comprehension of the simulation results, this work adopts the notation SFD(M,L) and SMRC(M,L), where M stands for the total number of subcarriers to be combined and L

(a) FD

(b) SC

(c) MRC
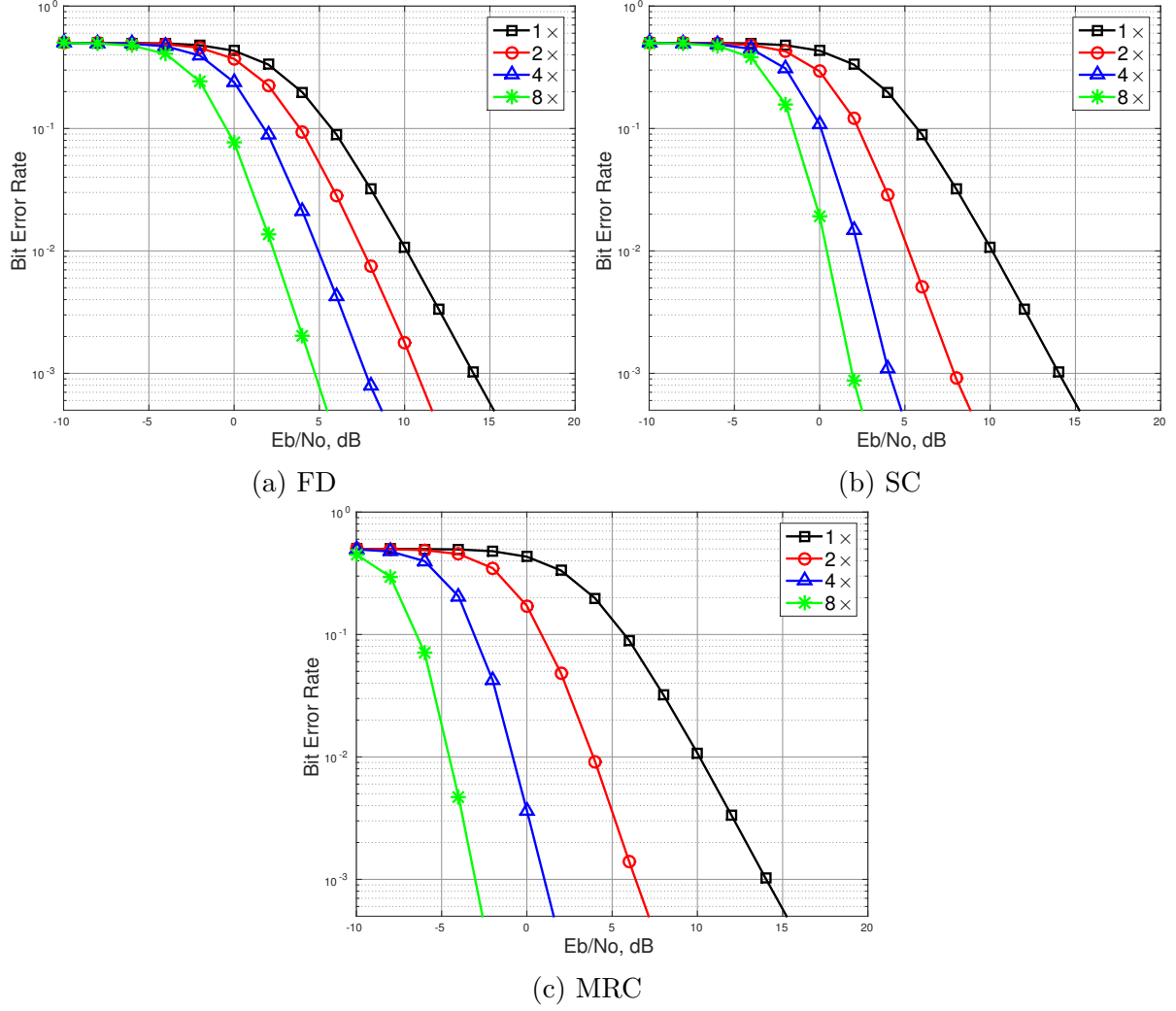
Figure 26 – Diversity combining technique performances according to the Spreading Factor for coded BPSK

stands for the number of selected subcarriers. Simulations with frequency by 2× are not described in Table 6, since SFD(2,1) and SMRC(2,1) performances are identical to the SC results in Fig. 26b, and SFD(2,2) and SMRC(2,2) performances are identical to the FD and MRC results in Fig. 26a and Fig. 26c, respectively.

The differences in SFD and SMRC performances according the number of selected subcarriers are depicted in Fig. 27. It is assumed BPSK modulation, convolutional coding with code rate 1/2, and spreading factor 4× selecting L subcarriers, $1sc \leq L \leq 4sc$. SFD(4,1) and SMRC(4,1) have similar performances, which are also similar to the SC performance for the same spreading factor. To reach a BER of 10^{-3}, SFD(4,1) and SMRC(4,1) need 4.10 dB. This is expected, since in these cases only one diversity branch is selected, so all the techniques coincide. The SFD presents its best performance when $L = 2$, reaching a BER of 10^{-3} with 3.03 dB. For more diversity branches, the performance of SFD decays as the number of selected subcarriers increases. It reaches its worst result with SFD(4,4), which is equivalent to the FD performance for the same configuration, i.e., both need 7.73

Table 6 – Hybrid combining techniques performance at E_b/N_0 (dB) for a BER of 10^{-3}

Spreading Factor	Modul.	Div. Comb. Techniques	Selected Subcarriers							
			1sc	2sc	3sc	4sc	5sc	6sc	7sc	8sc
4×	BPSK	SFD	4.10	3.03	3.68	7.73	-	-	-	-
		SMRC	4.09	2.12	1.34	1.03	-	-	-	-
	QPSK	SFD	4.79	3.62	4.68	9.33	-	-	-	-
		SMRC	4.79	2.72	1.97	1.61	-	-	-	-
	16-QAM	SFD	8.35	7.33	8.35	13.61	-	-	-	-
		SMRC	8.37	6.38	5.44	5.08	-	-	-	-
8×	BPSK	SFD	1.90	0.14	-0.79	-1.00	-0.87	-0.34	1.19	4.73
		SMRC	1.89	-0.31	-1.33	-2.06	-2.53	-2.80	-3.00	-3.03
	QPSK	SFD	2.53	0.58	-0.36	-0.54	-0.46	0.14	1.59	5.98
		SMRC	2.53	0.22	-1.01	-1.63	-2.10	-2.48	-2.66	-2.70
	16-QAM	SFD	5.69	3.83	2.96	2.72	2.93	3.56	5.10	9.98
		SMRC	5.67	3.49	2.33	1.66	1.25	0.94	0.68	0.70

dB to reach a BER of 10^{-3}.

On the other hand, SMRC performance improves as the number of selected subcarriers increases. SMRC(4,4) is its best performance and it is equivalent to the MRC BER curve. Both, SMRC(4,4) and MRC, reach a BER of 10^{-3} with 1.03 dB. SMRC(4,3) presents a performance close to SMRC(4,4), a difference of 0.3 dB approximately. The difference between SFD and SMRC behaviors as the number of selected subcarrier increases is justified by the way they combine the selected subcarriers (SIMON; ALOUINI, 2005). The SFD employs the same weights to the noisiest subcarriers and to the subcarriers considered as the most suitable; while the SMRC amplifies the strongest subcarriers and attenuates the ones least favorable.

(a) SFD   (b) SMRC
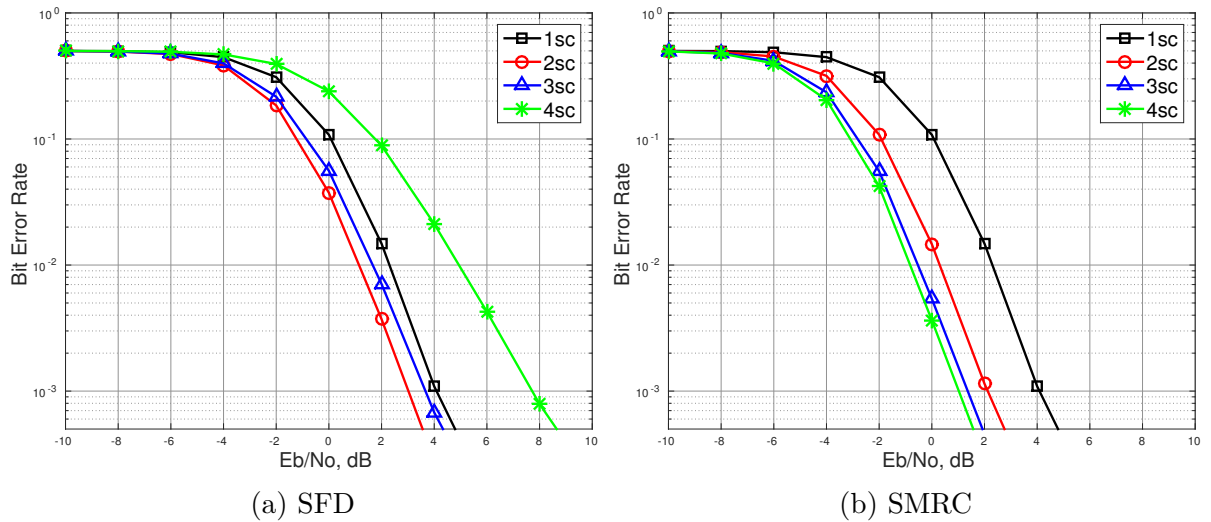
Figure 27 – Hybrid combining technique performances for coded BPSK 4× according to the number of selected subcarriers

For frequency spreading by 8×, the behavior of SFD and SMRC is similar to the 4× case. SFD reaches its best result when selecting 4 subcarriers and the worst result when selecting all the possible subcarriers. The SMRC performance still increases as the number of selected subcarriers increases. The performance provided by SMRC(8,L), for $L = 5$, 6 and 7, are close to the best case, with differences up to 0.5 dB approximately.

As described in Section 2.2.1, MRC provides the theoretical maximum gain that can be obtained with the use of diversity, but it also stands out as the most complex diversity combining technique. As an alternative to the MRC complexity, the hybrid techniques tend to provide an intermediate performance with an intermediate complexity. The SFD overcomes the FD and SC performances combining only half of the available subcarriers, while the SMRC provides performance close to the MRC even not employing all the available subcarriers.

Based on Section 3.2, in the OFDM context, the complexity of the diversity combining techniques is not clear as in systems with antenna diversity. Different from what happens in these systems, where the hybrid techniques exclude radio frequency circuits when do not select a certain path, in an OFDM receiver, its architecture suffers small changes. A significant change could be the derived from the MRC necessity of estimating all the subcarriers channel gain, which could be eliminated in SC, FD or hybrid techniques. However, in this work, the SC and the hybrid techniques select the subcarrier most suitable to be decoded based on the estimated channel gain. Moreover, even for the FD, that does not perform subcarrier selection, the incoming signal must be equalized previously using the estimated channel gain. The implementation complexity of the diversity combining techniques is addressed in the following chapter.

4.2.2 Extended Spreading Factor Performances

The results for the MCS proposals adopting extended spreading factors listed in Tables 3 and 4 are depicted in the following figures. For each data rate, the figures present comparisons between the performance of original and proposed MCS, both assuming convolutional coding with code rate 1/2. Moreover, the figures also show the PAPR reduction through the system CCDF. Finally, this section also provides the simulation results for the complete proposed method, i.e., MRC and MSC employing extended spreading factor. The complete proposed method is compared to a system employing FD and original MCS, which is defined as our benchmark for following sections.

In Fig. 28, for each data rate, the performances of proposed and original MCS adopting MRC are depicted. The results show gains up to 5.7 dB for the proposed MCS. The highest improvement is obtained with the MCS 1 proposal when adopting $\text{MCS}_{16-QAM,8\times}$, but it is close to the gain with $\text{MCS}_{QPSK,4\times}$, a difference of less than 1 dB. The similar performances for $\text{MCS}_{16-QAM,8\times}$ and $\text{MCS}_{QPSK,4\times}$, even adopting different spreading fac-

tors, are justified by the fact that, for a given SNR, the BER of 16-QAM modulation is worse than that of PSK. Still regarding the 16-QAM modulation, $\text{MCS}_{16-QAM,4\times}$ provides the worst improvement, around 2.24 dB. Analyzing the performance improvements of the proposed $\text{MCS}_{QPSK,4\times}$ and $\text{MCS}_{QPSK,8\times}$, their results corroborate the fact the diversity gain provided by MRC presents a diminishing marginal return. Even adopting the same modulations and diversity combining techniques, $\text{MCS}_{QPSK,8\times}$ presents a difference in performance of around 1 dB when compared to the $\text{MCS}_{QPSK,4\times}$ performance.

(a) MCS 0

(b) MCS 1

(c) MCS 2
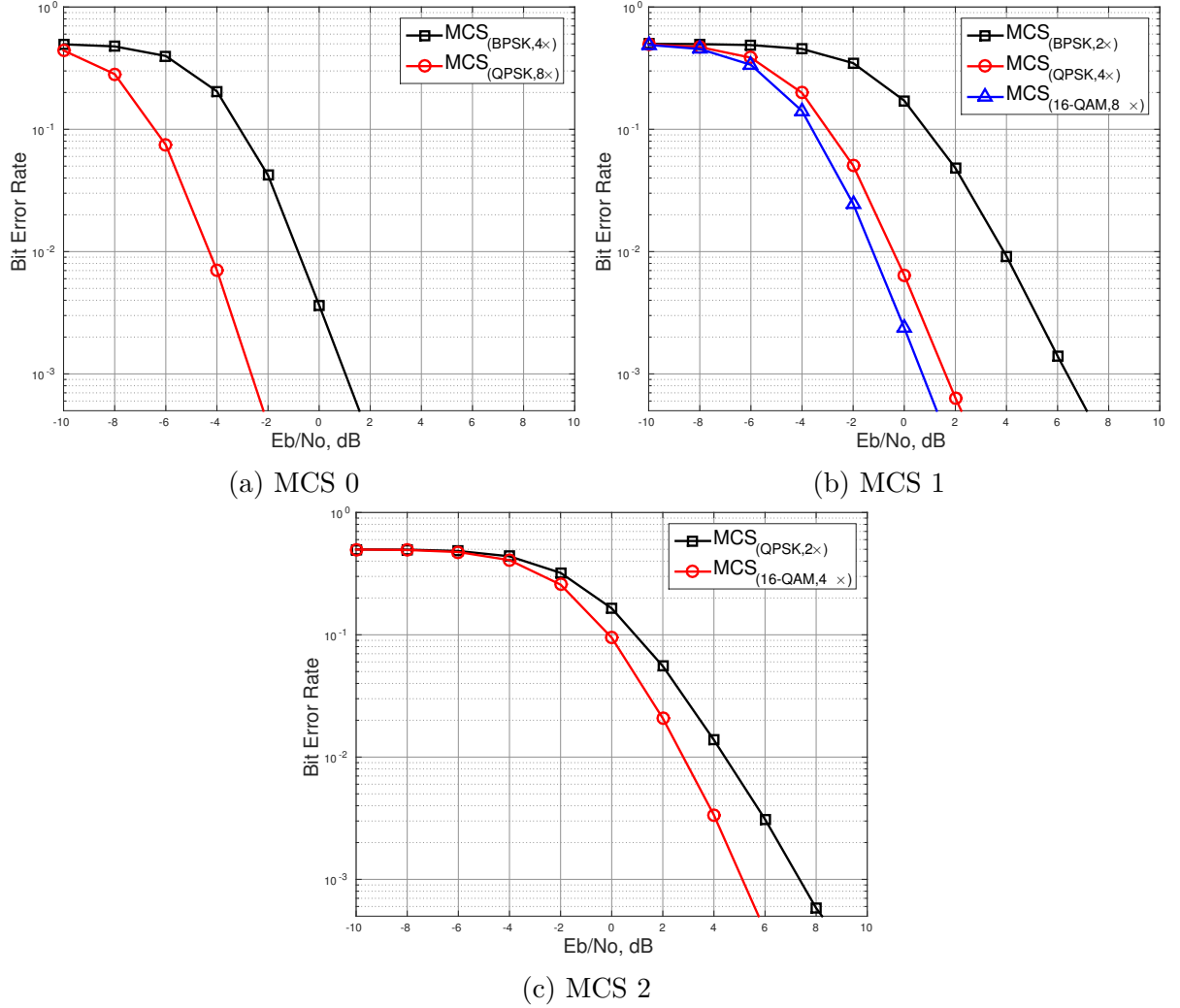
Figure 28 – Performance gain for MCS Proposals employing MRC in a coded system

    The PAPR reductions obtained by the use of extended spreading factors are depicted in Fig. 29. The curves presents, for each data rate, the CCDF of the PAPR employing original and proposed MCS. The CCDF is the probability, indicated by % in axis y, of the system PAPR to be above a certain power, indicated by dB in axis x. Thus, for a specific power, it is desired to achieve the lowest possible probability. The proposals $\text{MCS}_{(16-QAM,8\times)}$, $\text{MCS}_{(QPSK,4\times)}$, and $\text{MCS}_{(16-QAM,4\times)}$ provide improvements around 0.35 dB when compared to the original MCS of their data rates. Nevertheless, as mentioned in Section 3.3.1, the phase factors optimization affects the PAPR reduction provided by

FS, and, for 8×, the phase factors are chosen aiming at a simple MR-OFDM. The effects of this simplified choice for phase rotation in PAPR reduction is exemplified by $MCS_{(QPSK,8\times)}$ and $MCS_{(16-QAM,8\times)}$; both present similar PAPR reductions when compared to $MCS_{(BPSK,4\times)}$ and $MCS_{(QPSK,4\times)}$, respectively.

(a) MCS 0

(b) MCS 1

(c) MCS 2
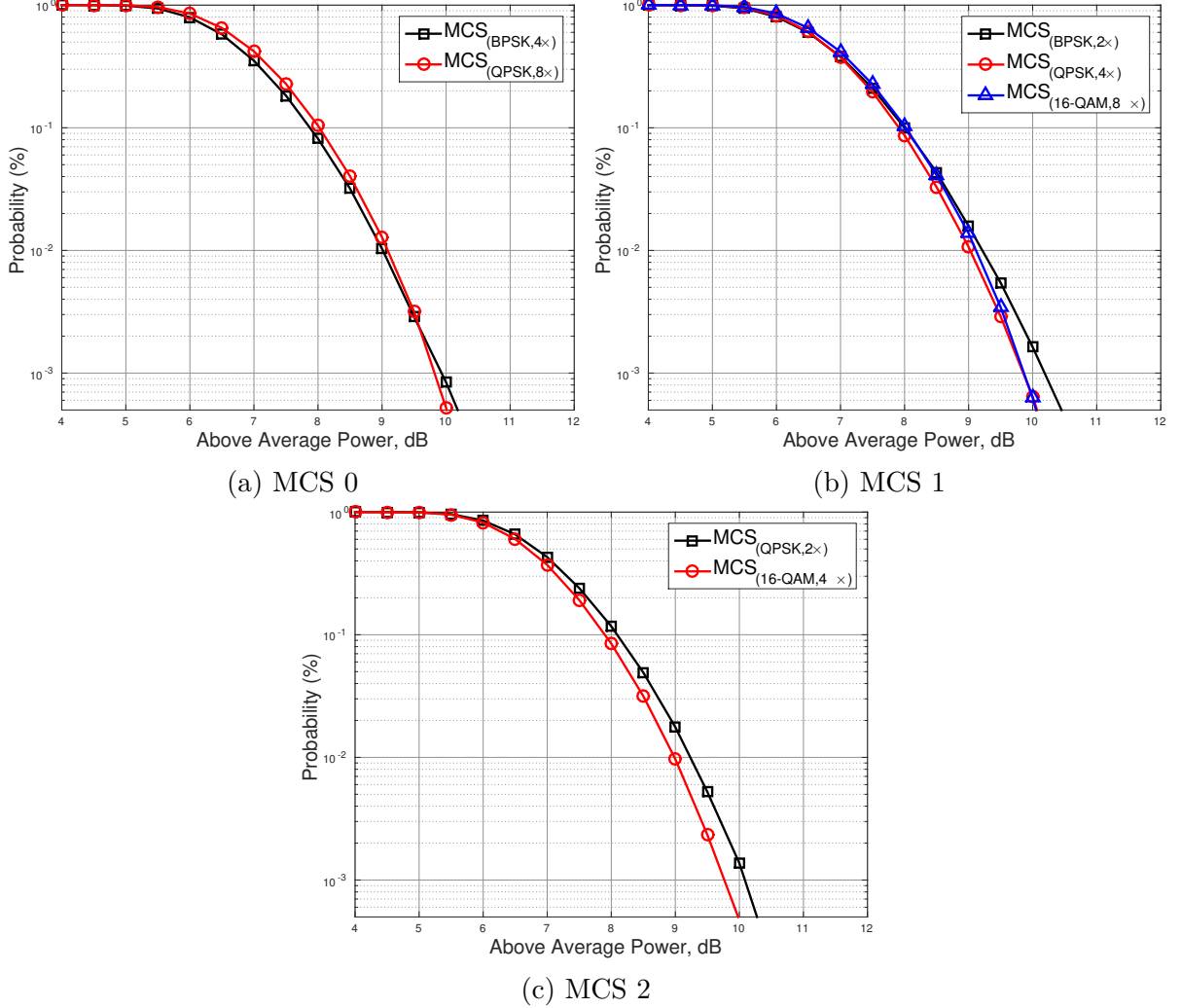
Figure 29 – PAPR reduction for MCS proposals in a coded system

Finally, Fig. 30 presents performance comparisons assuming both extended spreading factors and diversity combining techniques. For all data rates the original MCS employs FD while the proposed ones employ MRC. The system adopting the proposed MCS and MRC provides gains up to 10 dB when compared to the benchmark case. The highest improvement is obtained with $MCS_{(QPSK,8\times)}$ for a data rate of 100 kbps, which is around 10.30 dB. This proposal does not have any performance penalty due to modulation. On the other hand, the worst improvement is obtained with $MCS_{(16-QAM,4\times)}$ for a data rate of 400 kbps, providing a gain around 7.79 dB. These results corroborate the effects of the 16-QAM modulation on the method performance. For a data rate of 200 kbps, the highest improvement is with $MCS_{(16-QAM,8\times)}$, but it is close to the gain with $MCS_{(QPSK,4\times)}$, a difference less than 1 dB. In all the cases, the best results are presented

employing the highest extended spreading factor with a higher order modulation to avoid rate loss.

(a) MCS 0

(b) MCS 1

(c) MCS 2
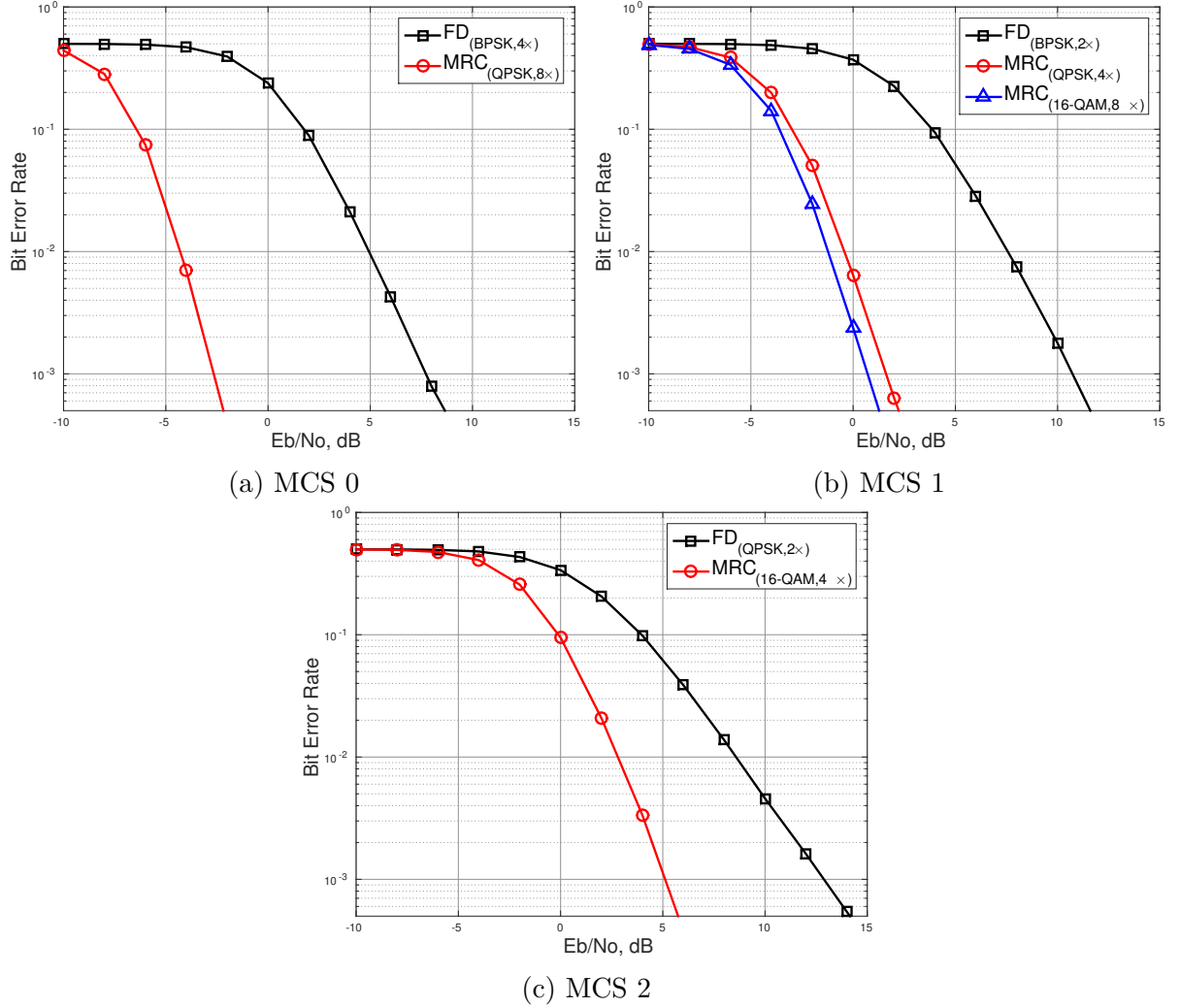
Figure 30 – Proposed method performances in a coded system

The results of this section show that the proposed frequency despreading method might be a significant evolution to the IEEE 802.15.4g standard in specific scenarios. Assuming that subcarrier repetition groups generated by the frequency spreading are independent and uncorrelated at the MR-OFDM receiver, there are improvements in both PAPR reduction and BER performance. All the adopted modulations are already comprised in the standard, the only new feature is the spreading factor 8×, which are defined aiming to maintain the simplicity of the other spreading factors.

4.2.3 Proposed Method Performances Under Different Simulation Scenarios

The same simulations performed in Section 4.2.1 and 4.2.2 are replicated in this section adopting different scenarios. The scenarios include the estimation of the channel frequency response instead of perfect knowledge of CSI, and the variation of the channel

coherence bandwidth instead of a fixed one. Based on the performance results it is possible to verify the robustness of the proposed frequency despreading method, employing MRC and proposed MCS configurations, to channel estimation in low SNR and subcarrier correlation.

Possible channel estimation errors due to low SNR tend to damage the performance of the diversity combining techniques since they all employ the estimated channel gain. Furthermore, depending on the channel coherence bandwidth, B_C, the subcarrier repetition groups created by frequency spreading in the transmission can be correlated. Subcarrier correlation affects the diversity gain provided by both the diversity combining techniques and extended spreading factors.

4.2.3.1   Channel Estimation Errors

For the following simulations, the channel estimation using zero forcing is performed based on pilot OFDM symbols transmitted along with the other OFDM symbols. The modeled channel is applied in all these OFDM symbols and estimated using only the pilot ones. The pilot OFDM symbols are discarded and the channel estimation is applied only to the remaining OFDM symbols. Table 7 summarizes the performances of FD, SC and MRC under channel estimation errors at E_b/N_0 (dB) for a BER of 10^{-3}. The simulations assume all the spreading factors and modulations encompassed by the original and proposed MCS configurations.

Table 7 – Conventional combining techniques performance at E_b/N_0 (dB) for a BER of 10^{-3} under channel estimation errors

Modulation	Diversity Combining Techniques	Spreading Factors			
		$1\times$	$2\times$	$4\times$	$8\times$
BPSK	FD	17.54	13.43	10.35	7.64
	SC	17.56	11.56	8.03	6.13
	MRC	17.56	10.35	5.69	2.47
QPSK	FD	19.43	15.58	11.38	8.30
	SC	19.45	12.15	8.35	6.15
	MRC	19.43	10.94	5.72	2.13
16-QAM	FD	24.83	21.01	17.09	13.58
	SC	24.81	17.29	12.83	10.81
	MRC	24.83	15.96	10.64	8.35

The performance degradation of the FD, SC, and MRC when comparing the cases with perfect CSI knowledge (dashed lines) and with channel estimation errors (solid lines) are depicted in Fig. 31. In practical systems, the MRC tends to be more sensitive to possible channel estimation errors than the other diversity combining techniques (SIMON; ALOUINI, 2005). This fact can be verified by these performance results. When comparing

both simulation cases, perfect CSI knowledge and channel estimation, the MRC, for a BER of 10^{-3}, presents a difference in performance of 3.96 dB for frequency spreading by $2\times$, 4.67 dB for frequency spreading by $4\times$, and 5.52 for frequency spreading by $8\times$.

Even though the other diversity combining techniques are not as affected as MRC, they are degraded as well, since the FD and SC are performed on equalized symbols. In the SC case, besides the equalized input, it also employs the channel estimation as a selection criterion. The SC, for a BER of 10^{-3}, presents a difference in performance of 2.68 dB for frequency spreading by $2\times$, 2.73 dB for frequency spreading by $4\times$, and 2.93 for frequency spreading by $8\times$, when comparing both simulation cases. Finally, the FD, for a BER of 10^{-3}, presents a difference in performance of 3.72 dB for frequency spreading by $2\times$, 3.98 dB for frequency spreading by $4\times$, and 4.23 for frequency spreading by $8\times$, when comparing both simulation cases. Other pattern that can be noticed in Fig. 31 is that the performance degradation worsens as the spreading factor increases.

(a) $2\times$
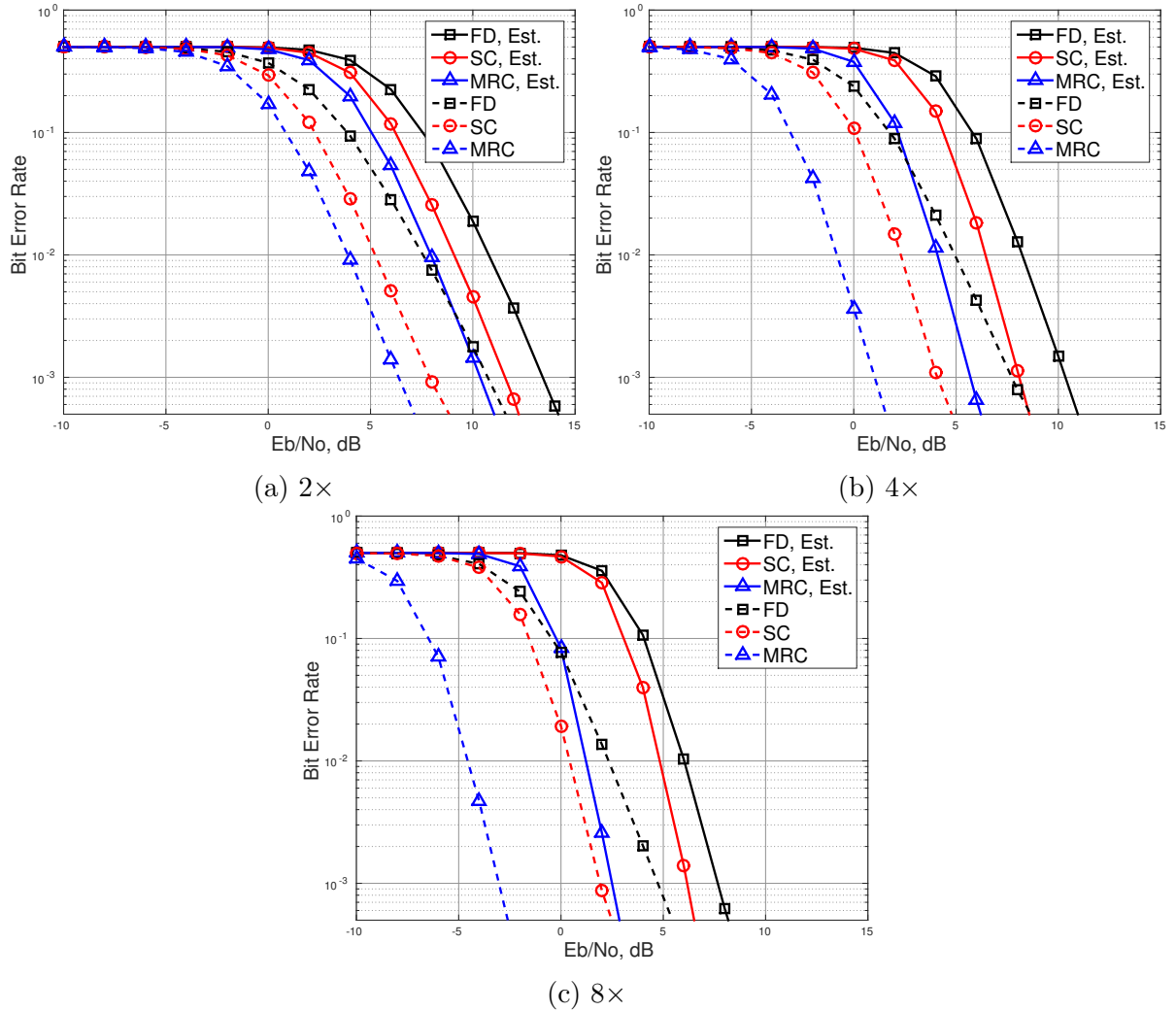
(b) $4\times$

(c) $8\times$

Figure 31 – Diversity combining technique performances for coded BPSK under channel estimation errors

The same behavior is presented in simulations adopting QPSK and 16-QAM modu-

lations, i.e., the MRC stands out as the most sensitive technique to the channel estimation errors, and for all the techniques the spreading factor 8× is the worst case. Based on these results, the 16-QAM modulation presents the worst results, being the modulation that is the most degraded due to this simulation scenario.

In Fig. 32 the proposed frequency despreading method performances are presented considering the possible channel estimation errors. For all data rates the original MCS employs the FD technique and is simulated assuming perfect CSI knowledge, which is defined as our benchmark. On the other hand, the proposed configurations employ MRC and are simulated assuming channel estimation. For $MCS_{(16-QAM,8\times)}$, the channel estimation errors lead to a loss in performance of approximately 8 dB when compared to the perfect CSI case. For the other MCS proposals, this loss in performance is around 5 dB. It can be justified by the fact the $MCS_{(16-QAM,8\times)}$ employs the modulation and the spreading factor more sensitive to the channel estimation errors. However, even presenting these performance losses, the proposed method, employing both MRC and extended spreading factor, under channel estimation errors outcomes the benchmark.

4.2.3.2   Channel Coherence Bandwidth

The variation of the channel B_C is directly related to the correlation among the subcarrier repetition groups. The larger the B_C the closer it gets to $\Delta f_{B_{sc}}$, and, consequently, the subcarriers that transmit the same symbols might become correlated. As mentioned previously, the gain provided by the techniques comprised in this work are affected by this correlation. The performance of FD, SC and MRC for both 2-tap and 32-tap channel at E_b/N_0 (dB) for a BER of 10^{-3} are summarized in Table 8. The simulations assume perfect knowledge of CSI, all the possible spreading factors and modulations.

The effect of subcarrier correlation in the diversity gain is exemplified in Fig. 33, which depicts the simulation results for the FD, SC and MRC, all of them employing all the possible spreading factors. The simulations assume a coded BPSK system and a 2-tap Rayleigh channel model. In this case, the channel presents a small channel time delay spread (σ_τ), i.e., the time interval between the arrival of the first received signal component, referred to the first tap, and the last received signal component of the same transmitted single pulse, referred to the second tap, is small. As B_C is inversely related to σ_τ, this channel presents a large B_C, and the subcarrier groups tends to be correlated. In the simulations presented in Section 4.2.1, only FD presents a quasi-constant marginal return as the spreading factor, M, increases, while SC and MRC present diminishing marginal return. Thus, instead of what happens in Section 4.2.1, in the 2-tap channel scenario, MRC and SC present a quasi-constant marginal return as the spreading factor, M, increases as well.

Besides the simulations assuming 2-tap channel, Fig. 34 also shows, for each spre-

(a) MCS 0

(b) MCS 1

(c) MCS 2
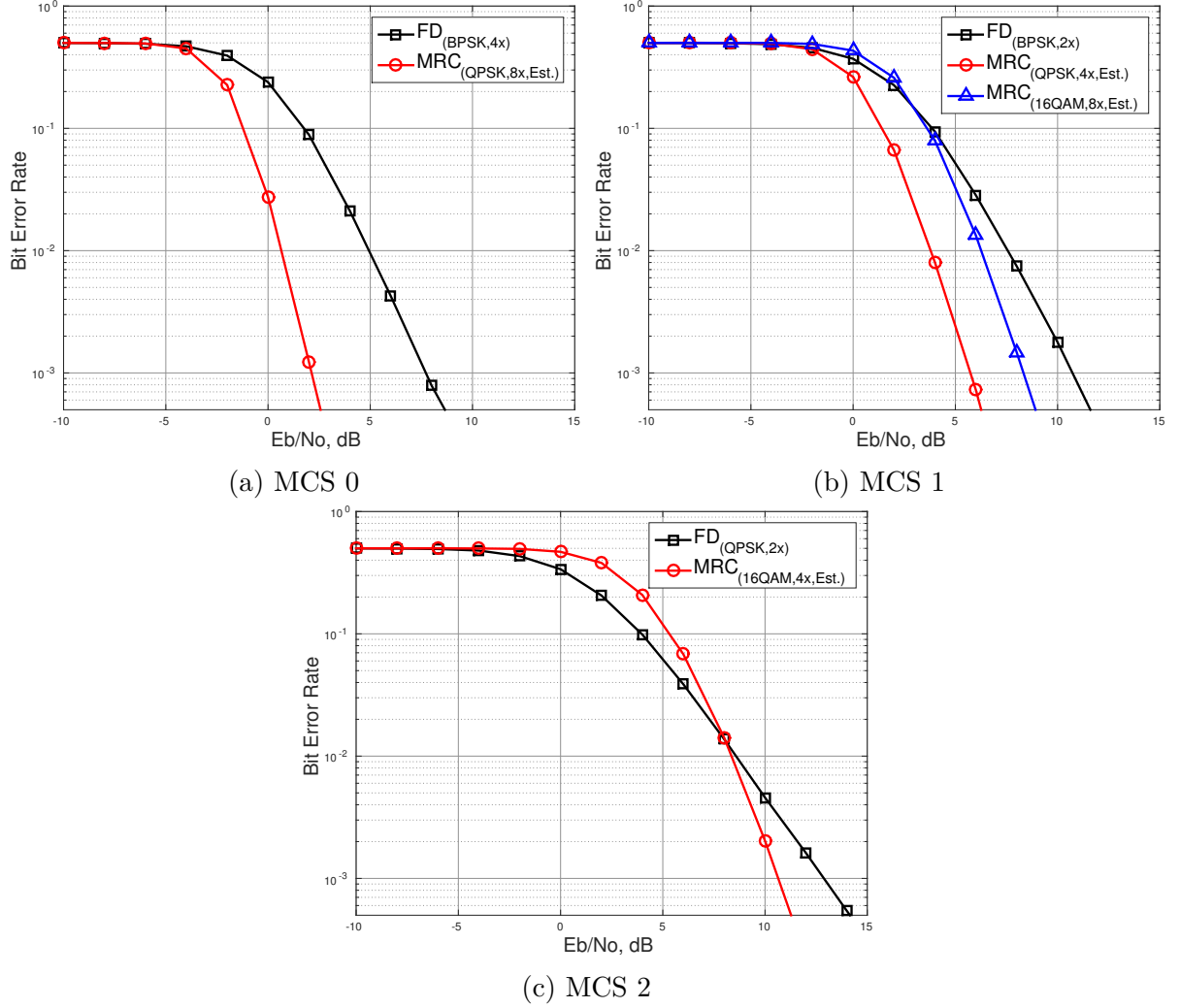
Figure 32 – Performance gain for the proposed method in a coded system under channel estimation errors

ading factor, the performances of FD, SC and MRC, assuming 32-tap channels in a coded BPSK system. The sensitivity of SC is particularly exemplified in Fig. 34c, where, for the 2-tap case, the SC provides worse performance than the one obtained with the FD. Similar behaviors are seen in simulations adopting QPSK and 16-QAM modulations, but the performances degrade as the modulation order increases.

The SC sensitivity to the B_C reflects directly in the performance of the hybrid technique SFD. Table 9 summarizes the SFD and SMRC performances according to the number of selected subcarriers in a coded system at E_b/N_0 (dB) for a BER of 10^{-3}. The simulations adopt frequency spreading by $2\times$ and $4\times$, BPSK, QPSK and 16-QAM modulations, 2-tap and 32-tap channel model, and perfect knowledge of CSI.

In Section 4.2.1, where it is assumed an ideal simulation scenario with a 10-tap channel, the SFD presents its best and worst results when selecting $M/2$ and M subcarriers, respectively. For the 32-tap case the behavior is the same, but for the 2-tap case it changes. For this case, with frequency spreading by $4\times$, the SFD presents its best and

Table 8 – Conventional combining techniques performance at E_b/N_0 (dB) for a BER of 10^{-3} under variation of channel B_C

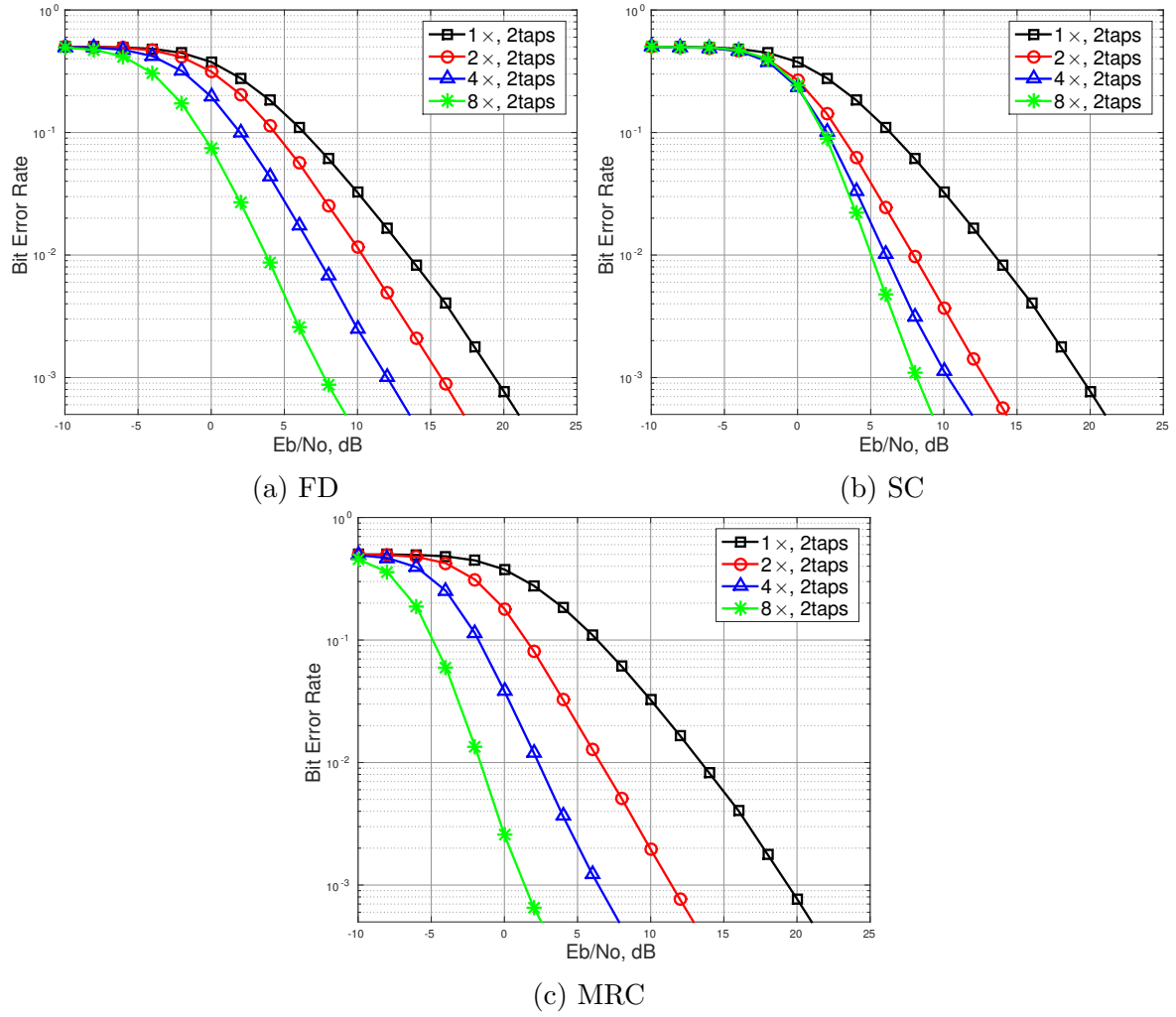| N-tap	Modulation	Diversity Combining Techniques	Spreading Factors			
			$1\times$	$2\times$	$4\times$	$8\times$
2 taps	BPSK	FD	19.34	15.70	12.03	7.69
		SC	19.38	12.81	10.32	8.15
		MRC	19.38	11.45	6.41	1.35
	QPSK	FD	21.94	17.58	14.01	10.51
		SC	21.93	13.45	12.01	10.32
		MRC	21.94	12.32	8.35	3.50
	16-QAM	FD	26.47	22.83	18.51	14.71
		SC	26.47	17.17	15.70	14.32
		MRC	26.48	15.96	11.81	7.75
32 taps	BPSK	FD	10.91	8.32	5.79	3.11
		SC	10.89	5.62	3.02	0.99
		MRC	10.89	4.35	-0.22	-3.98
	QPSK	FD	12.32	9.34	6.64	3.75
		SC	12.32	6.51	3.28	1.31
		MRC	12.31	5.22	0.15	-3.67
	16-QAM	FD	16.64	13.79	10.51	7.45
		SC	16.66	10.11	6.51	4.32
		MRC	16.66	8.64	3.31	-0.68

worst results when selecting 3 and 4 subcarriers, respectively. With frequency spreading by $8\times$, this technique provides its best result when selecting 5 subcarriers, but the worst result depends on the modulation, occurring when 1 subcarrier is selected for BPSK, and when 8 subcarriers are selected for the other cases. Nevertheless, with all the three modulations the difference between selecting only 1 subcarrier and all subcarriers are small, less than 0.5 dB.

The robustness of the proposed frequency despreading method to subcarrier correlation is analyzed through Fig. 35. For each data rate, the performances of the proposed MCS configurations employing MRC, assuming both 2-tap and 32-tap channel, is compared to the original MCS employing FD, assuming a 10-tap channel. It is worth mention that all the cases depicted in Fig. 35 are simulated assuming perfect CSI knowledge. The system employing an original MCS and FD, simulated in a 10-tap channel scenario, is defined as our benchmark. For the MRC with proposed MCS, the dashed line represents the simulations with a 32-tap channel while the solid one represents the ones with a 2-tap channel. As the results verify, even with a 2-tap channel, all the proposed MCS configurations employing MRC present performance gains when compared to the benchmark. When compared the results for the MRC with proposed MCS in a 2-tap channel and the same system in a 10-tap channel, presented in Section 4.2.2, the reduction in the

(a) FD

(b) SC

(c) MRC

Figure 33 – Spreading factor gain for coded BPSK under a large channel B_C

performance gains are around 6 and 7 dB for all the proposed MCS configurations.
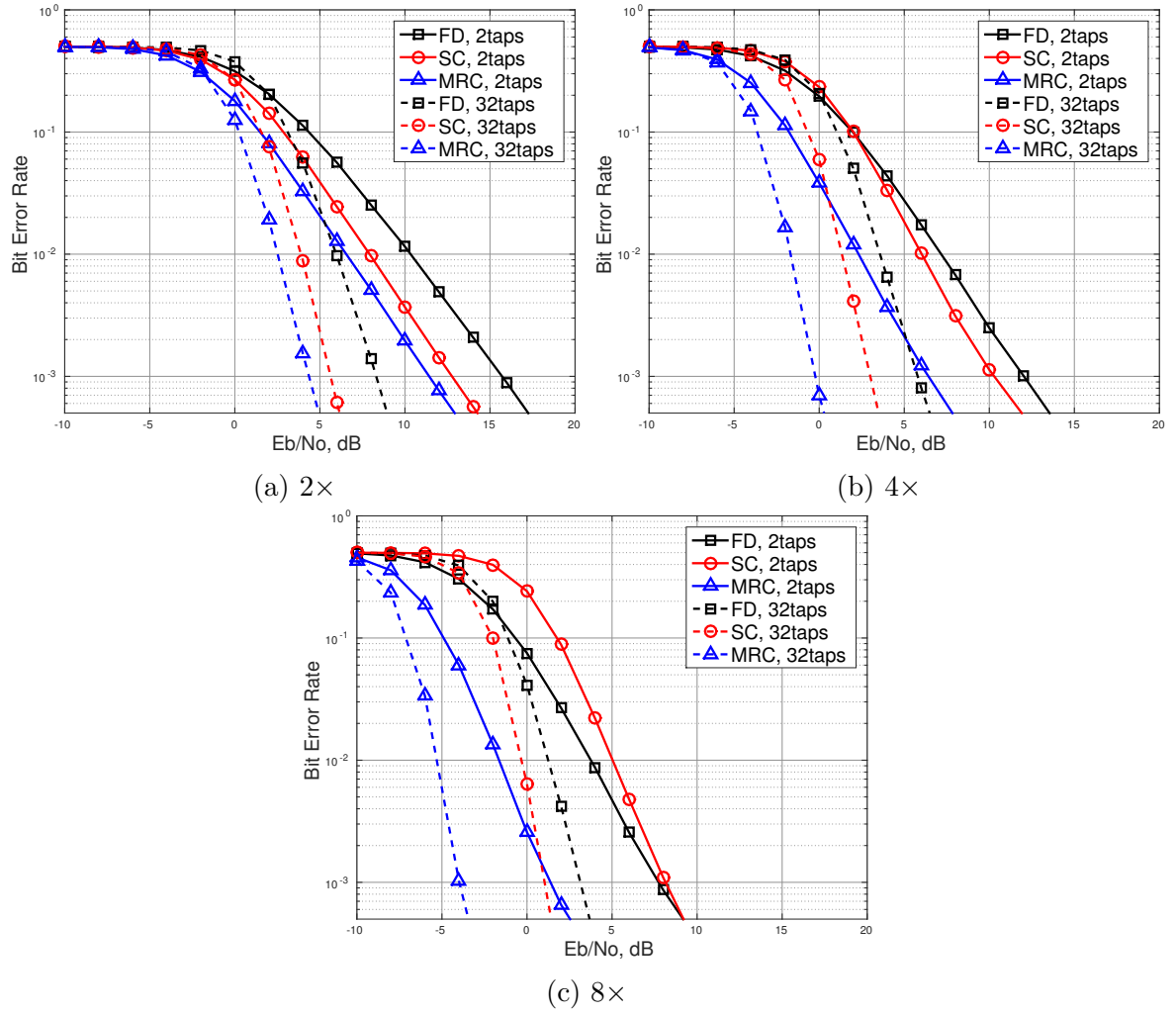
(a) 2×

(b) 4×

(c) 8×

Figure 34 – Diversity combining technique performances for coded BPSK under variation of channel B_C

Table 9 – Hybrid combining techniques performance at E_b/N_0 (dB) for a BER of 10^{-3} under variation of channel B_C

| N Taps	Spread. Factor	Modul.	Div. Comb. Tech.	Selected Subcarriers							
				1sc	2sc	3sc	4sc	5sc	6sc	7sc	8sc
2 taps	4×	BPSK	SFD	10.28	8.09	7.84	12.01	-	-	-	-
			SMRC	10.30	7.96	6.90	6.39	-	-	-	-
		QPSK	SFD	12.06	9.79	9.36	14.04	-	-	-	-
			SMRC	12.01	9.75	8.77	8.35	-	-	-	-
		16-QAM	SFD	15.70	13.09	13.19	18.45	-	-	-	-
			SMRC	15.78	13.07	12.09	11.77	-	-	-	-
	8×	BPSK	SFD	8.11	5.36	3.67	2.94	2.47	2.63	3.69	7.75
			SMRC	8.15	5.33	3.69	2.85	2.15	1.77	1.48	1.31
		QPSK	SFD	10.30	7.31	5.81	4.94	4.64	4.70	5.60	10.42
			SMRC	10.32	7.41	5.88	4.83	4.22	3.67	3.55	3.48
		16-QAM	SFD	14.32	11.70	10.03	9.19	8.85	9.24	10.15	14.73
			SMRC	14.30	11.62	10.03	8.94	8.58	8.18	7.86	7.72
32 taps	4×	BPSK	SFD	2.99	1.71	2.30	5.76	-	-	-	-
			SMRC	2.99	0.92	0.10	-0.25	-	-	-	-
		QPSK	SFD	3.26	2.11	2.75	6.58	-	-	-	-
			SMRC	3.26	1.16	0.39	0.13	-	-	-	-
		16-QAM	SFD	6.54	5.28	5.96	10.49	-	-	-	-
			SMRC	6.51	4.41	3.64	3.31	-	-	-	-
	8×	BPSK	SFD	1.05	-0.85	-1.67	-1.96	-1.92	-1.36	-0.37	3.11
			SMRC	1.02	-1.14	-2.37	-3.01	-3.38	-3.70	-3.65	-3.96
		QPSK	SFD	1.28	-0.71	-1.45	-1.67	-1.62	-1.14	-0.03	3.75
			SMRC	1.28	-1.01	-2.22	-2.81	-3.22	-3.48	-3.60	-3.72
		16-QAM	SFD	4.32	2.39	1.54	1.28	1.26	1.90	3.14	7.41
			SMRC	4.35	2.11	0.82	0.20	-0.18	-0.49	-0.71	-0.71

(a) MCS 0

(b) MCS 1

(c) MCS 2
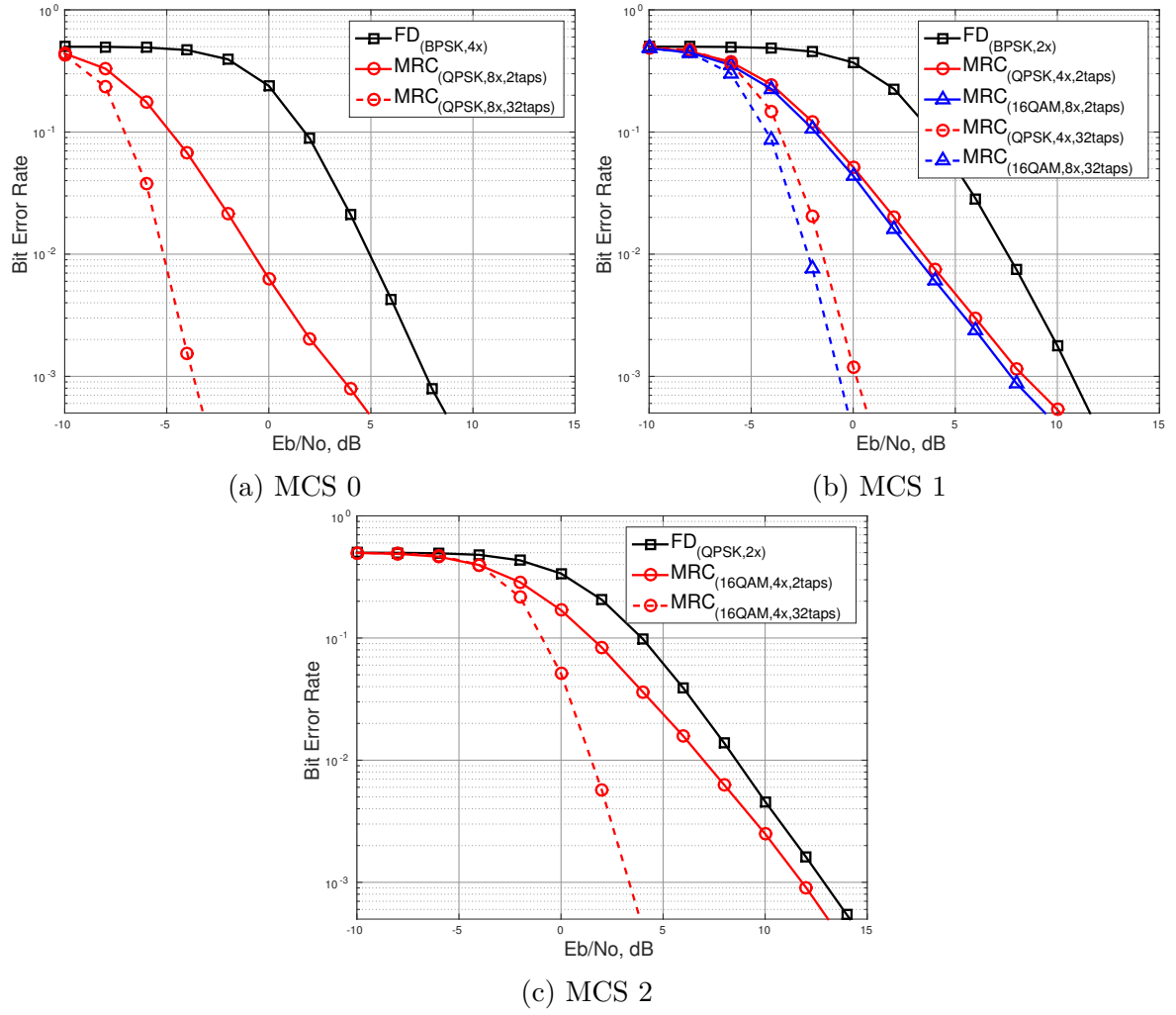
Figure 35 – Performance gain for the proposed method in a coded system under variation of channel B_C

5 Synthesis and Prototyping Results

In order to revert the frequency spreading applied in the MR-OFDM, this work proposes the FD technique, presented in Section 3.1. Moreover, the use of diversity combining techniques to combine the spreaded subcarriers in a way to exploit the frequency diversity provided by the frequency spreading is proposed as well. Section 3.2 describes the techniques MRC, SC, SFD and SMRC applied in the OFDM frequency despreading. This chapter, in turn, describes the hardware implementation of the FD and the mentioned diversity combining techniques in the OFDM context.

The implementation of the frequency despreading method is part of a major project under development, which focuses on an ASIC transceiver that must be compliant with the IEEE802.15.4g standard. In addition to MR-OFDM, the ASIC will contain the remaining IEEE802.15.4g standard PHYs, MR-FSK and MR-O-QPSK. Most part of the three PHYs are already implemented, making possible to verify the functionality of the proposed method within the project. The project has strict requirements for area and implementation complexity. The results presented in this chapter focus on these mentioned requirements.

5.1 MR-OFDM PHY Prototyped in FPGA

The proposed method is implemented in VHDL and integrated to the MR-OFDM baseband modem architecture containing the transmitter and receiver blocks presented in the following figures. As can be seen in Fig. 36, the MR-OFDM transmitter is implemented as established by the reference modulator diagram depicted by Fig. 11 in (IEEE, 2012). The differences between the diagrams are the use of IFFT instead of IDFT, the memory defined as Baud Rate First In First Out (FIFO), and some minor blocks as the Padder and Hanlder.
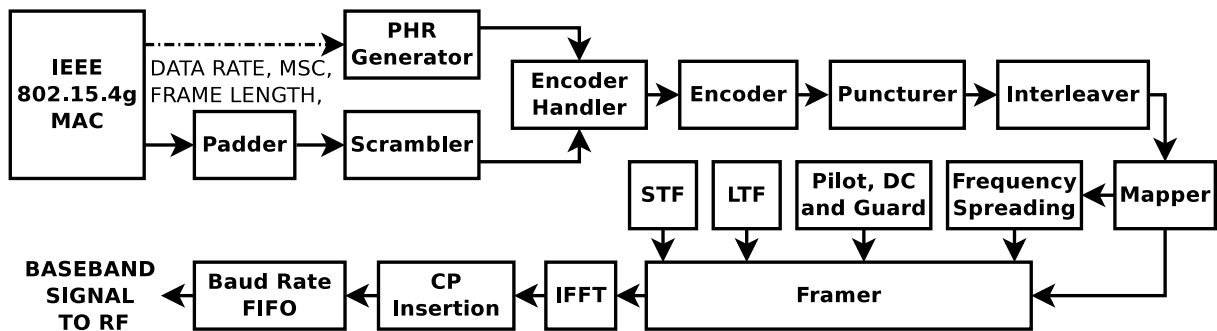

Figure 36 – Transmitter MR-OFDM in FPGA

The MR-OFDM Receiver is devoted to recover the transmitted data and deal with

synchronization issues associated to OFDM systems and errors derived from transmission impairments, such as offsets in timing, frequency and symbol boundary. Furthermore, the receiver has to compensate the influence of the channel over the received signal. The designed receiver for this work, depicted in Fig. 37, does not tackle the synchronization issues nor the errors due to transmission impairments. It includes only the sub-blocks equalize the incoming signal and then extract the transmitted data from the received frame.
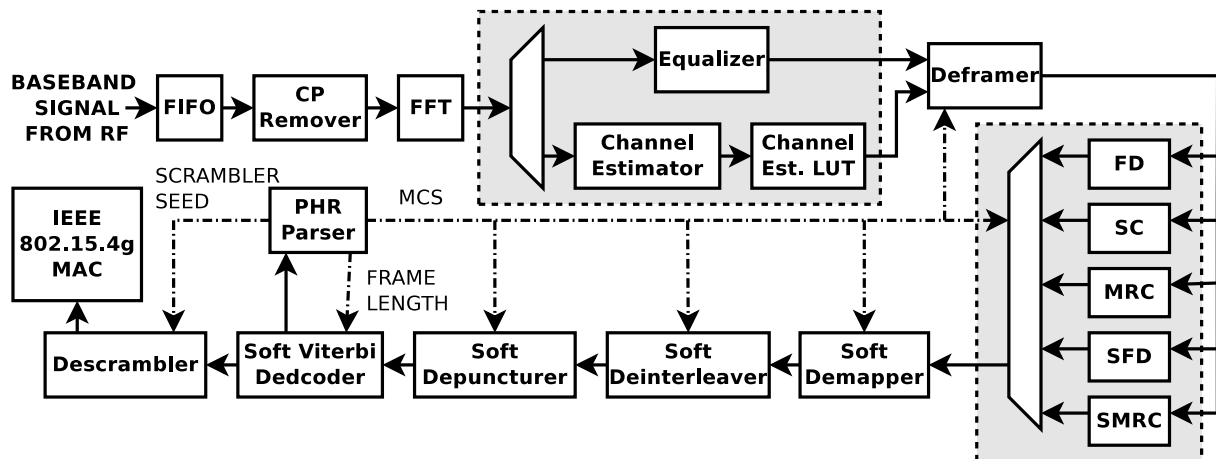

Figure 37 – Receiver MR-OFDM in FPGA

The architectures of the FD and the diversity combining techniques covered in this work are integrated to a demo version of the MR-OFDM PHY (QUEIROZ *et al.*, 2015), constituted by the depicted MR-OFDM Transmitter and Receiver in Fig. 36 and Fig. 37, respectively. The implemented system is more complex than the simulated one in MA-TLAB due to specific requirements of this PHY, as STF and LTF fields, Puncturer/Soft Depuncturer and Interleaver/Deinterleaver modules.

Moreover, the MR-OFDM Receiver architecture presents redundant modules, such as the Channel Estimator and the Channel Estimator LUT. Both blocks are originally placed within the Equalizer. However, when MRC and SMRC are adopted, the Equalizer is not necessary since they already perform symbol equalization by weighting the diversity branches. As these diversity combining techniques need CSI, channel estimation must be performed outside the equalizer, resulting in the block redundancy. The muxes highlighted in the architecture change the data flows according to the combining technique to be tested.

Through the depicted architectures, the functionality of the method is validated. Moreover, in order to validate the method performance, a platform is designed employing partially the simulation environment modeled in MATLAB and the MR-OFDM system demo version prototyped in FPGA, both described previously. The platform is shown in Fig. 38. Due to the necessity of a controlled environment between MR-OFDM transmitter and receiver, we opted to insert the Rayleigh channel and AWGN through Matlab. From

Data Generation to the data tones from the Deframer, the flow is performed in MATLAB. It stores in the FPGA memories the data to be despreaded, CSI, configuration signals, and bits used as reference to calculate the number of errors at the end of the reception. From the memories output to the BER Counter, the data flow is performed in FPGA, employing the stored data and configuration signals.
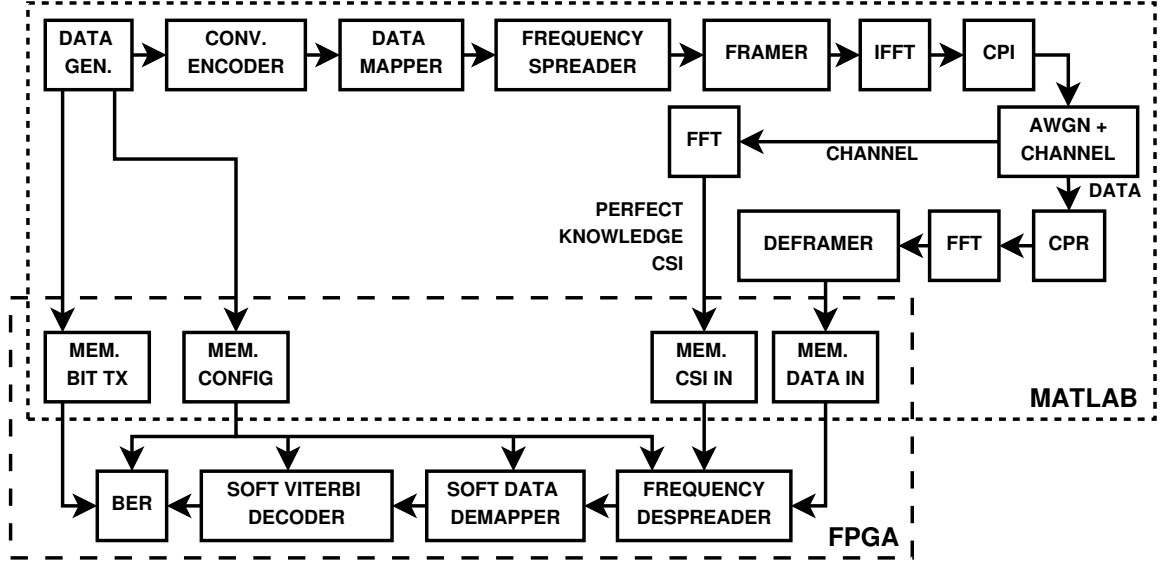
Figure 38 – BER platform employing MATLAB and FPGA

Some of the results obtained using the platform are presented in Fig. 39, where they are compared to the simulated results detailed in previous chapter. The performances of the proposals for $MCS_{BPSK,2\times}$ are used as reference since they adopt all the modulations and spreading factors in the scope of this work. Besides the coded case, results for an uncoded system are also presented. The simulated BER results are close to the ones obtained with FPGA. There is a difference in the BER curves which is a result of quantization noise. The proposed hardware architectures for the Frequency Despreader adopting the diversity combining techniques discussed in this work - SC, MRMC, SFD and SMRC - are addressed in the following section.

5.2 Proposed Hardware Architectures

The following sections describes the proposed hardware architectures for the FD and the diversity combining techniques described previously - SC, MRC, SFD, SMRC. In all the architectures, their sub-blocks are grouped into structures according to their functionality in order to facilitate the analysis and comparisons.

(a) FD/MRC MCS 1 Coded (b) FD/MRC MCS 1 Uncoded

Figure 39 – Extended Spreading Factor gain in FPGA

5.2.1 FD Hardware Architecture
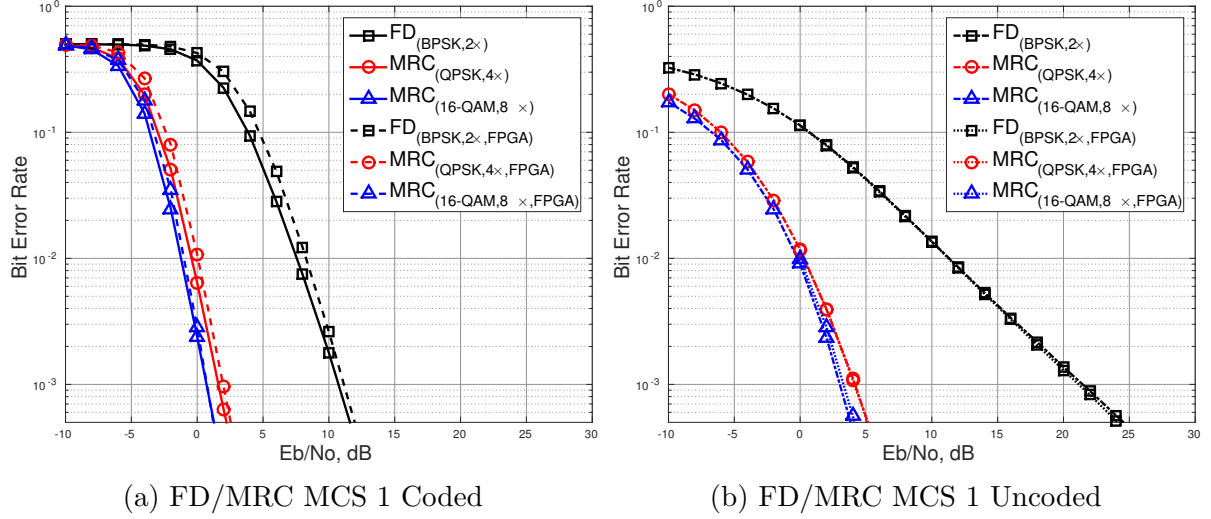
The proposed architecture for the FD is depicted in Fig. 40. It contains three structures: Derotator, Controller and Combiner. In the Derotator structure the phase rotations applied in the transmission for PAPR reduction are reverted. As detailed in Section 2.3.1.1, the phase rotations depend on the number of repetitions, the subcarrier repetition group and the subcarrier position within the group.
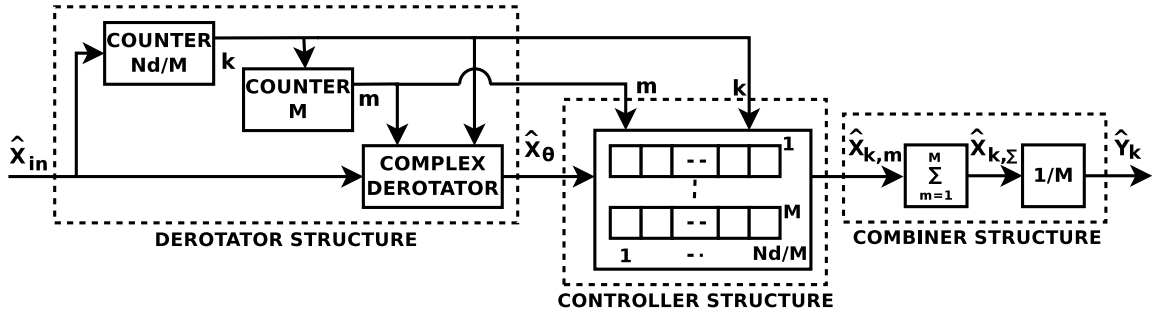
Figure 40 – FD Architecture

In order to decide which phase rotation must be applied in the incoming symbol, $\hat{x}_{in}$, the Derotator structure contains two counters, the N_d/M and the M, where N_d stands for the number of data tones in an OFDM symbol and M stands for the spreading factor (or the number of subcarrier repetition groups). The counter N_d/M is incremented by the incoming data tones, and establishes the symbol position within a subcarrier repetition group. In turn, this counter increments the counter M, establishing which repetition group the incoming symbol belongs. Based on their results the complex derotator uses a determined phase, as expressed in (3.2) and (3.3).

Moreover, the Controller structure arranges the N_d derotated subcarriers in M sequences of N_d/M symbols to be send to the Combiner structure. As the phase rotations,

this arrangement is also based on the counter results. The M sequences are equivalent to diversity branches, and must be combined. Thus, the M symbols related to each specific position k, for $1 \leq k \leq N_d/M$, are accumulated and averaged within the Combiner structure, providing an estimation of the kth transmitted symbol, $\hat{y}_k$. It is worth to mention that the FD is applied in equalized symbols, $\hat{X}_k$, so, the Controller structure provides the expression in (3.4).

5.2.2 SC Hardware Architecture

The SC architecture is depicted in Fig. 41. As the FD architecture, it contains the Derotator structure with the counter N_d/M, counter M and complex derotator controlled by the counters. This architecture does not contain the Combiner structure; instead it has the Multiplier structure. It is composed by the complex multiplier and the complex conjutate (X^*) sub-blocks, which provide the channel powers across all the subcarriers, $|\hat{H}|^2$, based on the channel state information, CSI_{in}. The channel powers are used as the selection criterion by the Controller structure.
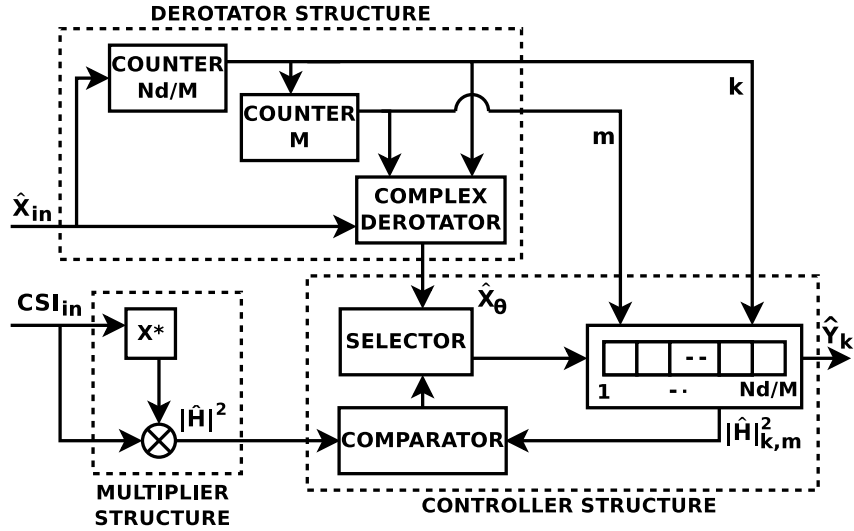
Figure 41 – SC Architecture

In this architecture the Controller structure contains the selector and comparator modules. They compare the incoming $|\hat{H}|^2$ with a stored channel power in order to choose the most suitable subcarrier for each k tone, for $1 \leq k \leq N_d/M$. The buffer where the result of the comparison is stored is formed by two lines with N_d/M registers, one line for the derotated symbols and the other for the channel powers. Besides the Multiplier structure, these extra logic in the Controller structure - selector and comparator - adds hardware complexity to the SC architecture.

The selection procedure starts with the first N_d/M derotated symbols and channel powers that are buffered in the Controller structure. It is worth mentioning that, as FD, the SC is applied to equalized symbols. When the following equalized symbols come, for

each position k, the Comparator analyzes the incoming channel power. If it is higher than the channel power related to the stored symbol, the selector updates the register. After all the N_d incoming symbols, the buffer provides the N_d/M symbols with the highest channel gains for each position k, as expressed in (3.5).

5.2.3 MRC Hardware Architecture

A proposed architecture for the MRC is depicted in Fig. 42. In terms of structures, it has the same ones already contemplated in the FD and SC architectures - Derotator, Combiner, Controller, and Multiplier. However, except for the Derotator, all the other structures are implemented differently. As detailed in Section 2.2.1.2, the incoming sub-carriers must be weighted in order to optimize the resultant signal. Moreover, the optimal weights are defined as the estimated channel gain, $\hat{H}$, on each subcarrier. Thus, once more based on the channel state information, CSI_{in}, the Multiplier structure is responsible not only for providing the channel powers across all the subcarriers, $|\hat{H}|^2$, but also for multiplying the incoming subcarriers by their related conjugated channel response, $R_{k,m}\hat{H}^*$. It is composed by two complex multipliers and the complex conjugated (X^*) sub-block.
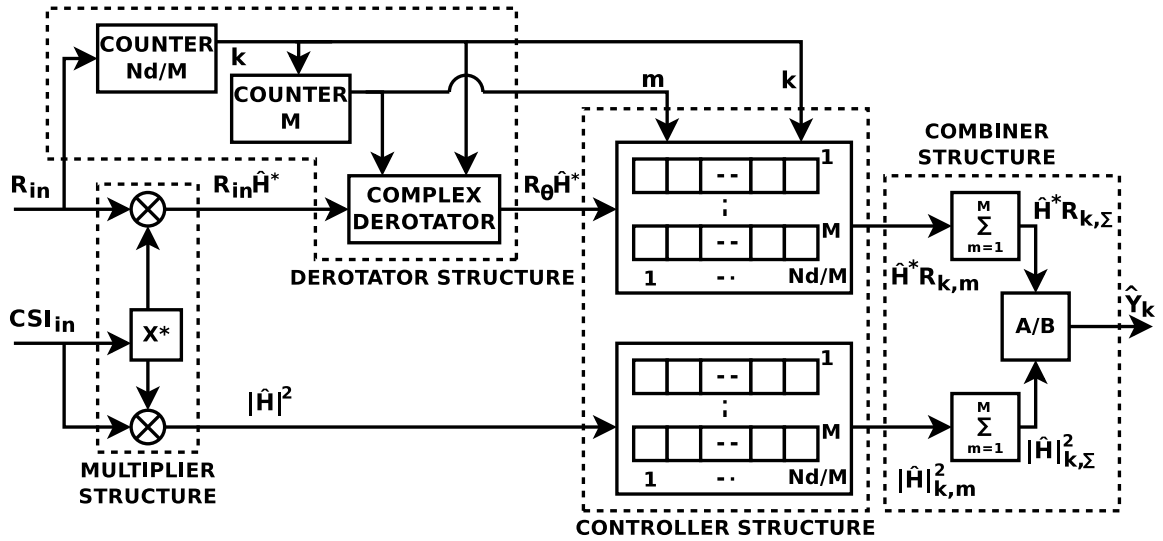
Figure 42 – MRC Architecture

The Controller structure is fed not only by the weighted derotated symbols but also the channel powers, hence arranging the incoming data in $2M$ sequences of N_d/M registers. The Combiner structure, in turn, accumulates both $R_{k,m}\hat{H}^*$ and $|\hat{H}|^2_{k,m}$ and divide them. The division result is an estimation of the kth transmitted symbol, $\hat{y}_k$, as in equation (3.7). It is worth mentioning that the MRC is applied to the received symbols prior equalization, since this technique already equalizes them.

The major differential in the MRC architecture is the divider module at the end of the Combiner structure. It is implemented using a CORDIC (VOLDER, 1959), increasing the architecture implementation complexity. For each position k, all the M symbols and

channel powers are accumulated and processed by the divider sub-block, as numerator and denominator, respectively.

5.2.4   SFD Hardware Architecture

As a hybrid diversity combining technique that merges both SC and FD, the SFD architecture also merges the SC and FD architectures, as shown in Fig. 43. It is composed by the same structures of the SC and FD architectures - Derotator, Multiplier, Controller, and Combiner. Following SC and FD, SFD is applied to equalized symbols. As in SC, the Multiplier structure provides the channel power across all the subcarriers, $|\hat{H}|^2$, which are used by the selection procedure to arrange the derotated symbols. Later, as in FD, the L symbols with the highest received power are accumulated and averaged in the Combiner structure, resulting in an estimation of the transmitted symbol, as expressed in (3.6).
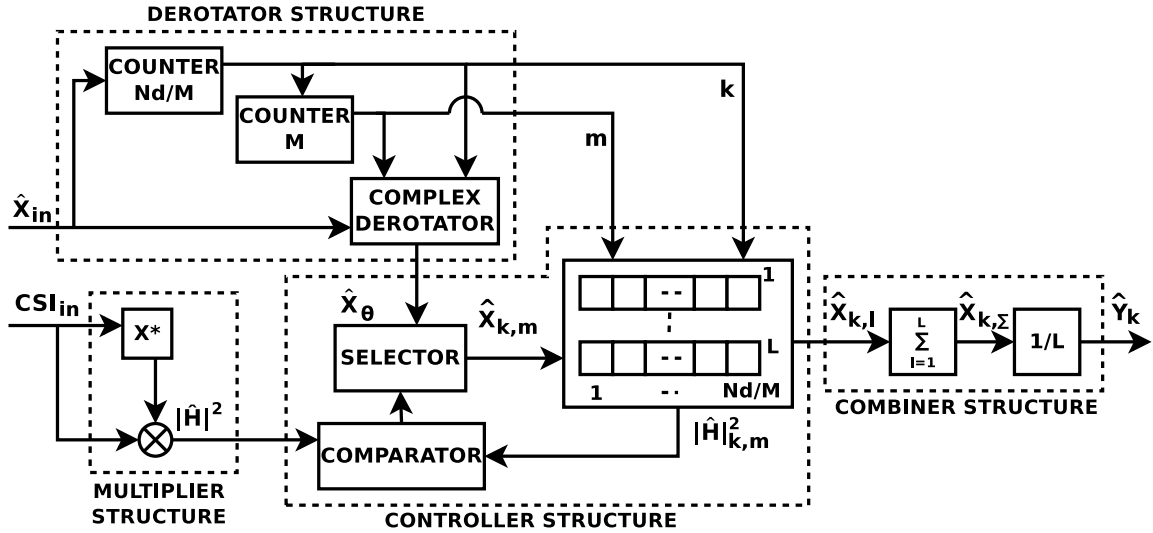
Figure 43 – SFD Architecture

This feature influences the hardware architecture directly. Both Controller and Combiner structures must be implemented in a way to support $1 \leq L \leq 8$, where 8 is the maximum extended spreading factor supported by the MR-OFDM to ensure that the frequency spreading provides frequency diversity to the system, as established in Section 3.3. For the Combiner structure it does not add a lot of implementation complexity, only to the average sub-block. Averaging requires dividing by L, which is implemented by a simple shift when L is a power of two, and, for the other cases, the average multiplies the accumulated symbol by a constant equals to $1/L$. On the other hand, in order to send only the subcarriers related to the L highest channel powers to the Combiner structure, the Controller ends up sorting the symbols as they arrive. The arrangement of the derotated symbols in an increasing order is complex to implement in hardware, which increases the overall SFD implementation complexity.

5.2.5 SMRC Hardware Architecture

The SMRC is also a hybrid diversity combining technique, and its architecture merges the structures of SC and MRC architectures - Derotator, Multiplier, Controller, Combiner - as depicted in Fig. 44. The SMRC architecture employs the channel powers across all the subcarriers, $|\hat{H}|^2$, as selection criterion and weighs the incoming symbols by $\hat{H}^*$. As in MRC, the weighting procedure already equalizes the incoming symbol, so, this technique is applied to the symbols prior equalization. After being arranged by the Controller structure, the L highest channel powers and the subcarriers related to them are accumulated and fed to the divider sub-block, as denominator and numerator, respectively. The division result is an estimation of the kth transmitted symbol, as expressed in (3.8).
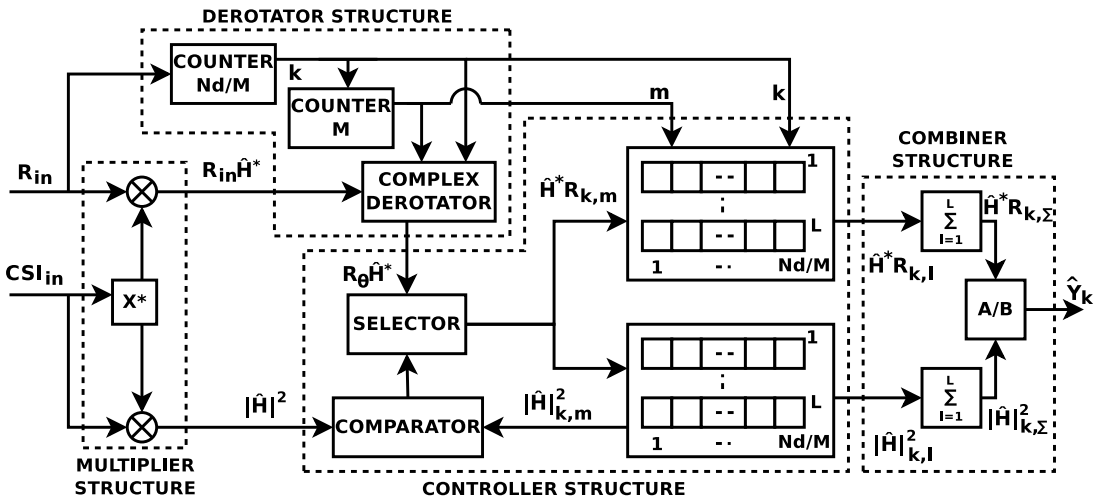
Figure 44 – SMRC Architecture

As the SFD, this architecture must support all the L possible values, $1 \leq L \leq 8$. The Combiner structure is equal to the MRC case, not being affected by the selection of the L most suitable subcarriers. It is composed by two accumulators and the divider implemented with a CORDIC. The Multiplier structure is equal to the one presented in the MRC architecture. On the other hand, the Controller structure is fed by $\hat{H}^*R_{k,m}$ and $|\hat{H}|^2$ and sorts both data as they arrive in the same way that happens in SFD architecture. The derotated symbol arrangement performed within the Controller structure, the CORDIC and the two complex multipliers make the SMRC architecture the most complex of the proposed ones.

5.3 Synthesis Results

All the architectures described in the early sections are synthesized in Altera Cyclone V GX FPGA, which is optimized for the lowest cost and power requirement for 614 Mbps to 3.125 Gbps transceiver applications (Altera Corporation, 2016). Table 10 summarizes the FPGA resource utilization results for each on of the discussed architectures.

The results are separated according to the implemented structures and any possible extra logic is included in the Total results.

The comparisons among the techniques are performed based on Altera logic blocks called Adaptive Logic Modules (ALMs), memory and Digital Signal Processing (DSP) blocks. The ALM is the key to the high-performance, area-efficient architecture of Altera FPGA. In the Cyclone V family it consists of Adaptive Look-Up Tables (ALUTs), two registers, and two adders. The ALUTS, the combinational portion of the ALMs, are Altera's patented LUT technology (Altera Corporation, 2006). It is worth mentioning that the same structure can be synthesized in different entities and presents different results due to the available resources. For instance, the Derotator structure is employed in all the entities without any difference in its instantiation. However their resource utilization results are similar but not identical.

Table 10 – Proposed Frequency Despreading method FPGA resource utilization

Entity	Structure	ALM	Combinational ALUT	Dedicated Logic Register	Block Memory Bits	DSP Block
FD	Combiner	169.4	239	161	0	0
	Derotator	155.8	266	42	0	4
	Controller	1924.6	1488	3895	0	2
	Total	2332	2100	4176	0	6
SC	Combiner	38.2	6	82	0	0
	Multiplier	26.3	50	0	0	2
	Derotator	160.1	263	42	0	4
	Controller	5458.6	9239	5815	0	1
	Total	5798.5	9737	6057	0	7
MRC	Combiner	786.3	1332	1437	144	2
	Multiplier	94.6	184	0	0	6
	Derotator	189.2	286	42	0	4
	Controller	2728.1	2125	5835	0	2
	Total	3942.4	4191	7392	144	14
SFD	Combiner	188	234	161	0	8
	Multiplier	26.2	50	0	0	2
	Derotator	160.2	263	42	0	4
	Controller	11965.9	9122	14215	0	0
	Total	12455.3	9846	14539	0	14
SMRC	Combiner	737.5	1323	1423	144	2
	Multiplier	95.2	184	0	0	6
	Derotator	192.3	283	42	0	4
	Controller	13028.9	11091	14475	0	0
	Total	14199.9	13141	16021	144	12

The FD presents the simplest architecture, which is reflected in the results in Table 10. It employs the least number of ALMs, memory and DSP blocks. Besides the Derotator, which is the same in all the entities, the other structures - Controller and Combiner - present the simplest implementation when compared to the other architectures. The Controller does not perform subcarrier selection and only arranges the incoming data. Moreover, the average performed after the symbol accumulation within the Combiner is implemented as a simple shift register since the spreading factors M are always a number of two. It justifies the small number of DSP blocks when compared to other architectures that average or divide the accumulated data.

In terms of the amount of used resource, the FD is followed by the MRC architecture. Compared to FD, MRC contains an extra structure, the Multiplier. Furthermore, its Controller structure consumes more resources than FD because it arranges not only the derotated symbols but the channel powers as well. Finally, the accumulator implemented in the MRC, instead of averaging the incoming data, uses a CORDIC within the divider. The CORDIC is responsible for memory bits.

Focusing on the remaining techniques, the results are worse than the ones obtained with FD and MRC. It is mostly due to the Controller structure, which includes the subcarrier selection in its resources. For the SC architecture, the other structures listed in the results do not require as many extra resources as the Controller. For instance, the Combiner is only responsible for conditioning the resultant signal to the SC output range, and is not even depicted in Fig. 41. Compared to the Multiplier listed in MRC, the SC one has smaller complexity because it employs only one complex multiplier.

When it comes to the hybrid techniques architectures - SFD and SMRC, the Controller structure is even more complex than the SC version. In order to support the possibility of choosing L subcarriers, it sorts the derotated symbols in an increasing order. The sorting process within the Controler structure increases the number of employed ALMs. In the SMRC case, this number of required resources is bigger than in the SC case since it also arranges the channel powers. Besides, their Combiner structure is also more complex. The SFD divides the accumulated data based by the number of selected subcarriers instead. This cannot always be done with shifting, and usually requires more DSP blocks. The SMRC, as the MRC, utilizes memory bits due the CORDIC.

As described in Chapter 3, the techniques FD, SC and SFD are applied to equalized symbols; while the remaining techniques - MRC and SMRC - are applied to the incoming symbols prior equalization. Even performing symbol equalization, these two techniques need CSI estimation to optimal combine the subcarriers. Thus, to a complete analyzes of the FPGA resources utilized by each of these techniques, it is necessary the results summarized in Table 11.

Based on the performance and resource utilization results, the MRC superiority

Table 11 – Equalizer and CSI Estimator FPGA resource utilization

Entity	ALM	Combinational ALUT	Dedicated Logic Register	Block Memory Bits	DSP Block
Equalizer	1808	1681	2865	3160	18
CSI Estimator	1099	659	1865	2048	1

is clear. Compared to the other diversity combining techniques, it presents the best performance results. Referring to the FPGA resource results of the techniques, Equalizer and CSI Estimator, the FD is the option that utilizes the least number of resources. Nevertheless, the MRC does not utilize much more resources than FD.

Conclusion

Even though the frequency spreading is a method for reducing the MR-OFDM symbol PAPR, it can introduce frequency diversity to the MR-OFDM PHY. In order to exploit diversity among subcarriers, this work proposes a method to perform frequency despreading using diversity combining techniques and extended spreading factors. Also, new MCS configurations adopting modulations with higher number of bits per symbol are proposed to compensate data rate loss.

The diversity combining techniques provided gain performances when compared to the proposed FD, which reverts the frequency spreading without fully exploiting frequency diversity. MRC and SMRC are the most effective techniques, being followed by SFD, and SC as the worst case. Due to the phase rotations applied to the extended spreading factors, when compared to the original MCS, the MCS proposals presented a higher PAPR reduction. Employing both approaches simultaneously, the MRC and the extended spreading factor, the method provides gains up to 10.35 dB, 10.00 dB and 7.80 dB when compared to the system using FD and $\text{MCS}_{(BPSK,4\times)}$, $\text{MCS}_{(BPSK,2\times)}$ and $\text{MCS}_{(QPSK,2\times)}$, respectively.

Furthermore, the MR-OFDM system employing the proposed method with MRC and proposed MCS configurations were simulated in scenarios with a variation of channel coherence bandwidth and channel estimation errors. Even affecting more the modulations with a higher number of bits per symbol and the spreading factor with a higher number of repetitions, the method is robust to the effects of channel estimation in low SNR and subcarrier correlation. The system employing MRC and proposed MCS configurations still provides BER improvements when compared to the MR-OFDM PHY adopting both the original configuration and the FD technique in the first simulated scenario, perfect knowledge CSI and 10-tap channel model. For $\text{MCS}_{(BPSK,4\times)}$, $\text{MCS}_{(BPSK,2\times)}$ and $\text{MCS}_{(QPSK,2\times)}$, the gains are reduced to 5.59 dB, 5.03 dB and 2.26 dB when the method is under channel estimation errors; and to 4.22 dB, 2.4 dB and 1.09 dB when under a B_C related to the 2-tap Rayleigh channel mode.

The method is part of a major project that aims to implement an integrated circuit capable of handling the three PHYs defined in the IEEE802.15.4g standard: MR-FSK, MR-O-QPSK, and MR-OFDM. Thus, along with the whole MR-OFDM, the method was implemented in VHDL and prototyped in FPGA. This implementation allows the verification of the method functionality and validation of its performance. Moreover, the frequency despreading is synthesized in FPGA employing the different diversity combining techniques. The FPGA resource utilization results corroborate the choice of the MRC as

the most suitable diversity combining technique for the MR-OFDM PHY. It employs the least amount of resource when compared to the other diversity combining techniques. Moreover, even when compared to the FD, the number of the used resource is not critical since the MRC already performs symbol equalization.

Based on the results presented in this work, extended spreading factors along with diversity combining techniques provide significant BER improvement to the system due to frequency diversity. Moreover, it can be considered as an evolution for the IEEE802.15.4g standard, allowing the MR-OFDM to be used in applications not considered originally.

References

Altera Corporation. *FPGA Architecture*. 2006. <https://www.altera.com/en_US/pdfs/literature/wp/wp-01003.pdf> [Accessed 4th Jan 2018]. Quoted on page 73.

Altera Corporation. *Cyclone V Device Overview*. 2016. <https://www.altera.com/en_US/pdfs/literature/hb/cyclone-v/cv_51001.pdf> [Accessed 14th Jun 2016]. Quoted on page 72.

ALVES, D. C.; SILVA, G. S. da; LIMA, E. R. de; CHAVES, C. G.; URDANETA, D.; PEREZ, T.; GARCIA, M. Architecture design and implementation of key components of an ofdm transceiver for ieee 802.15. 4g. In: IEEE. *Circuits and Systems (ISCAS), 2016 IEEE International Symposium on.* [S.l.], 2016. p. 550–553. Quoted on page 31.

BAHAI, A.; SALTZBERG, B.; ERGEN, M. *Multi-Carrier Digital Communications: Theory and Applications of OFDM*. Springer, 2004. (Information Technology: Transmission, Processing and Storage). ISBN 9780387225753. Disponível em: <https://books.google.com.br/books?id=ypXRF-5zYp4C>. Quoted on page 17.

CHANDRASEKARAN, N. Diversity techniques in wireless communication systems. *Wireless Communication Technologies*, p. 1–8, 2005. Quoted on page 24.

DIETZE, K. Analysis of a two-branch maximal ratio and selection diversity system with unequal branch powers and correlated inputs for a rayleigh fading channel. 2001. Quoted on page 23.

DINIS, R.; MONTEZUMA, P.; GUSMAO, A. Performance trade-offs with quasi-linearly amplified ofdm through a two-branch combining technique. In: IEEE. *Vehicular Technology Conference, 1996. Mobile Technology for the Human Race., IEEE 46th.* [S.l.], 1996. v. 2, p. 899–903. Quoted on page 22.

ENG, T.; KONG, N.; MILSTEIN, L. B. Comparison of diversity combining techniques for rayleigh-fading channels. *IEEE Transactions on communications*, IEEE, v. 44, n. 9, p. 1117–1129, 1996. Quoted 2 times on pages 28 e 38.

FELICIE, A. *Multipath Propagation*. Salv, 2012. ISBN 9786136321837. Disponível em: <https://books.google.com.br/books?id=fjx9LwEACAAJ>. Quoted on page 40.

GOLDSMITH, A. *Wireless communications*. [S.l.]: Cambridge university press, 2005. Quoted 8 times on pages , 17, 18, 19, 23, 24, 25 e 26.

IEEE, C. S. *IEEE Standard for local and metropolitan area networks; Part 15.4: Low-Rate Wireless Personal Area Networks (LR-WPANs); Amendment 3: Physical Layer (PHY) Specifications for Low-Data-Rate, Wireless, Smart Metering Utility Networks*. 2012. IEEE 802.15.4g-2012 (Amendment to IEEE 802.15.4-2011). Quoted 13 times on pages 15, 16, 17, 21, 29, 30, 31, 32, 41, 42, 45, 46 e 65.

JAIN, R. Channel models: A tutorial. In: *WiMAX forum AATG*. [S.l.: s.n.], 2007. p. 1–6. Quoted on page 18.

JONG, J.-H.; YANG, K.; STARK, W. E.; HADDAD, G. I. Power optimization of ofdm systems with dc bias controlled nonlinear amplifiers. In: IEEE. *Vehicular Technology Conference, 1999. VTC 1999-Fall. IEEE VTS 50th.* [S.l.], 1999. v. 1, p. 268–272. Quoted on page 22.

KATO, T. *Standardization and Certification Process for "Wi-SUN" Wireless Communication Technology.* 2015. Quoted on page 28.

KOZHAKHMETOV, T. Reduction of peak-to-average power ratio in ofdm systems using companding schemes. *Project work, Studien/Diplomarbeit, UniBwH, Professur ANT*, 2008. Quoted 2 times on pages 21 e 22.

LEE, W. C. *Mobile Communications Engineering.* [S.l.]: McGraw-Hill Professional, 1982. ISBN 0070370397. Quoted on page 26.

LI, Y. G.; STUBER, G. L. *Orthogonal frequency division multiplexing for wireless communications.* [S.l.]: Springer Science & Business Media, 2006. Quoted on page 21.

MARCHETTI, N.; RAHMAN, M. I.; KUMAR, S.; PRASAD, R. Ofdm: Principles and challenges. *New directions in wireless communications research*, Springer, p. 29–62, 2009. Quoted 2 times on pages 17 e 18.

MISHRA, H. B. *PAPR reduction of OFDM signals using selected mapping technique.* Tese (Doutorado), 2012. Quoted 2 times on pages 22 e 43.

MITIĆ, D.; LEBL, A.; TRENKIĆ, B.; MARKOV, Ž. An overview and analysis of ber for three diversity techniques in wireless communication systems. *Yugoslav Journal of Operations Research*, v. 25, n. 2, p. 251–269, 2015. Quoted 4 times on pages 23, 24, 25 e 35.

MITRA, A. Lecture notes on mobile communication. *A Curriculum Development Cell project Under QIP, IIT Guwahati*, 2009. Quoted on page 20.

MOLISCH, A. F. *Wireless communications.* [S.l.]: John Wiley & Sons, 2012. v. 34. Quoted 2 times on pages 22 e 46.

POLYDOROU, P. *Analysis of hybrid diversity receivers in Rayleigh fading channels.* Tese (Doutorado) — Theses (School of Engineering Science)/Simon Fraser University, 2004. Quoted on page 23.

PURKAYASTHA, B. B.; SARMA, K. K. *A digital phase locked loop based signal and symbol recovery system for wireless channel.* [S.l.]: Springer, 2015. Quoted on page 42.

QUEIROZ, A. F.; SILVA, G. S. da; CHAVES, C. G.; PEREZ, T. D.; URDANETTA, D. G.; ALVES, D. C.; GARCIA, M. C.; LIMA, E. R. de. Demo: Fpga implementation of an ieee802. 15.4 g mr-ofdm baseband modem for smart metering utility networks. In: IEEE. *Consumer Electronics (GCCE), 2015 IEEE 4th Global Conference on.* [S.l.], 2015. p. 125–126. Quoted on page 66.

SALEHI, M.; PROAKIS, J. *Digital Communications.* McGraw-Hill Education, 2007. ISBN 9780072957167. Disponível em: <https://books.google.com.br/books?id= HroiQAAACAAJ>. Quoted 2 times on pages 15 e 22.

SENGAR, P. P. B. S. Performance improvement in ofdm system by papr reduction. *Signal Image Processing An International Journal (SIPIJ)*, v. 3, n. 2, 2012. Quoted 2 times on pages 18 e 21.

SIMON, M.; ALOUINI, M. *Digital Communication over Fading Channels*. Wiley, 2005. (Wiley Series in Telecommunications and Signal Processing). ISBN 9780471715238. Disponível em: <https://books.google.com.br/books?id=OYrDN0Q6BacC>. Quoted 6 times on pages 26, 27, 28, 38, 51 e 56.

SKLAR, B. Rayleigh fading channels in mobile digital communication systems. i. characterization. *IEEE Communications magazine*, IEEE, v. 35, n. 9, p. 136–146, 1997. Quoted 4 times on pages , 19, 20 e 34.

STÜBER, G. *Principles of Mobile Communication*. Springer US, 2000. ISBN 9780792379980. Disponível em: <https://books.google.com.br/books?id= WO2GQy-SktcC>. Quoted on page 24.

TSE, D.; VISWANATH, P. *Fundamentals of Wireless Communication*. New York, NY, USA: Cambridge University Press, 2005. ISBN 0-5218-4527-0. Quoted 4 times on pages 15, 19, 46 e 49.

TU, X. H. P.; DUTKIEWICZ, E. Performance of an interleaved spread spectrum ofdm system over multipath fading channels. *Transactions on Electrical Engineering, Electronics, and Communications*, 2009. Quoted 2 times on pages 15 e 22.

VARAHRAM, P.; ALI, B. M. A low complexity partial transmit sequence for peak to average power ratio reduction in ofdm systems. *Radioengineering*, v. 20, n. 3, p. 677–682, 2011. Quoted 2 times on pages 22 e 43.

VOLDER, J. E. The cordic trigonometric computing technique. *IRE Transactions on electronic computers*, IEEE, n. 3, p. 330–334, 1959. Quoted on page 70.

WEINSTEIN, S.; EBERT, P. Data transmission by frequency-division multiplexing using the discrete fourier transform. *IEEE transactions on Communication Technology*, IEEE, v. 19, n. 5, p. 628–634, 1971. Quoted on page 17.

WI-SUN. *Wi-SUN Alliance*. 2017. Disponível em: <https://www.wi-sun.org/index.php>. Quoted on page 29.

YACOUB, M. D. *Wireless technology: protocols, standards, and techniques*. [S.l.]: CRC press, 2001. Quoted on page 25.